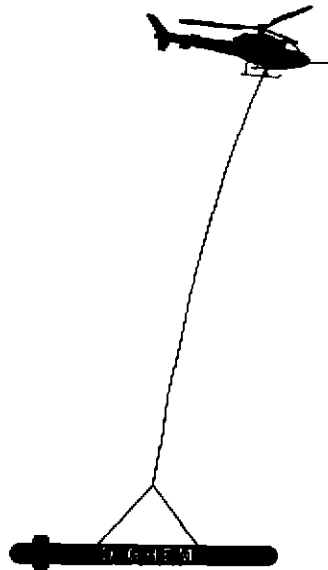


**DIGHEM<sup>V</sup> SURVEY  
FOR  
TOKLAT RESOURCES INC.  
HARRISON LAKE AREA  
BRITISH COLUMBIA**

**NTS 92H/5**



**GEOLOGICAL SURVEY BRANCH**  
A Department of Natural Resources Canada

**26,717**

Fugro Airborne Surveys Corp.  
Mississauga, Ontario

Paul A. Smith  
Geophysicist

October 18, 2001

## SUMMARY

This report describes the logistics and results of a DIGHEM<sup>V</sup> airborne geophysical survey carried out for Toklat Resources Inc, over a property located in the Harrison Lake area, British Columbia. Total coverage of the survey block amounted to 215 km. The survey was flown on October 15, 2001.

The purpose of the survey was to detect zones of auriferous quartz veins in diorite stocks, to locate alteration zones, and to provide information that could be used to map the geology and structure of the survey area. This was accomplished by using a DIGHEM<sup>V</sup> multi-coil, multi-frequency electromagnetic system, supplemented by a high sensitivity cesium magnetometer and a 256 channel spectrometer. The information from these sensors was processed to produce maps which display the magnetic, radiometric and conductive properties of the survey area. A GPS electronic navigation system ensured accurate positioning of the geophysical data with respect to the base maps. Visual flight path recovery techniques were used to confirm the location of the helicopter where visible topographic features could be identified on the ground.

The survey property contains several anomalous features, many of which are considered to be of moderate to high priority as exploration targets. Most of the inferred bedrock conductors appear to warrant further investigation using appropriate surface exploration techniques. Areas of interest may be assigned priorities on the basis of supporting geophysical, geochemical and/or geological information. After initial investigations have

been carried out, it may be necessary to re-evaluate the remaining anomalies based on information acquired from the follow-up program.

# CONTENTS

1.	INTRODUCTION.....	1.1
2.	SURVEY EQUIPMENT .....	2.1
	Electromagnetic System.....	2.1
	Magnetometer .....	2.4
	Magnetic Base Stations.....	2.4
	Spectrometer.....	2.5
	Radar Altimeter .....	2.6
	Barometric Pressure and Temperature Sensors .....	2.6
	Analog Recorder .....	2.7
	Digital Data Acquisition System.....	2.7
	Video Flight Path Recording System.....	2.8
	Navigation (Global Positioning System).....	2.10
	Field Workstation .....	2.12
3.	PRODUCTS AND PROCESSING TECHNIQUES .....	3.1
	Base Maps .....	3.1
	Electromagnetic Anomalies .....	3.2
	Apparent Resistivity.....	3.3
	EM Magnetite (optional) .....	3.4
	Total Magnetic Field .....	3.4
	Magnetic Derivatives (optional) .....	3.5
	Calculated Vertical Magnetic Gradient (optional).....	3.5
	Radiometrics .....	3.6
	Multi-channel Stacked Profiles .....	3.15
	Contour, Colour and Shadow Map Displays .....	3.16
	Resistivity-depth Sections (optional).....	3.18
4.	SURVEY RESULTS .....	4.1
	General Discussion .....	4.1
	Magnetics.....	4.3
	Apparent Resistivity.....	4.5
	Electromagnetic Anomalies .....	4.6
	Conductors in the Survey Area.....	4.9
5.	CONCLUSIONS AND RECOMMENDATIONS.....	5.1

## APPENDICES

- A. List of Personnel
- B. Statement of Cost
- C. Background Information
- D. EM Anomaly List
- E. Statement of Qualifications
- F. Radiometric Processing Control File

### Location and Access

The Abo (Harrison Gold) property is located in the extreme southern portion of British Columbia, approximately 130km east of Vancouver above the southeast shores of Harrison Lake. The main showing (Jenner Gold Zone) is situated 4.5km northeast of the village of Harrison Hot Springs. The geographic centre of the property is located at 49° north latitude and 121°41' west longitude, on mapsheet 92H5.

Access to the claim area is via Trans Canada Highway #1, and by Highway 9 which leads north from the Trans Canada highway at Agassiz to Harrison Hot Springs. Access to various parts of the claims is by rough tote roads which start at a paved road which accesses Sasquatch Provincial Park, approximately 4.5 km north of Harrison Hot Springs.

### Topography, Vegetation and Climate

The property is located in the Coast Mountain physiographic province of B.C., with slopes varying from 10° to 40° (averaging 25°), and elevations from a few meters above sea level up to 1035 meters ASL on top of Bear Mountain. The area has been previously logged off, resulting in a thick cover of second-growth comprised of small (less than 20 cm. diameter) mixed deciduous and coniferous trees, as well as numerous patches of "devils club". The mean annual precipitation for the area ranges from 1500 mm to 2500 mm per year. (60-100 inches).

### Tenure

The Abo property consists of 76 contiguous MGS and 2-post claim units, owned 100% by Eagle Plains Resources. Tenure details are included in Table 1, below.

**Table 1- Abo Claim Data**

TENURE NUMBER	CLAIM NAME	MAP NUMBER	EXPIRY DATE	MINING DIVISION	UNITS	TAG NUMBER
382167	ABO 1	92H032	2006DEC26	New West.	20	221001
382168	ABO 2	92H032	2006DEC26	New West.	9	221002
384241	ABO 3	92H032	2006DEC26	New West.	6	234658
384242	ABO 4	92H032	2006DEC26	New West.	20	234659
384243	ABO 5	92H032	2006DEC26	New West.	12	210556
384244	ABO 6	92H032	2006DEC26	New West.	1	702936M
384245	ABO 7	92H032	2006DEC26	New West.	1	702937M
383387	JILL	92H032	2006DEC26	New West.	1	698761M
235557	HOT 4	92H032	2006DEC26	New West.	6	4774

### History and Previous Work

Mineralization within the property area was first located in the early 1970s, when the original GEO claim was staked.

Between 1972 and 1982 a small tonnage was mined from the property area, producing 30.44 kg gold, 10.14 kg silver, and 616 kg copper from 643 tonnes of

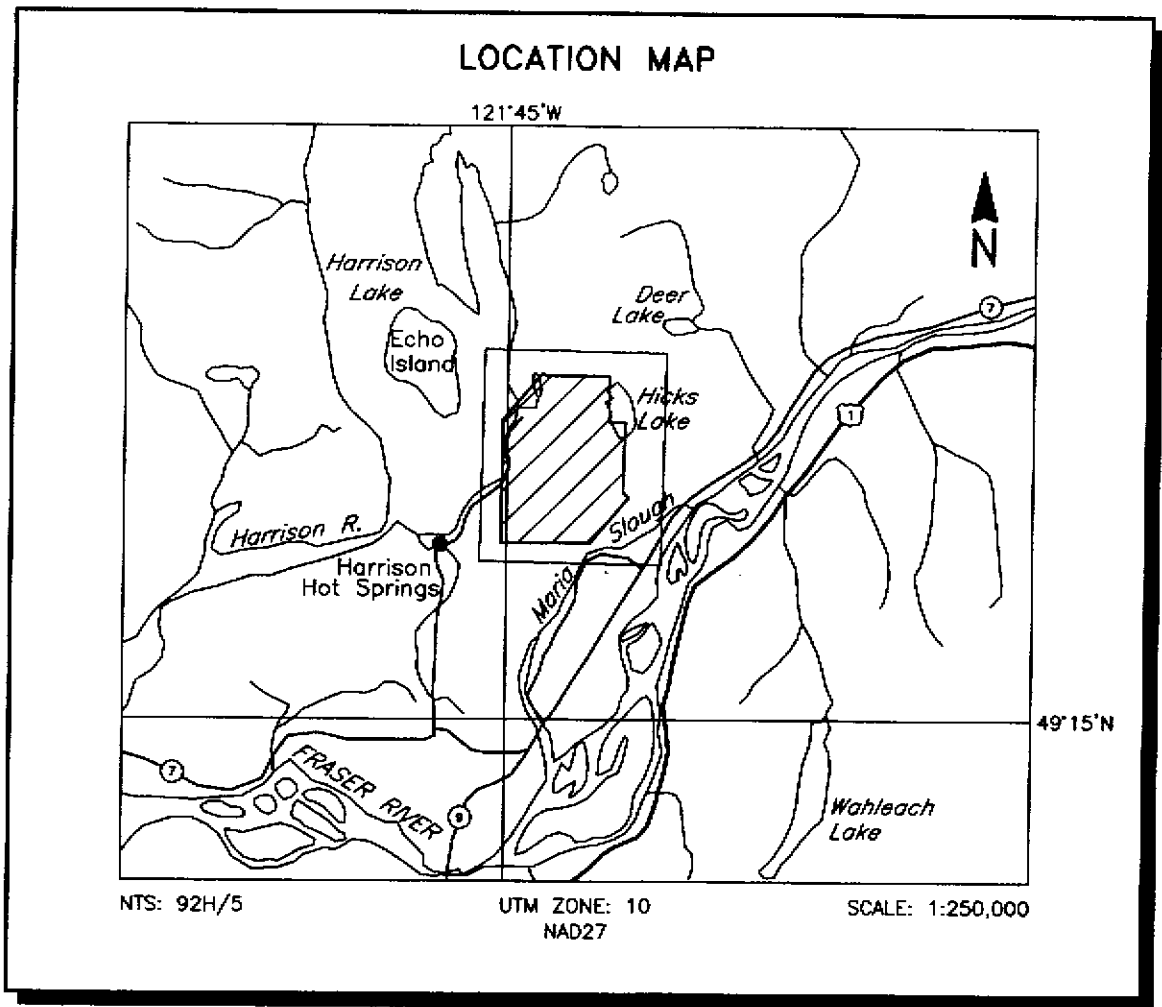


Figure 1  
Toklat Resources Inc.  
Harrison Lake Area, BC  
Job #2066A

ore. This was mined from the Portal Stock adit, which was 50m long and included four raises up to 15m in length. The ore consisted of quartz-pyrrhotite veins containing visible gold.

Abo Oil Corporation (later known as Abo Resource Corporation "Abo") acquired the property in 1982, and conducted surface exploration in 1982 and 1983. Work consisted of geological mapping, soil sampling, and EM surveying. This was followed by a drilling program of 17 diamond drill holes totalling 2,588 metres. In 1984, Sawyer Consultants of Vancouver, BC reviewed all data for Abo and made recommendations for further work, including drill targeting in areas other than the Portal Stock. Abo drilled a further seven diamond drill holes in 1984 totalling 754 metres, including the deepening of two previously drilled holes. Gold mineralization was intersected in three of these holes (DDH 84-28, 84-29, and 84-30). The best intersection was a 64 metre interval in hole 84-28 which averaged 3.77 g/t gold. These holes were the first within the newly discovered Jenner Stock area.

In late 1984, Kerr entered into a joint-venture with Abo to continue exploration. In 1985, Kerr re-mapped the property and carried out substantial stream, soil and rock geochemical sampling. This was followed by a four-hole, 834 metre drilling program (with a number of previous holes deepened).

In 1986 Kerr completed a major exploration program on the property. Geological mapping, based on gold geochemical anomalies, indicated the presence of a number of newly located quartz-diorite stocks located to the south and east of the Jenner stock, as well as a 1,000 metre long, 100 metre wide north-trending feldspar porphyry dyke.

In February, 1987, Kerr signed a letter of intent with Bema International Resources Inc. (Bema) whereby Bema could earn a 55% interest in Kerrs' 60% interest in the property (net 35% equity) by spending \$750,000 in exploration in 1987. Bema could earn a further 5% interest by spending an additional \$250,000.

During 1987, a 1,000 tonne bulk sample was procured from the Jenner Stock through a drift driven at the 187m elevation level. Over 1,500 samples were recovered through extensive rib, face, and muck sampling. The results from the underground sampling indicated that there was as significant upgrading from drill hole assay results (as much as 50%).

Kerr concluded from the 1987 sampling program that the assay average computed from the extensive underground sampling program was the most accurate, compared to drill assays. Kerr calculated an estimated grade and tonnage for the Jenner Stock, with the general assumption that the average grade resulting from underground workings would extend to surface and depth, and that the footwall zones appeared to be the most prospective targets for development. A grade of 3.2 to 4.1 g/t gold was indicated from underground sampling, with an inferred tonnage of 1.3 million tonnes between surface and 100m above sea level, and 2.2 million tonnes from surface down to sea level for the "Footwall Zone".



By early 1988, Bema had earned its equity position from Kerr by spending \$1,000,000. The joint venture then spent an additional \$357,000 to vest their combined interest in the property. In August 1988, Bema purchased Kerr's remaining 25% interest in the property for shares and cash. Abo Resource Corp. then had 40% equity, but this was reduced to 25% when Abo decided not to contribute to future work programs. Bema subsequently acquired control of Abo Resource Corp.

Bema became operator-manager of the Harrison Gold Project in July, 1988. From July to October of 1988, Bema completed an aggressive re-evaluation which included the completion of various geologic studies on the Jenner-Portal area; reconnaissance mapping and rock sampling; orthophoto map production, soil geochemical sampling, additional claim staking, grid establishment, geophysical surveys, road construction, and construction of a core handling and storage facility.

From mid-October to December of 1988, drilling was carried out by the Bema/Kerr JV based on target selection by Kahlert and Associates Ltd. Work was focussed on the Jenner-Portal area within the North Grid area, and from outlined geological, geochemical and geophysical targets on the Hill, Lake, and Breccia zones in the South Grid area.

Pacific Comox Resources Ltd. had an option in 1992 to earn from 49% to 76 % interest in the property by expending \$5 million over 5 years in staged bi-annual payments continuing to February 1997, and completing a positive feasibility study. Bema Resources Corp. retained the right to back in for 51% interest if gold reserves outlined in the feasibility study exceed 1 million troy ounces.

Pacific Comox entered into a tentative agreement on December 1, 1992, (extended to January 13, 1993) with Alaskon Resources Ltd. to form a joint venture to explore the property, but Alaskon failed to secure financing and relinquished the option.

Pacific Comox Resources Ltd. drilled 2 core drill holes in 1993 but failed to complete the work schedule, to complete a feasibility study or to secure financing to complete the purchase of the property, and in 1996, the property was returned to the original vendors.

In 1997, Global Gold Inc. was granted exclusive option to acquire a 100% interest in the property (less a 2% Net Smelter Royalty) by paying the vendors \$1,000,000. The purchase price was payable in cash and/or shares over a period of 3 years.

In October, 2000, Global Gold let the claims comprising most of the property lapse. Eagle Plains immediately acquired the core property area by staking. Additional claims were added in December, 2000 and February, 2001. A single remnant claim from the Bema project area (Hot 4) was purchased from the original vendors in October, 2002. With the purchase of this claim came all original data from past programs. Review of this data during 2001 prompted the

decision by Eagle Plains to complete the airborne geophysical program as described in this report

## **Geology**

The Harrison Lake shear zone is a right-lateral transcurrent fault which splays northward into an imbricate fan of high angle brittle faults. In part it passes along, and parallel to, Harrison Lake. The Harrison Gold property comprises a stratigraphic succession of sedimentary and volcanic rocks of the Cretaceous Brokenback Hill and Peninsula formations (Fire Lake Group) bounded on the east by the major Harrison fault and Tertiary granodiorite of the "Hicks Lake batholith". The Harrison fault separates Fire Lake Group rocks from Cretaceous and/or Tertiary, mainly greenschist facies, mafic to intermediate volcanics and phyllite of the Stollicum Schist. The Harrison fault is a 1-2 kilometre wide fracture zone with a well-developed cleavage dipping 50-70 degrees east but with no marked linear fabric within it. Several possible fault splays cut across the Harrison Gold property.

The Harrison Gold occurrence is underlain by sediments and volcanics of the Brokenback Hill Formation comprising green crystal tuff, volcanic conglomerate and tuffaceous sandstone in the lower part of the section, and volcanic flows, pyroclastics, argillite and sandstone in the upper parts. This sequence conformably overlies a coquina bed of the Peninsula Formation. The sediments and volcanics have been intruded by numerous quartz diorite stocks which are probably related to the "Hicks Lake batholith" (Chilliwack batholith). The age of one such stock, the Jenner stock, has been dated at 23-25 Ma. A feldspar porphyry dike also intrudes the package. Pelites of the Devonian to Permian Chilliwack Group are in fault contact with the Brokenback Hill Formation in the southern parts of the property.

Gold mineralization invariably occurs mainly as free visible flakes up to 2 millimetres in size (generally 0.2-0.6 millimetre or less) within quartz veins (approaching a weak stockwork system). The mineralized quartz veins are confined to quartz diorite intrusive bodies (Jenner, Portal, Hill and Lake stocks), or their immediate periphery. Gold mineralization is not known to occur more than 2 to 3 metres outside the quartz diorite intrusions. Gold also occurs in association with open space sulphide-fillings within a hydrothermally altered breccia pipe (Breccia zone).

The Jenner stock is a small irregular plug or apophysis of quartz diorite which has intruded sedimentary and volcanic rocks of the Brokenback Hill Formation. It is comprised of two main intrusive phases: a medium to coarse grained hornblende-biotite quartz diorite phase which occupies the central and upper portions of the stock; and a fine grained biotite-(hornblende) quartz diorite phase found mainly in the lower portions. Numerous thin, high angle felsic and less commonly mafic dikes are present throughout the stock. Disseminated and

evenly distributed mineralization within the Jenner stock consists of 1-3 per cent pyrrhotite, minor pyrite and chalcopyrite, and traces of molybdenite. In its upper levels, the stock is roughly circular to elliptical (80-110 metres in plan) becoming more elongated (60 by 150 metres) with depth. It plunges 80-85 degrees to the east and its overall three dimensional shape can be described as pipe-like. Portions of the stock, mainly along its footwall contact, are occupied by a contact breccia phase which is transitional from a breccia containing both quartz diorite and country rock fragments in a quartz diorite matrix, to one containing only country rock fragments. Several large xenoliths (40 by 20 by 5 metres) or roof pendants are also found within the stock.

The main deposit is the Jenner Stock zone. Gold-bearing vein systems within the Jenner stock are predominantly low-angle structures. The quartz veins which contain gold mineralization are associated with gently dipping (15-40 degrees) veins which form a conjugate set and bisectrix; minor subvertical veins also contain gold. In addition to these low-angle veins, the dominant features are large, low angle, west and east dipping compressive reverse faults which cut both country rocks and the stock. These faults have resulted in thrust development, shearing and localized vein offsets. The higher grade portions of the Jenner stock tend to be at its margins. A northwest trending, possibly post-mineralization fault, the Jenner fault, passes through the stock. Shearing and faulting is commonly associated with an assemblage of pyrite, carbonate and chlorite. Weak to locally strong propylitic alteration of the stock is ubiquitous and consists primarily of chlorite and carbonate.

The veins which contain the gold mineralization are comprised of a gangue of quartz with minor calcite, chlorite and sericite. The major sulphide mineral is pyrrhotite with minor to trace amounts of pyrite, chalcopyrite, molybdenite, scheelite, arsenopyrite, galena and sphalerite. Bismuth-silver tellurides are present and have been observed as intergrowths with native gold grains. The amount of native gold present in a given vein does not appear to correlate directly with the presence of any sulphide nor with its relative concentration. The highest gold concentrations are found along the mineralized western contact (Footwall zone) of the Jenner stock. Strong sericitic alteration envelopes with widths up to several centimetres are commonly developed around mineralized quartz veins.

The Portal stock is located 300 metres southwest from the Jenner stock. It is separated into two distinct domains: the western portion is a roughly circular body with an average diameter of 140 metres and smooth or regular contacts; the eastern portion is dike-like, narrowing from approximately 100 metres in the west to 40-50 metres near the eastern contact, with irregular or bulging contacts. The entire stock is plunging approximately 70 degrees to the east.

Gold-bearing quartz vein attitudes (gold zones) appear to be oriented horizontally to subhorizontally within the Portal stock. Overall, the zones appear to be dipping

15-20 degrees to the west and 5-20 degrees to the south. Drilling to date suggests that gold grades within the zones improve towards the intrusive contacts, particularly the northern contact. A drill intersection of a well mineralized zone averaged 3.17 grams per tonne gold across 30 metres (Assessment Report 19584). The sericite in these veins from the Portal stock adit gives a potassium-argon age of 24.5 Ma +/- 1 Ma (Fieldwork 1984). Gold mineralization also appears to be associated with the northern contact or footwall of a felsic dike. The dike is a quartz-flooded granite or diorite with intense associated chlorite-sericite-biotite-silica alteration along internal fractures and quartz veins, and 2-10 per cent disseminated pyrrhotite.

The Lake stock is located 1650 metres south from the Jenner stock and is the largest and best exposed of the gold-bearing diorite stocks. It is massive in texture with little variation in composition from margin to margin except for local variations in the size of amphibole and the amount of biotite. The stock locally contains up to 3 per cent finely disseminated pyrrhotite. Quartz veins are not common, and are found predominantly near the margins of the stock. The occasional vein contains visible gold with grades up to 2.24 grams per tonne (Assessment Report 19584).

The Hill stock is located 700 metres south from the Lake stock. Gold-silver mineralization is associated with quartz +/- carbonate- pyrrhotite-pyrite, +/- molybdenite, +/- arsenopyrite veins. These veins pass into the sedimentary country rock but the amount of gold and strength of veining generally decreases substantially and finally dies out within a short distance of the host quartz diorite. The mineralized zone containing the veins weakens laterally outward, is relatively flat lying and controlled by low angle veining similar to the Jenner-Portal style mineralization. Gold-silver grades range up to 23 grams per tonne and 57 grams per tonne respectively, across a 1 metre drill intersection (Assessment Report 20144).

A sulphide-bearing (pyrrhotite-sphalerite-chalcopyrite) breccia pipe (Breccia zone) which is strongly sericitized, chloritized and silicified, is spatially related to the Hill stock. It occurs on the west margin of the Hill stock. The breccia contains fragments of the surrounding country rocks as well as occasional fragments of quartz diorite. Fragments are mainly 5-10 centimetres in diameter with some rotation but no apparent milling or grinding. Sulphide mineralization occurs as open-space fillings. The zone has surface dimensions of 325 by 100 metres. A zone of 29 metres averaging 1.56 grams per tonne gold, 4.4 grams per tonne silver, 0.56 per cent zinc and 0.04 per cent copper including 7 metres averaging 3.56 grams per tonne gold, 9.3 grams per tonne silver, 1.2 per cent zinc and 0.049 per cent copper, occurs at the margins of the breccia pipe (Assessment Report 20144). Recent drilling has indicated that the strength of both hydrothermal alteration and grade of gold-silver- zinc mineralization has weakened downdip and laterally outward from the aforementioned 29 metre zone of mineralization.

## 1. INTRODUCTION

A DIGHEM<sup>V</sup> electromagnetic/resistivity/magnetic/radiometric survey was flown for Toklat Resources Inc., on October 15, 2001, over a survey block located about 21 km west of Hope, B.C. The survey area can be located on NTS map sheet 92H/5 (Figure 1).

Survey coverage consisted of approximately 215 line-km, comprising 202 km on 49 traverse lines and 13 km on 3 orthogonal tie lines. Flight lines were flown in an azimuthal direction of 040°/220° with a line separation of 100 metres. Three tie lines were flown northwest/southeast.

The survey employed the DIGHEM<sup>V</sup> electromagnetic system. Ancillary equipment consisted of a magnetometer, a 256 channel spectrometer, radar and barometric altimeters, video camera, analog and digital recorders, and an electronic navigation system. The instrumentation was installed in an AS350B2 turbine helicopter (Registration C-GZTA) which was provided by Questral Helicopters Ltd. The helicopter flew at an average airspeed of 80 km/h with an EM sensor height of approximately 30 m.

Section 2 provides details on the survey equipment, the data channels, their respective sensitivities, and the navigation/flight path recovery procedure. Noise levels of less than 2 ppm are generally maintained for wind speeds up to 35 km/h. Higher winds may cause the system to be grounded because excessive bird swinging produces difficulties in flying

the helicopter. The swinging results from the 5 m<sup>2</sup> of area which is presented by the bird to broadside gusts.

Powerlines are evident along the southeastern and northwestern edges of the survey area. Due to the presence of buildings and other cultural features in the survey area, any interpreted conductors which occur in close proximity to cultural sources, should be confirmed as bedrock conductors prior to drilling.

## 2. SURVEY EQUIPMENT

This section provides a brief description of the geophysical instruments used to acquire the survey data and the calibration procedures employed.

### Electromagnetic System

Model: DIGHEM<sup>V</sup>

Type: Towed bird, symmetric dipole configuration operated at a nominal survey altitude of 30 metres. Coil separation is 8 metres for 900 Hz, 1000 Hz, 5500 Hz and 7200 Hz, and 6.3 metres for the 56,000 Hz coil-pair.

Coil orientations/frequencies:	<u>orientation</u>	<u>nominal</u>	<u>actual</u>
	coaxial /	1000 Hz	1081 Hz
	coplanar /	900 Hz	876 Hz
	coaxial /	5500 Hz	5525 Hz
	coplanar /	7200 Hz	7158 Hz
	coplanar /	56,000 Hz	55,370 Hz

Channels recorded: 5 in-phase channels  
5 quadrature channels  
4 monitor channels

Sensitivity: 0.06 ppm at 1000 Hz Cx  
0.12 ppm at 900 Hz Cp  
0.12 ppm at 5,500 Hz Cx  
0.24 ppm at 7,200 Hz Cp  
0.60 ppm at 56,000 Hz Cp

Sample rate: 10 per second, equivalent to 1 sample every 3.3 m, at a survey speed of 120 km/h.

The electromagnetic system utilizes a multi-coil coaxial/coplanar technique to energize conductors in different directions. The coaxial coils are vertical with their axes in the flight direction. The coplanar coils are horizontal. The secondary fields are sensed simultaneously by means of receiver coils which are maximum coupled to their respective transmitter coils. The system yields an in-phase and a quadrature channel from each transmitter-receiver coil-pair.

The Dighem calibration procedure involves four stages; primary field bucking, phase calibration, gain calibration, and zero adjust. At the beginning of the survey, the primary field at each receiver coil is cancelled, or "bucked out", by precise positioning of five bucking coils.

The phase calibration adjusts the phase angle of the receiver to match that of the transmitter. A ferrite bar, which produces a purely in-phase anomaly, is positioned near each receiver coil. The bar is rotated from minimum to maximum field coupling and the responses for the in-phase and quadrature components for each coil pair/frequency are measured. The phase of the response is adjusted at the console to return an in-phase only response for each coil-pair. Phase checks are performed daily.

The gain calibration uses external coils designed to produce an equal response on in-phase and quadrature components for each frequency/coil-pair. The coil parameters and distances are designed to produce pre-determined responses at the receiver, due to the current induced in the calibration coil by the transmitter when a switch closes the



loop at the coil. The gain at the console is adjusted to yield secondary responses of 100 ppm (coaxial) and 200 ppm (coplanar). Gain calibrations are carried out at the beginning and end of the survey.

The phase and gain calibrations each measure a relative change in the secondary field, rather than an absolute value. This removes any dependency of the calibration procedure on the secondary field due to the ground, except under circumstances of extreme ground conductivity.

During each survey flight, internal (Q-coil) calibration signals are generated to recheck system gain and to establish zero reference levels. These calibrations are carried out at intervals of approximately 20 minutes with the system out of ground effect. At a sensor height of more than 250 m, there is no measurable secondary field from the earth. The remaining residual is therefore established as the zero level of the system. Linear system drift is automatically removed by re-establishing zero levels between the Q-coil calibrations.

## **Magnetometer**

Model: Picodas 3340 processor with Geometrics G822 sensor  
Type: Optically pumped cesium vapour  
Sensitivity: 0.01 nT  
Sample rate: 10 per second

The magnetometer sensor is housed in the EM bird, 28 m below the helicopter.

## **Magnetic Base Stations**

Model: GEM Systems GSM-19T (in survey area)  
Type: Digital recording proton precession  
Sensitivity: 0.10 nT  
Sample rate: 0.2 per second

Model: Fugro CF-1 with Picodas MEP-710 processor  
Type: Digital recording cesium vapour  
Sensitivity: 0.01 nT  
Sample rate: 1 per second

The CF-1 GPS/Mag base station was located about 20 km east of the survey block,

at latitude 49° 22' 10.77"N, longitude 121° 30' 27.7168"W at an ellipsoidal elevation of 22.6m.

A digital recorder was operated in conjunction with the base station magnetometer to record the diurnal variations of the earth's magnetic field. The clock of the base station is synchronized with that of the airborne system to permit subsequent removal of diurnal drift.

## **Spectrometer**

Manufacturer:	Exploranium
Model:	GR-820
Type:	256 Multichannel, Potassium stabilized
Accuracy:	1 count/sec.
Update:	1 integrated sample/sec.

The GR-820 Airborne Spectrometer employs four downward looking crystals (1024 cu.in.) and one upward looking crystal (256 cu.in.). The downward crystal records the radiometric spectrum from 410 KeV to 3 MeV over 256 discrete energy windows, as well as a cosmic ray channel which detects photons with energy levels above 3.0 MeV. From these 256 channels, the standard Total Count, Potassium, Uranium and Thorium channels are extracted. The upward crystal is used to measure and correct for Radon.

The shock-protected Sodium Iodide (Thallium) crystal package is unheated, and is automatically stabilized with respect to the Potassium peak. The GR-820 provides raw or

Compton stripped data which has been automatically corrected for gain, base level, ADC offset and dead time.

The system is calibration before and after each flight using three accurately positioned hand-held sources. Additionally, fixed-site hover tests are carried out to determine if there are any differences in background. This procedure allows corrections to be applied to each survey flight, to eliminate any differences, which might result from changes in temperature or humidity.

### **Radar Altimeter**

Manufacturer: Honeywell/Sperry  
Model: AA220  
Type: Short pulse modulation, 4.3 GHz  
Sensitivity: 0.3 m at 60 m survey height  
Sample rate: 2 per second

The radar altimeter measures the vertical distance between the helicopter and the ground. This information is used in the processing algorithm which determines conductor depth.

### **Barometric Pressure and Temperature Sensors**

Model: DIGHEM D 1300

Type: Motorola MPX4115AP analog pressure sensor  
AD592AN high-impedance remote temperature sensors

Sensitivity: Pressure: 150 mV/kPa  
Temperature: 100 mV/°C or 10 mV/°C (selectable)

Sample rate: 10 per second

The D1300 circuit is used in conjunction with one barometric sensor and up to three temperature sensors. Two sensors (baro and temp) are installed in the EM console in the aircraft, to monitor pressure and internal operating temperatures.

## **Analog Recorder**

Manufacturer: RMS Instruments

Type: DGR33 dot-matrix graphics recorder

Resolution: 4x4 dots/mm

Speed: 1.5 mm/sec

The analog profiles are recorded on chart paper in the aircraft during the survey. Table 2-1 lists the geophysical data channels and the vertical scale of each profile.

## **Digital Data Acquisition System**

Manufacturer: RMS Instruments

Model: DGR 33

Recorder: 48 Megabyte Flash Card

The data are stored on a 48 Mb Flash card and are downloaded to the field workstation PC at the survey base for verification, backup and preparation of in-field products.

### **Video Flight Path Recording System**

Type: Panasonic VHS Colour Video Camera (NTSC)

Model: AG 2400/WVCD132

Fiducial numbers are recorded continuously and are displayed on the margin of each image. This procedure ensures accurate correlation of analog and digital data with respect to visible features on the ground.

**Table 2-1. The Analog Profiles**

Channel Name	Parameter	Scale units/mm	Designation on Digital Profile
1X9I	coaxial in-phase ( 1000 Hz)	2.5 ppm	CXI1000
1X9Q	coaxial quad ( 1000 Hz)	2.5 ppm	CXQ1000
3P9I	coplanar in-phase ( 900 Hz)	2.5 ppm	CPI900
3P9Q	coplanar quad ( 900 Hz)	2.5 ppm	CPQ900
2P7I	coplanar in-phase ( 7200 Hz)	5 ppm	CPI7200
2P7Q	coplanar quad ( 7200 Hz)	5 ppm	CPQ7200
4X7I	coaxial in-phase ( 5500 Hz)	5 ppm	CXI5500
4X7Q	coaxial quad ( 5500 Hz)	5 ppm	CXQ5500
5P5I	coplanar in-phase ( 56000 Hz)	10 ppm	CPI56K
5P5Q	coplanar quad ( 56000 Hz)	10 ppm	CPQ56K
ALTR	altimeter (radar)	3 m	ALTBIRDM
MAGC	magnetics, coarse	20 nT	MAG100
MAGF	magnetics, fine	2.0 nT	MAG10
CXSP	coaxial spherics monitor		CXSP
CPSP	coplanar spherics monitor		CPSP
CXPL	coaxial powerline monitor		CXPL
CPPL	coplanar powerline monitor		CPPL
1KPA	altimeter (barometric)	30 m	
2TDC	internal (console) temperature	1° C	
3TDC	external temperature	1° C	
TC	total radiometric counts	100 cps	TC
K	potassium counts	10 cps	K
U	uranium counts	10 cps	U
TH	thorium counts	10 cps	TH

## Navigation (Global Positioning System)

### Airborne Receiver

Model:	Ashtech Glonass GG24
Type:	SPS (L1 band), 24-channel, C/A code at 1575.42 MHz, S code at 0.5625 MHz, Real-time differential.
Sensitivity:	-132 dBm, 0.5 second update
Accuracy:	Manufacturer's stated accuracy is better than 10 metres real-time
Recorder:	48 Mb flash card

### Base Station

Model:	Marconi Allstar OEM, CMT-1200 (in CF-1)
Type:	Code and carrier tracking of L1 band, 12-channel, C/A code at 1575.42 MHz
Sensitivity:	-90 dBm, 1.0 second update
Accuracy:	Manufacturer's stated accuracy for differential corrected GPS is 2 metres

The Ashtech GG24 is a line of sight, satellite navigation system which utilizes time-coded signals from at least four of forty-eight available satellites. Both Russian GLONASS and American NAVSTAR satellite constellations are used to calculate the position and to provide real time guidance to the helicopter. The Ashtech system can be combined with a RACAL or similar GPS receiver to further improve the accuracy of the flying and subsequent flight path recovery to better than 5 metres. The differential corrections, which



are obtained from a network of virtual reference stations, are transmitted to the helicopter via a spot-beam satellite. This eliminates the need for a local GPS base station. However, the Marconi Allstar OEM (CMT-1200) was used as a backup and to provide post-survey differential corrections.

The Marconi Allstar OEM (CMT-1200), part of the CF-1 base station, utilizes time-coded signals from at least four of the twenty-four NAVSTAR satellites. The base station raw XYZ data are recorded, thereby permitting post-survey processing for theoretical accuracies of better than 5 metres.

The Ashtech receiver is coupled with a PNAV 2100 navigation system for real-time guidance.

Although the base station receiver is able to calculate its own latitude and longitude, a higher degree of accuracy can be obtained if the reference unit is established on a known benchmark or triangulation point. For this survey, the CF-1/GPS station was located at latitude  $49^{\circ}22'10.77''N$ , longitude  $121^{\circ}30'20.7168''W$  at an elevation of 22.6 m (ellipsoidal). The GPS records data relative to the WGS84 ellipsoid, which is the basis of the revised North American Datum (NAD83). Conversion software is used to transform the WGS84 coordinates to the NAD27 UTM system displayed on the base maps.

## **Field Workstation**

A PC is used at the survey base to verify data quality and completeness. Flight data are transferred to the PC hard drive to permit the creation of a database using a proprietary software package (typhoon-version 17.01.04). This process allows the field operators to display both the positional (flight path) and geophysical data on a screen or printer.

### 3. PRODUCTS AND PROCESSING TECHNIQUES

Table 3-1 lists the maps and products, which have been provided under the terms of the survey agreement. Other products can be prepared from the existing dataset, if requested. These include magnetic enhancements or derivatives, radiometric ratios or ternary plots, percent magnetite, digital terrain or resistivity-depth sections. Most parameters can be displayed as contours, profiles, or in colour.

#### Base Maps

Base maps of the survey area have been produced by digitally scanning published topographic maps. This provides a relatively accurate, distortion-free base which facilitates correlation of the navigation data to the UTM grid. The scanned (.bmp) topographic files are combined with the geophysical data for plotting the final maps. All maps are created using the following parameters:

#### Projection Description:

Datum:	NAD27 (B.C.)
Ellipsoid:	Clarke 1866
Projection:	UTM (Zone: 10)
Central Meridian:	123° W
False Northing:	0
False Easting:	500000
Scale Factor:	0.9996
WGS84 to Local Conversion:	Molodensky
Datum Shifts:	DX: +7    DY: -162    DZ: -188

### **Table 3-1 Survey Products**

The geophysical data have been presented on a single map sheet at a scale of 1:10,000.

Maps accompanying this report include colour sets of the following products:

- EM anomalies with 5500 Coaxial/7200 Coplanar profiles
- Total magnetic field
- Apparent resistivity (7200 Hz)
- Radiometrics total count

Additional products include:

- Digital XYZ archive in Geosoft ASCII format (CD-ROM)
- Digital grid archives in Geosoft format (CD-ROM)
- Survey report
- Multi-channel stacked profiles
- Analog chart records
- Flight path video cassettes

*Note: Other products can be produced from existing survey data, if requested.*

### **Electromagnetic Anomalies**

EM data are processed at the recorded sample rate of 10 samples/second. If necessary, appropriate spheric rejection median or Hanning filters are applied to reduce noise to acceptable levels. EM test profiles are then created to allow the interpreter to select the most appropriate EM anomaly picking controls for a given survey area. The EM picking parameters depend on several factors but are primarily based on the dynamic range of the resistivities within the survey area, and the types and expected geophysical responses of the targets being sought.

Anomalous electromagnetic responses are selected and analysed by computer to provide a preliminary electromagnetic anomaly map. The automatic selection algorithm is intentionally oversensitive to assure that no meaningful responses are missed. Using the preliminary map in conjunction with the multi-parameter stacked profiles, the interpreter then classifies the anomalies according to their source and eliminates those that are not substantiated by the data. The final interpreted EM anomaly map includes bedrock, surficial and cultural conductors. A map containing only bedrock conductors can be generated, if desired.

### **Apparent Resistivity**

The apparent resistivity in ohm-m can be generated from the in-phase and quadrature EM components for any of the frequencies, using a pseudo-layer half-space model. A resistivity map portrays all the EM information for that frequency over the entire survey area. This contrasts with the electromagnetic anomaly map which provides information only over interpreted conductors. The large dynamic range makes the resistivity parameter an excellent mapping tool.

The preliminary resistivity maps and images are carefully inspected to locate any lines or line segments which might require levelling adjustments. Subtle changes between in-flight calibrations of the system can result in line to line differences, particularly in resistive (low signal amplitude) areas. If required, manual levelling is carried out to eliminate or minimize resistivity differences which can be caused by changes in operating

temperatures. These levelling adjustments are usually very subtle, and do not result in the degradation of anomalies from valid bedrock sources.

After the manual levelling process is complete, revised resistivity grids are created. The resulting grids can be subjected to a microlevelling filter in order to smooth the data for contouring. The coplanar resistivity parameter has a broad 'footprint' which requires very little filtering.

Colour maps of the 7200 Hz apparent resistivity have been presented at a scale of 1:10,000. The calculated resistivities for all three coplanar frequencies are included in the XYZ archives. Values are in ohm-metres on all final products.

### **EM Magnetite (optional)**

The apparent percent magnetite by weight is computed wherever magnetite produces a negative in-phase EM response. This calculation is more meaningful in resistive areas.

### **Total Magnetic Field**

The aeromagnetic data are corrected for diurnal variation using the magnetic base station data. Manual adjustments are applied to any lines that require levelling, as indicated by

shadowed images of the gridded magnetic data or tie line/traverse line intercepts. The IGRF gradient has not been removed from the corrected total field data.

### **Magnetic Derivatives (optional)**

The total magnetic field data can be subjected to a variety of filtering techniques to yield maps of the following:

- enhanced magnetics
- first or second vertical derivatives
- reduction to the pole/equator
- magnetic susceptibility with reduction to the pole
- upward/downward continuations
- analytic signal

All of these filtering techniques improve the recognition of near-surface magnetic bodies, with the exception of upward continuation. Any of these parameters can be produced on request.

### **Calculated Vertical Magnetic Gradient (optional)**

The diurnally-corrected total magnetic field data are subjected to a processing algorithm which enhances the response of magnetic bodies in the upper 500 m and attenuates the

response of deeper bodies. The resulting vertical gradient map provides better definition and resolution of near-surface magnetic units. It also identifies weak magnetic features which may not be evident on the total field map. However, regional magnetic variations and changes in lithology may be better defined on the total magnetic field map.

## **Radiometrics**

All radiometric data reductions performed by Fugro Airborne Surveys rigorously follow the procedures described in the IAEA Technical Report<sup>1</sup>.

All processing of radiometric data was undertaken at the natural sampling rate of the spectrometer, i.e., one second. The data were not interpolated to match the fundamental 0.1 second interval of the EM and magnetic data.

The following sections describe each step in the process.

### **Pre-filtering**

The radar altimeter data were processed with a 49-point median filter to remove spikes.

---

<sup>1</sup> Exploranium, I.A.E.A. Report, Airborne Gamma-Ray Spectrometer Surveying, Technical Report No. 323, 1991.



### Reduction to Standard Temperature and Pressure

The radar altimeter data were converted to effective height ( $h_e$ ) in feet using the acquired temperature and pressure data, according to the following formula:

$$h_e = h * \frac{273.15}{T + 273.15} * \frac{P}{1013.25}$$

where:  $h$  is the observed crystal to ground distance in feet  
 $T$  is the measured air temperature in degrees Celsius  
 $P$  is the barometric pressure in millibars

### Live Time Correction

The spectrometer, an Exploranium GR-820, uses the notion of "live time" to express the relative period of time the instrument was able to register new pulses per sample interval. This is the opposite of the traditional "dead time", which is an expression of the relative period of time the system was unable to register new pulses per sample interval.

The GR-820 measures the live time electronically, and outputs the value in milliseconds. The live time correction is applied to the total count, potassium, uranium, thorium, upward uranium and cosmic channels. The formula used to apply the correction is as follows:

$$C_{lt} = C_{raw} * \frac{1000.0}{L}$$

where:  $C_{lt}$  is the live time corrected channel in counts per second

$C_{raw}$  is the raw channel data in counts per second

$L$  is the live time in milliseconds

### Intermediate Filtering

Two parameters were filtered, but not returned to the database:

- Radar altimeter was smoothed with a 5-point Hanning filter ( $h_{ef}$ ).
- The Cosmic window was smoothed with a 29-point Hanning filter ( $Cos_f$ ).

### Aircraft and Cosmic Background

Aircraft background and cosmic stripping corrections were applied to the total count, potassium, uranium, thorium and upward uranium channels using the following formula:

$$C_{ac} = C_{lt} - (a_c + b_c * Cos_f)$$

where:  $C_{ac}$  is the background and cosmic corrected channel

$C_{lt}$  is the live time corrected channel

$a_c$  is the aircraft background for this channel

$b_c$  is the cosmic stripping coefficient for this channel

$Cos_f$  is the filtered Cosmic channel

### **Radon Background**

The determination of calibration constants that enable the stripping of the effects of atmospheric radon from the downward-looking detectors through the use of an upward-looking detector is divided into two parts:

- 1) Determine the relationship between the upward- and downward-looking detector count rates for radiation originating from the ground.
  
- 2) Determine the relationship between the upward- and downward-looking detector count rates for radiation due to atmospheric radon.

The procedures to determine these calibration factors are documented in IAEA Report #323 on airborne gamma-ray surveying. The calibrations for the first part were determined as outlined in the report.

The latter case normally requires many over-water measurements where there is no contribution from the ground. From these tests, any change in the downward uranium window due to variations in radon background would be directly related to variations in the upward window and the other downward windows.

The validity of this technique rests on the assumption that the radiation from the ground is essentially constant from flight to flight. Inhomogeneities in the ground, coupled with deviations in the flight path between test runs, add to the inaccuracy of the accumulated results. Variations in flying heights and other environmental factors also contribute to the uncertainty.

Tests were carried out over the Fraser River, at the start and end of the day. Data were acquired over a four-minute period at the nominal survey altitude (60 m). The data were then corrected for livetime, aircraft background and cosmic activity.

Once the survey was completed, the relationships between the counts in the downward uranium window and in the other four windows due to atmospheric radon were determined using linear regression for each of the three hover sites. The equations solved for were:

$$u_r = a_u U_r + b_u$$

$$K_r = a_K U_r + b_K$$

$$T_r = a_T U_r + b_T$$

$$I_r = a_I U_r + b_I$$

where:  $u_r$  is the radon component in the upward uranium window  
 $K_r$ ,  $U_r$ ,  $T_r$  and  $I_r$  are the radon components in the various windows of the downward detectors

the various "a" and "b" coefficients are the required calibration constants

In practice, only the "a" constants were used in the final processing. The "b" constants, which are normally near zero for over-water calibrations, were of no value as they reflected the local distribution of the ground concentrations measured in the five windows.

The thorium, uranium and upward uranium data for each line were copied into temporary arrays, then smoothed with 21, 21 and 51 point Hanning filters to product  $Th_f$ ,  $U_f$ , and  $u_f$  respectively. The radon component in the downward uranium window was then determined using the following formula:

$$U_d = \frac{u_f - a_1 * U_f - a_2 * Th_f + a_2 * b_{Th} - b_u}{a_u - a_1 - a_2 * a_{Th}}$$

where:  $U_d$  is the radon component in the downward uranium window  
 $u_f$  is the filtered upward uranium  
 $U_f$  is the filtered uranium  
 $Th_f$  is the filtered thorium  
 $a_1$ ,  $a_2$ ,  $a_u$  and  $a_{Th}$  are proportionality factors and  
 $b_u$  and  $b_{Th}$  are constants determined experimentally

The effects of radon in the downward uranium are removed by simply subtracting  $U_r$  from  $U_{ac}$ . The effects of radon in the total count, potassium, thorium and upward uranium are then removed based upon previously established relationships with  $U_r$ . The corrections are applied using the following formula:

$$C_{rc} = C_{ac} - (a_r * U_r + b_c)$$

where:  $C_{rc}$  is the radon corrected channel  
 $C_{ac}$  is the background and cosmic corrected channel  
 $U_r$  is the radon component in the downward uranium window  
 $a_r$  is the proportionality factor and  
 $b_c$  is the constant determined experimentally for this channel

### Compton Stripping

Following the radon correction, the potassium, uranium and thorium are corrected for spectral overlap. First  $\alpha$ ,  $\beta$ , and  $\gamma$  the stripping ratios, are modified according to altitude. Then an adjustment factor based on  $a$ , the reversed stripping ratio, uranium into thorium, is calculated. (Note: the stripping ratio altitude correction constants are expressed in change per metre. A constant of 0.3048 is required to conform to the internal usage of height in feet):

$$\alpha_h = \alpha - h_{ef} * 0.00049$$

$$\beta_h = \beta + h_{ef} * 0.00065$$

$$\gamma_h = \gamma + h_{ef} * 0.00069$$

where:  $\alpha, \beta, \gamma$  are the Compton stripping coefficients  
 $\alpha_h, \beta_h, \gamma_h$  are the height corrected Compton stripping coefficients  
 $h_{ef}$  is the height above ground in metres

The stripping corrections are then carried out using the following formulas:

$$\alpha_r = \frac{1}{1 - a\alpha_h - g\gamma_h + ag\beta_h}$$
$$Th_c = ((1 - g\gamma_h)Th_{rc} - aU_{rc} + agK_{rc}) * \alpha_r$$
$$U_c = (Th_{rc}(g\beta_h - \alpha_h) + U_{rc} - K_{rc}^g) * \alpha_r$$
$$K_c = (Th_{rc}(a\alpha_h - \beta_h) + U_{rc}(a\beta_h - \gamma_h) + K_{rc}(1 - a\alpha_h)) * \alpha_r$$

where:  $U_c, Th_c$  and  $K_c$  are corrected uranium, thorium and potassium  
 $\alpha_h, \beta_h, \gamma_h$  are the height corrected Compton stripping coefficients  
 $U_{rc}, Th_{rc}$  and  $K_{rc}$  are radon-corrected uranium, thorium and potassium  
 $\alpha_r$  is the backscatter correction  
 $a$  is the reverse stripping ratio U into Th  
 $g$  is the reverse stripping ratio K into uranium

### Attenuation Corrections

The total count, potassium, uranium and thorium data are then corrected to a nominal survey altitude, in this case 60 m (200 ft). This is done according to the equation:

$$C_a = C * e^{\mu(h_{ef} - h_0)}$$

where:  $C_a$  is the output altitude corrected channel  
 $C$  is the input channel  
 $\mu$  is the **attenuation** correction for that channel  
 $h_{ef}$  is the effective altitude, usually in m  
 $h_0$  is the nominal survey altitude used as datum

### **Adjustments**

Manual adjustments may have been made to the data in some parts of the survey area to minimize the effect of the problems which were not completely eliminated by the standard processing. However, the data may be of lower reliability in the areas covered by the affected lines. In this survey, no such adjustments were warranted by the data.

Due to very rugged terrain in the survey area, the survey altitude fluctuations are severe in some sections which is unavoidable for safety reasons. The attenuation corrections in such sections are not optimal and hence need to be further adjusted.

All coefficients used in processing the radiometric data are included in the Radiometric Processing Control Files appended to this report.



## **Multi-channel Stacked Profiles**

Distance-based profiles of the digitally recorded geophysical data are created at an appropriate scale. These profiles also contain the calculated parameters which are used in the interpretation process. These are produced as worksheets prior to interpretation, and are also presented in the final corrected form after interpretation. The profiles display the characteristics of the electromagnetic anomalies with their respective interpretive symbols. Table 3-2 shows the parameters and scales for the multi-channel stacked profiles.

In Table 3-2, the log resistivity scale of 0.06 decade/mm means that the resistivity changes by an order of magnitude in 16.6 mm. The resistivities at 0, 33 and 67 mm up from the bottom of the digital profile are respectively 1, 100 and 10,000 ohm-m.

## **Contour, Colour and Shadow Map Displays**

The geophysical data are interpolated onto a regular grid using a modified Akima spline technique. The resulting grid is suitable for generating contour maps of excellent quality.

The grid cell size is 25 metres, 25% of the line interval.

Colour maps are produced by interpolating the grid down to the pixel size. The parameter is then incremented with respect to specific amplitude ranges to provide colour "contour" maps. Colour maps of the total magnetic field are particularly useful in defining the lithology of the survey area.



Monochromatic shadow maps or images are generated by employing an artificial sun to cast shadows on a surface defined by the geophysical grid. There are many variations in the shadowing technique. These techniques can be applied to total field or enhanced magnetic data, magnetic derivatives, VLF, resistivity, etc. The shadow of the enhanced magnetic parameter is particularly suited for defining geological structures with crisper images and improved resolution.

### **Resistivity-depth Sections (optional)**

The apparent resistivities for all frequencies can be displayed simultaneously as coloured resistivity-depth sections. Usually, only the coplanar data are displayed as the close frequency separation between the coplanar and adjacent coaxial data tends to distort the section. The sections can be plotted using the topographic elevation profile as the surface. The digital terrain values, in metres a.m.s.l., can be calculated from the GPS Z-value or barometric altimeter, minus the aircraft radar altimeter.

Resistivity-depth sections can be generated in three formats:

- (1) Sengpiel resistivity sections, where the apparent resistivity for each frequency is plotted at the depth of the centroid of the in-phase current flow<sup>2</sup>; and,

---

<sup>2</sup> Sengpiel, K.P., 1988, Approximate Inversion of Airborne EM Data from Multilayered Ground: Geophysical Prospecting 36, 446-459.

- (2) Differential resistivity sections, where the differential resistivity is plotted at the differential depth<sup>3</sup>.
- (3) Occam<sup>4</sup> or Multi-layer<sup>5</sup> inversion.

Both the Sengpiel and differential methods are derived from the pseudo-layer half-space model. Both yield a coloured resistivity-depth section which attempts to portray a smoothed approximation of the true resistivity distribution with depth. Resistivity-depth sections are most useful in conductive layered situations, but may be unreliable in areas of moderate to high resistivity where signal amplitudes are weak. In areas where in-phase responses have been suppressed by the effects of magnetite, the computed resistivities shown on the sections may be unreliable.

Both the Occam and Multi-layer Inversions compute the layered earth resistivity model which would best match the measured EM data. The Occam inversion uses a series of thin, fixed layers (usually 20 x 5m and 10 x 10m layers) and computes resistivities to fit the

---

<sup>3</sup> Huang, H. and Fraser, D.C., 1993, Differential Resistivity Method for Multi-frequency Airborne EM Sounding: presented at Intern. Airb. EM Workshop, Tucson, Ariz.

<sup>4</sup> Constable et al, 1987, Occam's inversion: a practical algorithm for generating smooth models from electromagnetic sounding data: *Geophysics*, 52, 289-300.

<sup>5</sup> Huang H., and Palacky, G.J., 1991, Damped least-squares inversion of time domain airborne EM data based on singular value decomposition: *Geophysical Prospecting*, 39, 827-844.

EM data. The multi-layer inversion computes the resistivity and thickness for each of a defined number of layers (typically 3-5 layers) to best fit the data.

## 4. SURVEY RESULTS

### General Discussion

The survey results are presented on separate map sheets for each parameter at a scale of 1:10,000. Table 4-1 summarizes the EM responses in the survey area, with respect to conductance grade and interpretation.

The anomalies shown on the electromagnetic anomaly maps are based on a near-vertical, half plane model. This model best reflects "discrete" bedrock conductors. Wide bedrock conductors or flat-lying conductive units, whether from surficial or bedrock sources, may give rise to very broad anomalous responses on the EM profiles. These may not appear on the electromagnetic anomaly map if they have a regional character rather than a locally anomalous character. These broad conductors, which more closely approximate a half-space model, will be maximum coupled to the horizontal (coplanar) coil-pair and should be more evident on the resistivity parameter. Resistivity maps, therefore, may be more valuable than the electromagnetic anomaly maps, in areas where broad or flat-lying conductors are considered to be of importance. Coloured resistivity maps, based on the 7200 Hz coplanar data are included with this report.

**TABLE 4-1  
EM ANOMALY STATISTICS  
HARRISON LAKE AREA, B.C.**

CONDUCTOR GRADE	CONDUCTANCE RANGE SIEMENS (MHOS)	NUMBER OF RESPONSES
7	>100	0
6	50 - 100	0
5	20 - 50	2
4	10 - 20	19
3	5 - 10	49
2	1 - 5	193
1	<1	38
*	INDETERMINATE	69
TOTAL		370

CONDUCTOR MODEL	MOST LIKELY SOURCE	NUMBER OF RESPONSES
L	LINE SOURCE (CULTURE)	27
D	DISCRETE BEDROCK CONDUCTOR	76
B	DISCRETE BEDROCK CONDUCTOR	150
S	CONDUCTIVE COVER	21
H	ROCK UNIT OR THICK COVER	80
E	EDGE OF CONDUCTIVE UNIT	16
TOTAL		370

(SEE EM MAP LEGEND FOR EXPLANATIONS)



Excellent resolution and discrimination of conductors was accomplished by using a fast sampling rate of 0.1 sec and by employing a "common" frequency on two orthogonal coil-pairs (5500 Hz coaxial and 7200 Hz coplanar). The resulting "difference channel" parameters often permit differentiation of bedrock and surficial conductors, even though they may exhibit similar conductance values.

Anomalies which occur near the ends of the survey lines (i.e., outside the survey area), should be viewed with caution. Some of the weaker anomalies could be due to aerodynamic noise, i.e., bird bending, which is created by abnormal stresses to which the bird is subjected during the climb and turn of the aircraft between lines. Such aerodynamic noise is usually manifested by an anomaly on the coaxial in-phase channel only, although severe stresses can affect the coplanar in-phase channels as well.

## **Magnetics**

A Gem Systems GSM-19T proton precession magnetometer base station was operated at the survey site to record diurnal variations of the earth's magnetic field. The clock of the base station was synchronized with that of the airborne system to permit subsequent removal of diurnal drift. A second magnetic base station (with GPS) was located at the base of operations in Hope, approximately 20km east of the survey area.

The total magnetic field data have been presented as contours on the base maps using a contour interval of 10 nT where gradients permit. The maps show the magnetic properties of the rock units underlying the survey area.

There is some evidence on the magnetic map that suggests that the survey area has been subjected to deformation and/or alteration. These structural complexities are evident on the contour maps as variations in magnetic intensity, irregular patterns, and as offsets or changes in strike direction.

The magnetic results show a moderate dynamic range, with values of less than 56,530 nT to more than 58,800 nT. The east-central portion of the property is dominated by an elongate magnetic high that strikes north-northwest. In addition, there are several smaller, plug-like highs that could reflect diorite intrusions. Magnetic lows on lines 10220 and 10350 have been attributed to remanent magnetization, which could be indicative of alteration zones.

If a specific magnetic intensity can be assigned to the rock type which is believed to host the target mineralization, it may be possible to select areas of higher priority on the basis of the total field magnetic data. This is based on the assumption that the magnetite content of the host rocks will give rise to a limited range of contour values which will permit differentiation of various lithological units.

The magnetic results, in conjunction with the other geophysical parameters, have provided valuable information which can be used to effectively map the geology and structure in the survey area.

### **Apparent Resistivity**

Apparent resistivity maps, which display the conductive properties of the survey area, were produced from the 7200 Hz coplanar data. The maximum resistivity value calculated for the 7200 Hz is 8,000 ohm-m. This cutoff eliminates the erratic higher resistivities that would result from unstable ratios of very small EM amplitudes.

In general, the resistivity patterns show moderately good agreement with the magnetic trends. This suggests that many of the resistivity lows and highs are probably related to bedrock features, rather than culture or conductive overburden, although the broad, moderately conductive zones in Harrison Lake and four other smaller lakes, have been primarily attributed to conductive lake-bottom material. However, there are at least nine interesting resistivity lows in the land portion that are probably due to bedrock conductors. Although most of the resistivity lows appear to be associated with relatively non-magnetic rock units, approximately 25% of the EM anomalies yield direct magnetic correlation. Pyrrhotite is considered to be a contributing factor.

## **Electromagnetic Anomalies**

The EM anomalies resulting from this survey appear to fall within one of three general categories. The first type consists of discrete, well-defined anomalies that yield marked inflections on the difference channels. These anomalies are usually attributed to conductive sulphides or graphite and are generally given a "B", "T" or "D" interpretive symbol, denoting a bedrock source. Strong responses also occur over powerlines and other cultural objects. These anomalies are defined by 'L' or 'L?' symbols, denoting probable line sources.

The second class of anomalies comprises moderately broad responses which exhibit the characteristics of a half-space and do not yield well-defined inflections on the difference channels. Anomalies in this category are usually given an "S" or "H" interpretive symbol. The lack of a difference channel response usually implies a broad or flat-lying conductive source such as overburden. Some of these anomalies could reflect conductive rock units, zones of deep weathering, or alteration zones, all of which can often yield "non-discrete" signatures.

The effects of conductive overburden are evident in a few portions of the survey block, particularly in the water-covered areas. Although the difference channels (DIFI and DIFQ) are extremely valuable in detecting bedrock conductors which are partially masked by conductive overburden, sharp undulations in the bedrock/overburden interface can yield anomalies in the difference channels which may be interpreted as possible bedrock

conductors. Such anomalies usually fall into the "S?" or "B?" classification but may also be given an "E" interpretive symbol, denoting a resistivity contrast at the edge of a conductive unit.

The "?" symbol does not question the validity of an anomaly, but instead indicates some degree of uncertainty as to which is the most appropriate EM source model. This ambiguity results from the combination of effects from two or more conductive sources, such as overburden and bedrock, gradational changes, or moderately shallow dips. The presence of a conductive upper layer has a tendency to mask or alter the characteristics of bedrock conductors, making interpretation difficult. This problem is further exacerbated in the presence of magnetite.

The third anomaly category includes responses that are associated with magnetite. Magnetite can cause suppression or polarity reversals of the in-phase components, particularly at the lower frequencies in resistive areas. The effects of magnetite-rich rock units are evident on a few of the multi-parameter geophysical data profiles, as negative excursions of the 900 Hz in-phase channels.

In areas where EM responses are evident primarily on the quadrature components, zones of poor conductivity are indicated. Where these responses are coincident with magnetic anomalies, it is possible that the in-phase component amplitudes have been suppressed by the effects of magnetite. Most of these poorly conductive magnetic features give rise to resistivity anomalies that are only slightly above or slightly below background. If it is

expected that poorly conductive economic mineralization may be associated with magnetite-rich units, some of these weakly anomalous features will also be of interest. In areas where magnetite causes the in-phase components to become negative, the apparent conductance and depth of EM anomalies will be unreliable. Magnetite effects usually give rise to overstated (higher) resistivity values and understated (shallow) depth calculations.

As economic mineralization within the area may be associated with weakly disseminated sulphides, which may or may not be hosted by magnetite-rich rocks, it is impractical to assess the relative merits of EM anomalies on the basis of conductance. It is recommended that an attempt be made to compile a suite of geophysical "signatures" over any known areas of interest. Anomaly characteristics are clearly defined on the multi-parameter geophysical data profiles that are supplied as one of the survey products.

A complete assessment and evaluation of the survey data should be carried out by one or more qualified professionals who have access to, and can provide a meaningful compilation of, all available geophysical, geological and geochemical data.

## **Conductors in the Survey Area**

The electromagnetic anomaly map shows the anomaly locations with the interpreted conductor type, dip, conductance and depth being indicated by symbols. Direct magnetic correlation is also shown if it exists. The strike direction and length of the conductors are indicated only where anomalies can be correlated from line to line with a reasonable degree of confidence.

Approximately 226 of the 370 anomalous responses detected by the survey have been attributed to possible or probable bedrock conductors. Most of these comprise moderately strong responses. Although there are several thin, discrete sources, many of the anomalous zones are quite broad, or flat-dipping. In many areas, these broad zones are more conductive at depth, often being covered by a more resistive near-surface layer. One of these highly conductive zones is evident in the southwestern corner of the property, where anomaly 10320C indicates a resistivity of less than 1 ohm-m, at a depth of 40m. Although geothermal sources can yield very low resistivities, values of less than 1 ohm-m are normally attributed to salt water, graphite, or massive conductive sulphides.

There are other resistivity lows in the area, in addition to several S- or H-type responses that are coincident with magnetic highs. Some of these may also be of interest, as they could reflect broad, weakly mineralized zones near surface. Other anomalies appear to be coincident with magnetite-rich rock units, although the magnetite content tends to preclude

the development of an associated resistivity low. Some of these weakly-conductive, magnetite-rich zones could be indicative of skarn type mineralization.

In the search for vein-type or shear-hosted gold, even the weaker, poorly-defined responses are considered to be potential targets. Quartz veins often yield resistivities that are higher than the surrounding host rocks. If these veins are wide enough, they can show as resistive trends, particularly at the higher frequencies.



## 5. CONCLUSIONS AND RECOMMENDATIONS

This report provides a very brief description of the survey results and describes the equipment, procedures and logistics of the survey.

There are several moderately strong anomalies in the survey block which are typical of sulphide responses. The survey was also successful in locating numerous weak or broad conductors which may also warrant additional work. It is possible that any valid conductors that are located within 250m of the major powerlines, might have escaped detection due to the strong 60Hz interference that saturated the highly sensitive EM equipment on some lines.

The various maps included with this report display the magnetic, radiometric and conductive properties of the survey area. It is recommended that the survey results be reviewed in detail, in conjunction with all available geophysical, geological and geochemical information. Particular reference should be made to the multi-parameter geophysical data profiles which clearly define the characteristics of the individual anomalies.

Most anomalies in the area are moderately broad and well-defined. Some have been attributed to buried conductive layers or deep weathering, although a few appear to be associated with magnetite-rich rock units. Others coincide with magnetic gradients which

may reflect contacts, faults or shears. Such structural breaks are considered to be of particular interest as they may have influenced mineral deposition within the survey area.

The interpreted bedrock conductors defined by the survey should be subjected to further investigation, using appropriate surface exploration techniques. Anomalies which are currently considered to be of moderately low priority may require upgrading if follow-up results are favourable.

It is also recommended that image processing of existing geophysical data be considered, in order to extract the maximum amount of information from the survey results. Current software and imaging techniques often provide valuable information on structure and lithology, which may not be clearly evident on the contour and colour maps. These techniques can yield images which define subtle, but significant, structural details.

Respectfully submitted,

**FUGRO AIRBORNE SURVEYS CORP.**

A handwritten signature in black ink, appearing to read "Paul A. Smith". The signature is stylized and cursive, with a large initial "P" and "S".

Paul A. Smith  
Geophysicist

PAS/sdp

2066A

## APPENDIX A

### LIST OF PERSONNEL

The following personnel were involved in the acquisition, processing, interpretation and presentation of data, relating to a DIGHEM<sup>V</sup> airborne geophysical survey carried out for Toklat Resources Inc. in the Harrison Lake area, BC.

Dave Miles	Manager, Helicopter Operations
Troy Will	Supervisor, Helicopter Operations
Darcy Blouin	Geophysical Operator
César Perez	Field Geophysicist
Al Sweet	Pilot (Provincial Helicopters Ltd.)
Gordon Smith	Data Processing Supervisor
Dak Darbha	Geophysicist/Data Processor
Doug Robinson	Geophysicist/Data Processor
Paul A. Smith	Interpretation Geophysicist
Lyn Vanderstarren	Drafting Supervisor
Susan Pothiah	Word Processing Operator
Albina Tonello	Secretary/Expeditor

The survey consisted of 215 km of coverage, flown on October 15, 2001.

All personnel are employees of Fugro Airborne Surveys, except for the pilot who is an employee of Quesstral Helicopters Ltd.

**APPENDIX B**

**STATEMENT OF COST**

Date: October 18, 2001

**IN ACCOUNT WITH FUGRO AIRBORNE SURVEYS**

To: Fugro flying of agreement dated July 16<sup>th</sup>, 2001, pertaining to an Airborne Geophysical Survey in the Harrison Lake area, British Columbia

Survey Charges

215 line-km of flying	\$54,000.00
-----------------------	-------------

Allocation of Costs

-Data Acquisition	(80%)
-Data Processing	(10%)
-Interpretation, Report and Maps	(10%)

## BACKGROUND INFORMATION

### Electromagnetics

DIGHEM electromagnetic responses fall into two general classes, discrete and broad. The discrete class consists of sharp, well-defined anomalies from discrete conductors such as sulphide lenses and steeply dipping sheets of graphite and sulphides. The broad class consists of wide anomalies from conductors having a large horizontal surface such as flatly dipping graphite or sulphide sheets, saline water-saturated sedimentary formations, conductive overburden and rock, and geothermal zones. A vertical conductive slab with a width of 200 m would straddle these two classes.

The vertical sheet (half plane) is the most common model used for the analysis of discrete conductors. All anomalies plotted on the geophysical maps are analyzed according to this model. The following section entitled **Discrete Conductor Analysis** describes this model in detail, including the effect of using it on anomalies caused by broad conductors such as conductive overburden.

The conductive earth (half-space) model is suitable for broad conductors. Resistivity contour maps result from the use of this model. A later section entitled **Resistivity Mapping** describes the method further, including the effect of using it on anomalies caused by discrete conductors such as sulphide bodies.

## **Geometric Interpretation**

The geophysical interpreter attempts to determine the geometric shape and dip of the conductor. Figure C-1 shows typical DIGHEM anomaly shapes which are used to guide the geometric interpretation.

## **Discrete Conductor Analysis**

The EM anomalies appearing on the electromagnetic map are analyzed by computer to give the conductance (i.e., conductivity-thickness product) in siemens (mhos) of a vertical sheet model. This is done regardless of the interpreted geometric shape of the conductor.

This is not an unreasonable procedure, because the computed conductance increases as the electrical quality of the conductor increases, regardless of its true shape. DIGHEM anomalies are divided into seven grades of conductance, as shown in Table C-1. The conductance in siemens (mhos) is the reciprocal of resistance in ohms.

The conductance value is a geological parameter because it is a characteristic of the conductor alone. It generally is independent of frequency, flying height or depth of burial, apart from the averaging over a greater portion of the conductor as height increases.

Small anomalies from deeply buried strong conductors are not confused with small anomalies from shallow weak conductors because the former will have larger conductance values.

**Table C-1. EM Anomaly Grades**

Anomaly Grade	Siemens
7	> 100
6	50 - 100
5	20 - 50
4	10 - 20
3	5 - 10
2	1 - 5
1	< 1

Conductive overburden generally produces broad EM responses which may not be shown as anomalies on the geophysical maps. However, patchy conductive overburden in otherwise resistive areas can yield discrete anomalies with a conductance grade (cf. Table C-1) of 1, 2 or even 3 for conducting clays which have resistivities as low as 50 ohm-m. In areas where ground resistivities are below 10 ohm-m, anomalies caused by weathering variations and similar causes can have any conductance grade. The anomaly shapes from the multiple coils often allow such conductors to be recognized, and these are indicated by the letters S, H, and sometimes E on the geophysical maps (see EM legend on maps).

For bedrock conductors, the higher anomaly grades indicate increasingly higher conductances. Examples: DIGHEM's New Inasco copper discovery (Noranda, Canada) yielded a grade 5 anomaly, as did the neighbouring copper-zinc Magusi River ore body; Mattabi (copper-zinc, Sturgeon Lake, Canada) and Whistle (nickel, Sudbury, Canada) gave grade 6; and DIGHEM's Montcalm nickel-copper discovery (Timmins, Canada) yielded a grade 7 anomaly. Graphite and sulphides can span all grades but, in any

- Appendix C.4 -

*particular survey area, field work may show that the different grades indicate different types of conductors.*

Strong conductors (i.e., grades 6 and 7) are characteristic of massive sulphides or graphite. Moderate conductors (grades 4 and 5) typically reflect graphite or sulphides of a less massive character, while weak bedrock conductors (grades 1 to 3) can signify poorly connected graphite or heavily disseminated sulphides. Grades 1 and 2 conductors may not respond to ground EM equipment using frequencies less than 2000 Hz.

The presence of sphalerite or gangue can result in ore deposits having weak to moderate conductances. As an example, the three million ton lead-zinc deposit of Restigouche Mining Corporation near Bathurst, Canada, yielded a well-defined grade 2 conductor. The 10 percent by volume of sphalerite occurs as a coating around the fine grained massive pyrite, thereby inhibiting electrical conduction. Faults, fractures and shear zones may produce anomalies which typically have low conductances (e.g., grades 1 to 3). Conductive rock formations can yield anomalies of any conductance grade. The conductive materials in such rock formations can be salt water, weathered products such as clays, original depositional clays, and carbonaceous material.

For each interpreted electromagnetic anomaly on the geophysical maps, a letter identifier and an interpretive symbol are plotted beside the EM grade symbol. The horizontal rows of dots, under the interpretive symbol, indicate the anomaly amplitude on the flight record. The vertical column of dots, under the anomaly letter, gives the estimated depth. In areas



- Appendix C.5 -

where anomalies are crowded, the letter identifiers, interpretive symbols and dots may be obliterated. The EM grade symbols, however, will always be discernible, and the obliterated information can be obtained from the anomaly listing appended to this report.

The purpose of indicating the anomaly amplitude by dots is to provide an estimate of the reliability of the conductance calculation. Thus, a conductance value obtained from a large ppm anomaly (3 or 4 dots) will tend to be accurate whereas one obtained from a small ppm anomaly (no dots) could be quite inaccurate. The absence of amplitude dots indicates that the anomaly from the coaxial coil-pair is 5 ppm or less on both the in-phase and quadrature channels. Such small anomalies could reflect a weak conductor at the surface or a stronger conductor at depth. The conductance grade and depth estimate illustrates which of these possibilities fits the recorded data best.

The conductance measurement is considered more reliable than the depth estimate. There are a number of factors which can produce an error in the depth estimate, including the averaging of topographic variations by the altimeter, overlying conductive overburden, and the location and attitude of the conductor relative to the flight line. Conductor location and attitude can provide an erroneous depth estimate because the stronger part of the conductor may be deeper or to one side of the flight line, or because it has a shallow dip. A heavy tree cover can also produce errors in depth estimates. This is because the depth estimate is computed as the distance of bird from conductor, minus the altimeter reading. The altimeter can lock onto the top of a dense forest canopy. This situation yields an erroneously large depth estimate but does not affect the conductance estimate.

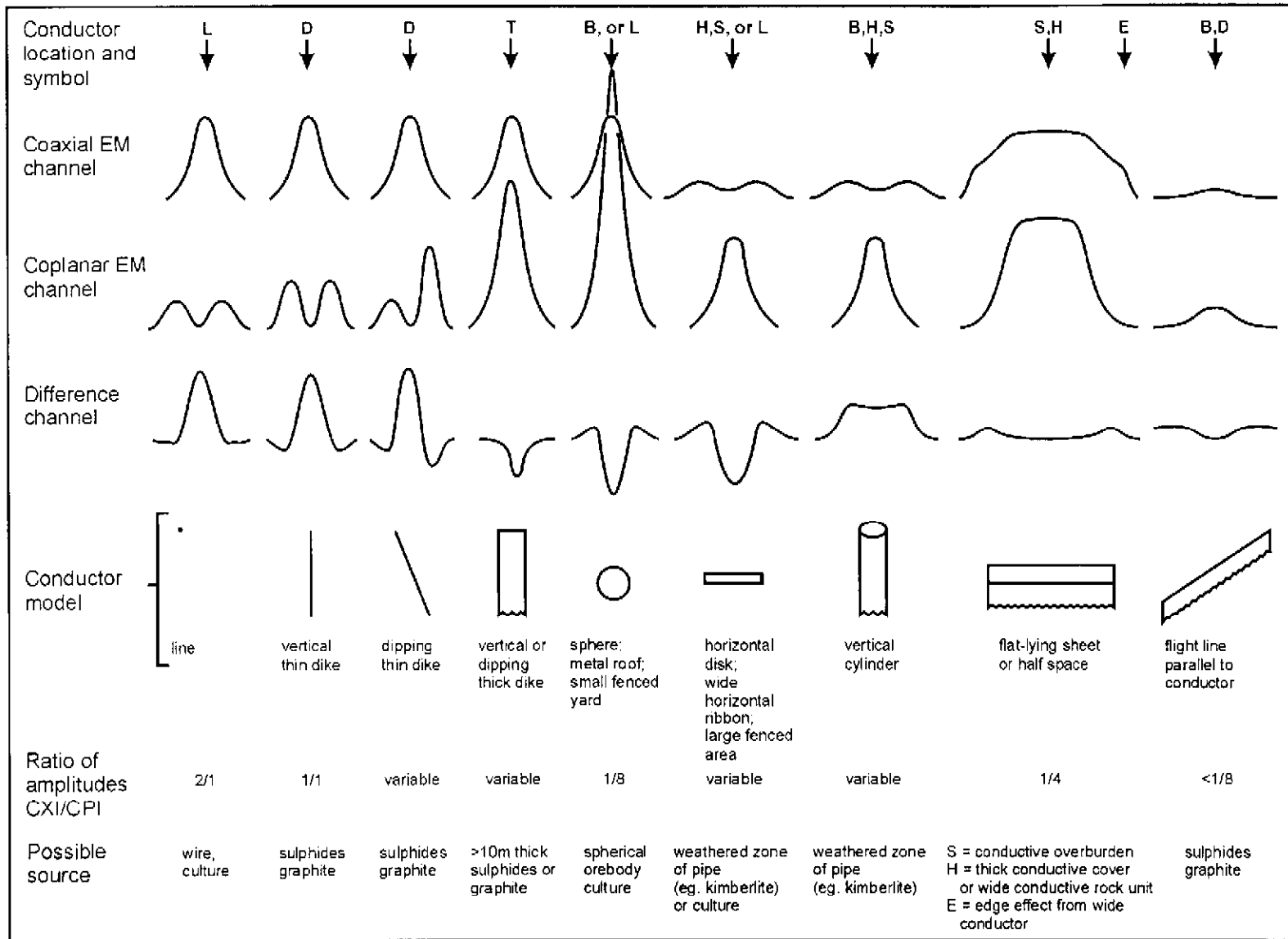
- Appendix C.6 -

Dip symbols are used to indicate the direction of dip of conductors. These symbols are used only when the anomaly shapes are unambiguous, which usually requires a fairly resistive environment.

A further interpretation is presented on the EM map by means of the line-to-line correlation of bedrock anomalies, which is based on a comparison of anomaly shapes on adjacent lines. This provides conductor axes which may define the geological structure over portions of the survey area. The absence of conductor axes in an area implies that anomalies could not be correlated from line to line with reasonable confidence.

DIGHEM electromagnetic anomalies are designed to provide a correct impression of conductor quality by means of the conductance grade symbols. The symbols can stand alone with geology when planning a follow-up program. The actual conductance values are printed in the attached anomaly list for those who wish quantitative data. The anomaly ppm and depth are indicated by inconspicuous dots which should not distract from the conductor patterns, while being helpful to those who wish this information. The map provides an interpretation of conductors in terms of length, strike and dip, geometric shape, conductance, depth, and thickness. The accuracy is comparable to an interpretation from a high quality ground EM survey having the same line spacing.

- Appendix C.7 -



**Typical DIGHEM anomaly shapes**  
**Figure C-1**

- Appendix C.8 -

The attached EM anomaly list provides a tabulation of anomalies in ppm, conductance, and depth for the vertical sheet model. The EM anomaly list also shows the conductance and depth for a thin horizontal sheet (whole plane) model, but only the vertical sheet parameters appear on the EM map. The horizontal sheet model is suitable for a flatly dipping thin bedrock conductor such as a sulphide sheet having a thickness less than 10 m. The list also shows the resistivity and depth for a conductive earth (half-space) model, which is suitable for thicker slabs such as thick conductive overburden. In the EM anomaly list, a depth value of zero for the conductive earth model, in an area of thick cover, warns that the anomaly may be caused by conductive overburden.

Since discrete bodies normally are the targets of EM surveys, local base (or zero) levels are used to compute local anomaly amplitudes. This contrasts with the use of true zero levels which are used to compute true EM amplitudes. Local anomaly amplitudes are shown in the EM anomaly list and these are used to compute the vertical sheet parameters of conductance and depth. Not shown in the EM anomaly list are the true amplitudes which are used to compute the horizontal sheet and conductive earth parameters.

### **Questionable Anomalies**

DIGHEM maps may contain EM responses which are displayed as asterisks (\*). These responses denote weak anomalies of indeterminate conductance, which may reflect one of the following: a weak conductor near the surface, a strong conductor at depth (e.g.,

## - Appendix C.9 -

100 to 120 m below surface) or to one side of the flight line, or aerodynamic noise. Those responses which have the appearance of valid bedrock anomalies on the flight profiles are indicated by appropriate interpretive symbols (see EM legend on maps). The others probably do not warrant further investigation unless their locations are of considerable geological interest.

### **The Thickness Parameter**

DIGHEM can provide an indication of the thickness of a steeply dipping conductor. The amplitude of the coplanar anomaly (e.g., CPI channel on the digital profile) increases relative to the coaxial anomaly (e.g., CXI) as the apparent thickness increases, i.e., the thickness in the horizontal plane. (The thickness is equal to the conductor width if the conductor dips at 90 degrees and strikes at right angles to the flight line.) This report refers to a conductor as thin when the thickness is likely to be less than 3 m, and thick when in excess of 10 m. Thick conductors are indicated on the EM map by parentheses "( )". For base metal exploration in steeply dipping geology, thick conductors can be high priority targets because many massive sulphide ore bodies are thick, whereas non-economic bedrock conductors are often thin. The system cannot sense the thickness when the strike of the conductor is subparallel to the flight line, when the conductor has a shallow dip, when the anomaly amplitudes are small, or when the resistivity of the environment is below 100 ohm-m.

## **Resistivity Mapping**

Resistivity mapping is useful in areas where broad or flat lying conductive units are of interest. One example of this is the clay alteration which is associated with Carlin-type deposits in the south west United States. The Dighem system was able to identify the clay alteration zone over the Cove deposit. The alteration zone appeared as a strong resistivity low on the 900 Hz resistivity parameter. The 7,200 Hz and 56,000 Hz resistivities show more of the detail in the covering sediments, and delineate a range front fault. This is typical in many areas of the south west United States, where conductive near surface sediments, which may sometimes be alkalic, attenuate the higher frequencies.

Resistivity mapping has proven successful for locating diatremes in diamond exploration. Weathering products from relatively soft kimberlite pipes produce a resistivity contrast with the unaltered host rock. In many cases weathered kimberlite pipes were associated with thick conductive layers which contrasted with overlying or adjacent relatively thin layers of lake bottom sediments or overburden.

Areas of widespread conductivity are commonly encountered during surveys. These conductive zones may reflect alteration zones, shallow-dipping sulphide or graphite-rich units or conductive overburden. In such areas, anomalies can be generated by decreases of only 5 m in survey altitude as well as by increases in conductivity. The typical flight record in conductive areas is characterized by in-phase and quadrature channels which are continuously active. Local EM peaks reflect either increases in conductivity of the

- Appendix C.11 -

earth or decreases in survey altitude. For such conductive areas, apparent resistivity profiles and contour maps are necessary for the correct interpretation of the airborne data. The advantage of the resistivity parameter is that anomalies caused by altitude changes are virtually eliminated, so the resistivity data reflect only those anomalies caused by conductivity changes. The resistivity analysis also helps the interpreter to differentiate between conductive bedrock and conductive overburden. For example, discrete conductors will generally appear as narrow lows on the contour map and broad conductors (e.g., overburden) will appear as wide lows.

The apparent resistivity is calculated using the pseudo-layer (or buried) half-space model defined by Fraser (1978)<sup>6</sup>. This model consists of a resistive layer overlying a conductive half-space. The depth channels give the apparent depth below surface of the conductive material. The apparent depth is simply the apparent thickness of the overlying resistive layer. The apparent depth (or thickness) parameter will be positive when the upper layer is more resistive than the underlying material, in which case the apparent depth may be quite close to the true depth.

The apparent depth will be negative when the upper layer is more conductive than the underlying material, and will be zero when a homogeneous half-space exists. The apparent depth parameter must be interpreted cautiously because it will contain any errors which may exist in the measured altitude of the EM bird (e.g., as caused by a dense tree

---

- Appendix C.12 -

cover). The inputs to the resistivity algorithm are the in-phase and quadrature components of the coplanar coil-pair. The outputs are the apparent resistivity of the conductive half-space (the source) and the sensor-source distance. The flying height is not an input variable, and the output resistivity and sensor-source distance are independent of the flying height when the conductivity of the measured material is sufficient to yield significant in-phase as well as quadrature responses. The apparent depth, discussed above, is simply the sensor-source distance minus the measured altitude or flying height. Consequently, errors in the measured altitude will affect the apparent depth parameter but not the apparent resistivity parameter.

The apparent depth parameter is a useful indicator of simple layering in areas lacking a heavy tree cover. The DIGHEM system has been flown for purposes of permafrost mapping, where positive apparent depths were used as a measure of permafrost thickness. However, little quantitative use has been made of negative apparent depths because the absolute value of the negative depth is not a measure of the thickness of the conductive upper layer and, therefore, is not meaningful physically. Qualitatively, a negative apparent depth estimate usually shows that the EM anomaly is caused by conductive overburden. Consequently, the apparent depth channel can be of significant help in distinguishing between overburden and bedrock conductors.



## Interpretation in Conductive Environments

Environments having low background resistivities (e.g., below 30 ohm-m for a 900 Hz system) yield very large responses from the conductive ground. This usually prohibits the recognition of discrete bedrock conductors. However, DIGHEM data processing techniques produce three parameters which contribute significantly to the recognition of bedrock conductors in conductive environments. These are the in-phase and quadrature difference channels (DIFI and DIFQ, which are available only on systems with common frequencies on orthogonal coil pairs), and the resistivity and depth channels (RES and DP) for each coplanar frequency.

The EM difference channels (DIFI and DIFQ) eliminate most of the responses from conductive ground, leaving responses from bedrock conductors, cultural features (e.g., telephone lines, fences, etc.) and edge effects. Edge effects often occur near the perimeter of broad conductive zones. This can be a source of geologic noise. While edge effects yield anomalies on the EM difference channels, they do not produce resistivity anomalies. Consequently, the resistivity channel aids in eliminating anomalies due to edge effects. On the other hand, resistivity anomalies will coincide with the most highly conductive sections of conductive ground, and this is another source of geologic noise. The recognition of a bedrock conductor in a conductive environment therefore is based on the anomalous responses of the two difference channels (DIFI and DIFQ) and the resistivity channels (RES). The most favourable situation is where anomalies coincide on all channels.

The DP channels, which give the apparent depth to the conductive material, also help to determine whether a conductive response arises from surficial material or from a conductive zone in the bedrock. When these channels ride above the zero level on the digital profiles (i.e., depth is negative), it implies that the EM and resistivity profiles are responding primarily to a conductive upper layer, i.e., conductive overburden. If the DP channels are below the zero level, it indicates that a resistive upper layer exists, and this usually implies the existence of a bedrock conductor. If the low frequency DP channel is below the zero level and the high frequency DP is above, this suggests that a bedrock conductor occurs beneath conductive cover.

## **Reduction of Geologic Noise**

Geologic noise refers to unwanted geophysical responses. For purposes of airborne EM surveying, geologic noise refers to EM responses caused by conductive overburden and magnetic permeability. It was mentioned previously that the EM difference channels (i.e., channel DIFI for in-phase and DIFQ for quadrature) tend to eliminate the response of conductive overburden.

Magnetite produces a form of geological noise on the in-phase channels of all EM systems. Rocks containing less than 1% magnetite can yield negative in-phase anomalies caused by magnetic permeability. When magnetite is widely distributed throughout a survey area, the in-phase EM channels may continuously rise and fall, reflecting variations in the magnetite percentage, flying height, and overburden thickness. This can lead to

difficulties in recognizing deeply buried bedrock conductors, particularly if conductive overburden also exists. However, the response of broadly distributed magnetite generally vanishes on the in-phase difference channel DIFI. This feature can be a significant aid in the recognition of conductors which occur in rocks containing accessory magnetite.

## **EM Magnetite Mapping**

The information content of DIGHEM data consists of a combination of conductive eddy current responses and magnetic permeability responses. The secondary field resulting from conductive eddy current flow is frequency-dependent and consists of both in-phase and quadrature components, which are positive in sign. On the other hand, the secondary field resulting from magnetic permeability is independent of frequency and consists of only an in-phase component which is negative in sign. When magnetic permeability manifests itself by decreasing the measured amount of positive in-phase, its presence may be difficult to recognize. However, when it manifests itself by yielding a negative in-phase anomaly (e.g., in the absence of eddy current flow), its presence is assured. In this latter case, the negative component can be used to estimate the percent magnetite content.

A magnetite mapping technique was developed for the coplanar coil-pair of DIGHEM. The method can be complementary to magnetometer mapping in certain cases. Compared to magnetometry, it is far less sensitive but is more able to resolve closely spaced magnetite zones, as well as providing an estimate of the amount of magnetite in the rock. The method is sensitive to 1/4% magnetite by weight when the EM sensor is at a height of 30 m above a magnetic half-space. It can individually resolve steep dipping narrow

magnetite-rich bands which are separated by 60 m. Unlike magnetometry, the EM magnetite method is unaffected by remanent magnetism or magnetic latitude.

The EM magnetite mapping technique provides estimates of magnetite content which are usually correct within a factor of 2 when the magnetite is fairly uniformly distributed. EM magnetite maps can be generated when magnetic permeability is evident as negative in-phase responses on the data profiles.

Like magnetometry, the EM magnetite method maps only bedrock features, provided that the overburden is characterized by a general lack of magnetite. This contrasts with resistivity mapping which portrays the combined effect of bedrock and overburden.

## **Recognition of Culture**

Cultural responses include all EM anomalies caused by man-made metallic objects. Such anomalies may be caused by inductive coupling or current gathering. The concern of the interpreter is to recognize when an EM response is due to culture. Points of consideration used by the interpreter, when coaxial and coplanar coil-pairs are operated at a common frequency, are as follows:

1. Channels CXP and CPP monitor 60 Hz radiation. An anomaly on these channels shows that the conductor is radiating power. Such an indication is normally a guarantee that the conductor is cultural. However, care must be taken to ensure

- Appendix C.17 -

that the conductor is not a geologic body which strikes across a power line, carrying leakage currents.

2. A flight which crosses a "line" (e.g., fence, telephone line, etc.) yields a centre-peaked coaxial anomaly and an m-shaped coplanar anomaly.<sup>7</sup> When the flight crosses the cultural line at a high angle of intersection, the amplitude ratio of coaxial/coplanar response is 8. Such an EM anomaly can only be caused by a line. The geologic body which yields anomalies most closely resembling a line is the vertically dipping thin dike. Such a body, however, yields an amplitude ratio of 4 rather than 8. Consequently, an m-shaped coplanar anomaly with a CXI/CPI amplitude ratio of 8 is virtually a guarantee that the source is a cultural line.
3. A flight which crosses a sphere or horizontal disk yields centre-peaked coaxial and coplanar anomalies with a CXI/CPI amplitude ratio (i.e., coaxial/coplanar) of 1/8. In the absence of geologic bodies of this geometry, the most likely conductor is a metal roof or small fenced yard.<sup>8</sup> Anomalies of this type are virtually certain to be cultural if they occur in an area of culture.
4. A flight which crosses a horizontal rectangular body or wide ribbon yields an m-shaped coaxial anomaly and a centre-peaked coplanar anomaly. In the absence of geologic bodies of this geometry, the most likely conductor is a large fenced

---

<sup>7</sup> See Figure C-1 presented earlier.

<sup>8</sup> It is a characteristic of EM that geometrically similar anomalies are obtained from: (1) a planar conductor, and (2) a wire which forms a loop having dimensions identical to the perimeter of

area.<sup>5</sup> Anomalies of this type are virtually certain to be cultural if they occur in an area of culture.

5. EM anomalies which coincide with culture, as seen on the camera film or video display, are usually caused by culture. However, care is taken with such coincidences because a geologic conductor could occur beneath a fence, for example. In this example, the fence would be expected to yield an m-shaped coplanar anomaly as in case #2 above. If, instead, a centre-peaked coplanar anomaly occurred, there would be concern that a thick geologic conductor coincided with the cultural line.
  
6. The above description of anomaly shapes is valid when the culture is not conductively coupled to the environment. In this case, the anomalies arise from inductive coupling to the EM transmitter. However, when the environment is quite conductive (e.g., less than 100 ohm-m at 900 Hz), the cultural conductor may be conductively coupled to the environment. In this latter case, the anomaly shapes tend to be governed by current gathering. Current gathering can completely distort the anomaly shapes, thereby complicating the identification of cultural anomalies. In such circumstances, the interpreter can only rely on the radiation channels and on the camera film or video records.

## **Magnetics**

Total field magnetics provides information on the magnetic properties of the earth materials in the survey area. The information can be used to locate magnetic bodies of *direct interest for exploration, and for structural and lithological mapping.*

The total field magnetic response reflects the abundance of magnetic material, in the source. Magnetite is the most common magnetic mineral. Other minerals such as ilmenite, pyrrhotite, franklinite, chromite, hematite, arsenopyrite, limonite and pyrite are also magnetic, but to a lesser extent than magnetite on average.

In some geological environments, an EM anomaly with magnetic correlation has a greater likelihood of being produced by sulphides than one which is non-magnetic. However, sulphide ore bodies may be non-magnetic (e.g., the Kidd Creek deposit near Timmins, Canada) as well as magnetic (e.g., the Mattabi deposit near Sturgeon Lake, Canada).

Iron ore deposits will be anomalously magnetic in comparison to surrounding rock due to the concentration of iron minerals such as magnetite, ilmenite and hematite.

Changes in magnetic susceptibility often allow rock units to be differentiated based on the total field magnetic response. Geophysical classifications may differ from geological classifications if various magnetite levels exist within one general geological classification.

- Appendix C.20 -

Geometric considerations of the source such as shape, dip and depth, inclination of the earth's field and remanent magnetization will complicate such an analysis.

In general, mafic lithologies contain more magnetite and are therefore more magnetic than many sediments which tend to be weakly magnetic. Metamorphism and alteration can also increase or decrease the magnetization of a rock unit.

Textural differences on a total field magnetic contour, colour or shadow map due to the frequency of activity of the magnetic parameter resulting from inhomogeneities in the distribution of magnetite within the rock, may define certain lithologies. For example, near surface volcanics may display highly complex contour patterns with little line-to-line correlation.

Rock units may be differentiated based on the plan shapes of their total field magnetic responses. Mafic intrusive plugs can appear as isolated "bulls-eye" anomalies. Granitic intrusives appear as sub-circular zones, and may have contrasting rings due to contact metamorphism. Generally, granitic terrain will lack a pronounced strike direction, although granite gneiss may display strike.

Linear north-south units are theoretically not well-defined on total field magnetic maps in equatorial regions due to the low inclination of the earth's magnetic field. However, most stratigraphic units will have variations in composition along strike which will cause the units to appear as a series of alternating magnetic highs and lows.



Faults and shear zones may be characterized by alteration which causes destruction of magnetite (e.g., weathering) which produces a contrast with surrounding rock. Structural breaks may be filled by magnetite-rich, fracture filling material as is the case with diabase dikes, or by non-magnetic felsic material.

Faulting can also be identified by patterns in the magnetic total field contours or colours. Faults and dikes tend to appear as lineaments and often have strike lengths of several kilometres. Offsets in narrow, magnetic, stratigraphic trends also delineate structure. Sharp contrasts in magnetic lithologies may arise due to large displacements along strike-slip or dip-slip faults.

## **Radiometrics**

Radioelement concentrations are measures of the abundance of radioactive elements in the rock. The original abundance of the radioelements in any rock can be altered by the subsequent processes of metamorphism and weathering.

Gamma radiation in the range which is measured in the thorium, potassium, uranium and total count windows is strongly attenuated by rock, overburden and water. Almost all of the total radiation measured from rock and overburden originates in the upper .5 metres. Moisture in soil and bodies of water will mask the radioactivity from underlying rock. Weathered rock materials which have been displaced by glacial, water or wind action will not reflect the general composition of the underlying bedrock. Where residual soils exist,

- Appendix C.22 -

they may reflect the composition of underlying rock except where equilibrium does not exist between the original radioelement and the products in its decay series.

Radioelement counts (expressed as counts per second) are the rates of detection of the gamma radiation from specific decaying particles corresponding to products in each radioelements decay series. The radiation source for uranium is bismuth (Bi-214), for thorium it is thallium (Tl-208) and for potassium it is potassium (K-40).

The uranium and thorium radioelement concentrations are dependent on a state of equilibrium between the parent and daughter products in the decay series. Some daughter products in the uranium decay are long lived and could be removed by processes such as leaching. One product in the series, radon (Rn-222), is a gas which can easily escape. Both of these factors can affect the degree to which the calculated uranium concentrations reflect the actual composition of the source rock. Because the daughter products of thorium are relatively short lived, there is more likelihood that the thorium decay series is in equilibrium.

Lithological discrimination can be based on the measured relative concentrations and total, combined, radioactivity of the radioelements. Feldspar and mica contain potassium. Zircon, sphene and apatite are accessory minerals in igneous rocks which are sources of uranium and thorium. Monazite, thorianite, thorite, uraninite and uranothorite are also sources of uranium and thorium which are found in granites and pegmatites.

- Appendix C.23 -

In general, the abundance of uranium, thorium and potassium in igneous rock increases with acidity. Pegmatites commonly have elevated concentrations of uranium relative to thorium. Sedimentary rocks derived from igneous rocks may have characteristic signatures which are influenced by their parent rocks, but these will have been altered by subsequent weathering and alteration.

Metamorphism and alteration will cause variations in the abundance of certain radioelements relative to each other. For example, alterative processes may cause uranium enrichment to the extent that a rock will be of economic interest. Uranium anomalies are more likely to be economically significant if they consist of an increase in the uranium relative to thorium and potassium, rather than a sympathetic increase in all three radioelements.

Faults can exhibit radioactive highs due to increased permeability which allows radon migration, or as lows due to structural control of drainage and fluvial sediments which attenuate gamma radiation from the underlying rocks. Faults can also be recognized by sharp contrasts in radiometric lithologies due to large strike-slip or dip-slip displacements. Changes in relative radioelement concentrations due to alteration will also define faults.

Similar to magnetics, certain rock types can be identified by their plan shapes if they also produce a radiometric contrast with surrounding rock. For example, granite intrusions will appear as sub-circular bodies, and may display concentric zonations. They will tend to lack a prominent strike direction. Offsets of narrow, continuous, stratigraphic units with

- Appendix C.24 -

contrasting radiometric signatures can identify faulting, and folding of stratigraphic trends will also be apparent.

---

**APPENDIX D**

**EM ANOMALY LIST**

---

## EM Anomaly List

Label Fid	Interp	XUTM (m.) YUTM (m.)	CX 5500HZ Real (ppm)	CX 5500HZ Quad (ppm)	CP 7200HZ Real (ppm)	CP 7200HZ Quad (ppm)	CP 900HZ Real (ppm)	CP 900HZ Quad (ppm)	Cond. (siemens)	DIKE DEPTH (m)	Mag. Corr (nT)
<b>LINE 10010 FLIGHT 5</b>											
A 1161.1	L?	591235 , 5466377	19.1	1.4	73.3	9.0	54.4	27.2	---	---	0
B 1137.4	S	591664 , 5466888	17.6	30.3	184.6	348.5	19.2	72.9	0.9	4	0
<b>LINE 10020 FLIGHT 5</b>											
A 1052.6	D	591298 , 5466277	12.7	5.7	119.7	11.1	98.6	48.7	3.9	36	0
B 1069.2	B?	591554 , 5466582	3.3	4.3	22.3	30.5	1.2	7.6	---	---	13
C 1077.6	S?	591718 , 5466804	29.3	40.5	278.8	385.3	16.9	105.4	1.3	0	0
<b>LINE 10030 FLIGHT 5</b>											
A 934.8	B?	591352 , 5466235	20.3	4.4	100.1	21.7	70.9	37.7	12.9	15	0
B 919.4	B?	591545 , 5466421	6.9	7.8	1.9	30.3	9.4	0.5	1.0	27	0
C 910.2	D	591691 , 5466588	12.5	18.6	70.1	99.1	5.1	28.2	0.9	0	73
D 908.2	S	591727 , 5466633	6.5	11.3	70.1	99.1	5.1	28.2	0.6	1	73
<b>LINE 10040 FLIGHT 5</b>											
A 796.0	B	591444 , 5466134	8.1	2.4	49.3	20.7	43.9	28.5	---	---	0
B 806.9	D	591530 , 5466269	10.3	10.4	83.9	26.3	52.3	35.3	1.3	28	0
C 820.2	B?	591690 , 5466464	7.3	5.1	55.3	35.5	10.4	21.8	---	---	0
D 827.4	S?	591821 , 5466620	18.9	55.4	119.7	319.0	8.7	54.7	0.6	0	0
<b>LINE 10050 FLIGHT 5</b>											
A 694.9	H	590603 , 5464995	8.0	15.9	160.1	207.1	119.5	152.2	0.6	13	0
B 658.5	H	591304 , 5465665	10.6	6.9	85.9	47.1	36.0	38.0	2.3	10	0
C 641.0	B?	591525 , 5466069	11.9	3.6	40.1	20.5	18.8	17.8	6.6	1	0
D 610.3	D	592094 , 5466773	8.9	4.7	64.4	37.8	25.8	37.6	2.7	34	37
<b>LINE 10060 FLIGHT 5</b>											
A 428.0	H	590655 , 5464931	28.8	21.2	88.2	154.8	18.7	151.2	2.7	9	0
B 442.8	L	590831 , 5465086	14.3	9.6	110.1	92.2	205.8	209.1	2.4	18	0
C 474.5	H	591329 , 5465685	35.1	18.6	131.1	74.2	51.4	70.8	4.4	0	0
D 492.3	H	591685 , 5466095	5.1	4.9	35.2	34.4	16.7	14.9	---	---	0
E 524.1	D	592251 , 5466800	23.0	16.2	91.5	65.1	34.6	40.3	2.7	19	0
Harrison Lake		CX=COAXIAL CP=COPLANAR	Note: EM values shown above are local amplitudes			*Estimated depth may be unreliable because the stronger part of the conductor may be deeper or to one side of the flight line, or because of a shallow dip or magnetite/overburden effects.					

## EM Anomaly List

Label Fid	Interp	XUTM (m.) YUTM (m.)	CX 5500HZ Real (ppm)	CX 5500HZ Quad (ppm)	CP 7200HZ Real (ppm)	CP 7200HZ Quad (ppm)	CP 900HZ Real (ppm)	CP 900HZ Quad (ppm)	Cond. (siemens)	DIKE DEPTH (m)	Mag. Corr (nT)
F 540.6	D	592475 , 5467066	19.1	14.0	70.9	53.7	34.8	34.7	2.4	11	65
<b>LINE 10070 FLIGHT 4</b>											
A 6241.0	H	590608 , 5464715	32.1	27.0	197.9	139.7	41.2	84.3	2.4	4	0
B 6257.0	L	590770 , 5465024	7.9	7.1	3.1	0.0	15.3	2.5	1.4	24	0
C 6298.9	D	591287 , 5465477	44.5	19.8	202.0	82.6	96.5	90.4	6.0	10	0
D 6302.1	B?	591327 , 5465526	24.1	19.8	202.0	82.6	96.5	90.4	---	---	0
E 6310.4	B?	591416 , 5465636	19.2	3.6	141.7	34.0	95.1	61.9	15.5	22	0
F 6365.8	B	592245 , 5466643	49.6	29.6	222.1	135.0	44.1	96.5	4.2	8	0
G 6378.3	B?	592438 , 5466886	6.2	7.2	61.9	89.8	0.5	26.1	1.0	34	173
H 6389.0	H	592543 , 5467013	9.0	18.6	15.0	38.8	30.5	17.2	0.6	1	0
<b>LINE 10080 FLIGHT 4</b>											
A 6209.3	H	590599 , 5464493	11.9	8.5	195.1	168.3	44.4	79.0	2.1	19	0
B 6168.4	B?	591212 , 5465199	19.3	10.5	123.4	49.2	49.0	54.2	3.5	7	0
C 6151.2	B?	591424 , 5465487	9.2	2.0	40.7	8.0	35.1	15.3	---	---	0
D 6134.0	D	591573 , 5465653	11.0	13.1	130.6	65.8	50.2	57.3	1.1	16	0
E 6092.1	B	592264 , 5466554	59.4	34.3	251.3	94.2	95.3	112.1	4.7	5	0
F 6086.0	E	592346 , 5466654	25.0	15.9	198.1	83.5	77.8	86.0	3.1	16	0
<b>LINE 10090 FLIGHT 4</b>											
A 5840.3	S	590621 , 5464317	25.4	39.4	363.7	392.1	56.9	62.6	1.1	1	0
B 5863.4	L	590935 , 5464650	7.8	3.6	107.5	35.9	87.3	75.4	3.3	23	0
C 5893.2	B	591268 , 5465104	21.8	6.7	142.8	60.4	76.2	73.0	8.0	25	0
D 5905.7	D	591436 , 5465304	33.6	12.1	131.8	64.4	66.6	54.2	7.3	10	22
E 5920.0	B?	591567 , 5465469	9.1	5.9	16.8	6.6	6.5	5.6	---	---	0
F 5927.3	D	591630 , 5465547	13.2	4.2	50.1	24.5	37.0	22.9	6.3	19	73
G 5938.8	B?	591707 , 5465673	9.0	10.0	41.2	24.8	12.3	20.4	1.1	13	0
H 5981.3	B	592350 , 5466466	22.9	5.9	131.0	94.1	59.0	63.2	10.3	29	0
I 5986.1	B?	592434 , 5466541	15.7	8.8	131.0	37.7	59.0	63.2	---	---	0
J 5993.6	H	592567 , 5466699	6.2	9.0	107.3	109.5	10.2	39.7	0.8	23	0
Harrison Lake		CX=COAXIAL CP=COPLANAR	Note: EM values shown above are local amplitudes			*Estimated depth may be unreliable because the stronger part of the conductor may be deeper or to one side of the flight line, or because of a shallow dip or magnetite/overburden effects.					

## EM Anomaly List

Label Fid	Interp	XUTM (m.) YUTM (m.)	CX 5500HZ Real (ppm)	CX 5500HZ Quad (ppm)	CP 7200HZ Real (ppm)	CP 7200HZ Quad (ppm)	CP 900HZ Real (ppm)	CP 900HZ Quad (ppm)	Cond. (siemens)	DIKE DEPTH (m)	Mag. Corr (nT)
<b>LINE 10100 FLIGHT 4</b>											
A 5678.1	S	590710 , 5464273	33.2	63.4	314.7	509.5	8.7	133.0	1.0	0	0
B 5667.1	L	590845 , 5464411	26.6	5.2	0.0	0.3	25.7	7.2	16.1	23	0
C 5655.9	L	590956 , 5464526	22.6	2.2	116.7	0.0	139.3	39.4	---	---	21
D 5619.9	B	591293 , 5465000	42.1	16.5	131.7	51.6	87.3	61.4	7.0	17	105
E 5612.0	B	591406 , 5465138	13.3	14.4	86.7	41.2	74.2	24.0	1.3	17	0
F 5600.7	B?	591547 , 5465310	10.1	1.9	9.6	4.1	4.7	1.7	---	---	0
G 5556.5	D	592231 , 5466157	10.8	10.9	52.1	45.0	11.3	24.1	1.4	22	0
H 5548.0	B	592377 , 5466343	40.3	25.1	173.0	72.8	60.9	85.4	3.7	8	76
I 5527.6	H	592683 , 5466718	8.8	6.3	53.4	51.3	12.1	18.1	1.9	33	0
<b>LINE 10110 FLIGHT 4</b>											
A 5254.6	S	590722 , 5464151	0.1	32.2	75.2	240.0	122.1	21.5	---	---	0
B 5264.0	L?	590854 , 5464323	39.2	15.8	33.3	51.6	133.0	91.6	6.5	9	0
C 5276.4	B	590970 , 5464459	20.6	1.0	155.3	22.9	140.4	58.7	---	---	30
D 5305.5	B	591258 , 5464783	36.8	13.1	120.8	58.0	55.9	55.4	7.6	13	0
E 5314.7	B	591383 , 5464932	80.6	19.6	399.9	92.6	293.9	153.2	---	---	0
F 5317.4	B	591418 , 5464973	77.4	18.2	399.9	92.6	293.9	153.2	17.7	5	41
G 5371.1	B	591924 , 5465640	35.2	24.0	124.0	97.7	18.8	47.4	3.2	5	0
H 5388.4	B	592130 , 5465885	10.8	9.7	41.1	37.1	6.5	19.0	1.5	24	0
I 5399.4	D	592275 , 5466065	27.1	29.0	83.6	83.7	20.3	35.8	1.7	13	0
J 5411.2	H	592415 , 5466234	18.1	9.9	70.2	34.9	15.6	27.6	3.4	34	131
K 5431.1	B	592717 , 5466573	48.8	31.0	189.2	92.7	46.0	84.0	3.9	7	23
L 5437.0	E	592773 , 5466655	23.2	22.4	156.6	89.3	33.1	69.1	1.8	12	20
<b>LINE 10120 FLIGHT 4</b>											
A 5206.8	S	590618 , 5463843	23.5	38.9	262.1	313.4	236.1	285.4	1.0	1	0
B 5189.1	L?	590949 , 5464221	32.4	12.5	128.2	65.7	137.1	140.0	6.5	15	37
C 5171.1	H	591164 , 5464496	9.2	3.1	2.7	9.6	0.8	0.8	5.1	39	0
D 5158.8	B	591298 , 5464675	46.4	11.7	98.9	27.4	49.3	44.6	13.4	8	36
Harrison Lake		CX=COAXIAL CP=COPLANAR	Note: EM values shown above are local amplitudes			*Estimated depth may be unreliable because the stronger part of the conductor may be deeper or to one side of the flight line, or because of a shallow dip or magnetite/overburden effects.					



## EM Anomaly List

Label Fid	Interp	XUTM (m.) YUTM (m.)	CX 5500HZ Real (ppm)	CX 5500HZ Quad (ppm)	CP 7200HZ Real (ppm)	CP 7200HZ Quad (ppm)	CP 900HZ Real (ppm)	CP 900HZ Quad (ppm)	Cond. (siemens)	DIKE DEPTH (m)	Mag. Corr (nT)
E 5147.9	B	591421 , 5464820	16.8	6.3	77.2	21.9	61.8	34.9	5.5	21	0
F 5139.2	E	591528 , 5464946	21.9	9.9	64.5	19.6	57.1	24.6	4.6	20	0
G 5096.8	B	591983 , 5465558	7.0	2.8	23.9	0.0	13.2	11.4	---	---	0
H 5081.4	II	592303 , 5465925	17.9	17.7	85.5	66.7	19.0	34.2	1.6	4	0
I 5055.3	H	592769 , 5466520	6.6	7.2	102.2	65.1	20.0	42.4	1.0	27	0
J 5052.9	D	592809 , 5466565	13.1	10.4	102.2	65.1	19.7	42.4	1.9	20	0
<b>LINE 10130 FLIGHT 4</b>											
A 4781.3	B	591379 , 5464612	47.6	14.9	189.9	60.3	122.4	83.3	10.0	14	214
B 4791.9	D	591496 , 5464767	51.0	14.1	141.2	48.0	106.6	56.2	12.2	10	0
C 4806.1	D	591672 , 5464991	40.8	24.1	143.7	65.7	59.4	67.6	4.0	3	0
D 4828.2	D	591872 , 5465208	11.6	8.2	9.7	9.8	10.3	1.3	2.1	24	0
E 4839.3	D	591931 , 5465295	22.2	10.3	39.8	28.1	11.2	17.5	4.5	3	0
F 4845.4	B?	591956 , 5465333	12.4	6.8	39.8	28.1	11.2	17.5	3.0	0	0
G 4868.5	H	592066 , 5465532	5.7	2.4	37.1	10.8	19.5	15.7	---	---	0
H 4907.8	E	592625 , 5466160	14.0	14.9	36.7	53.5	8.8	12.9	1.4	21	0
I 4944.7	B?	592979 , 5466595	3.1	0.4	15.9	6.4	13.2	7.0	---	---	0
<b>LINE 10140 FLIGHT 4</b>											
A 4597.1	B	591397 , 5464490	39.8	16.5	169.4	57.9	99.3	73.0	6.4	5	151
B 4593.3	B	591439 , 5464533	23.8	2.8	169.4	57.9	99.3	73.0	---	---	154
C 4583.7	D	591545 , 5464660	20.6	14.1	49.1	52.8	14.1	17.6	2.7	15	0
D 4566.7	B	591729 , 5464895	23.1	20.3	127.7	93.2	42.5	58.7	2.0	1	0
E 4560.8	E	591791 , 5464973	14.6	13.9	127.7	93.2	30.1	58.7	1.6	17	57
F 4523.9	D	592049 , 5465294	6.7	4.2	55.2	41.7	7.3	27.8	2.0	33	0
G 4512.4	H	592186 , 5465474	3.7	3.5	54.2	15.6	32.2	23.1	---	---	0
H 4494.1	H	592479 , 5465839	6.5	11.9	18.3	37.5	5.9	8.2	0.6	13	222
I 4485.3	B	592643 , 5466019	7.1	10.8	63.9	60.9	24.1	25.6	---	---	0
<b>LINE 10150 FLIGHT 4</b>											
A 3994.0	L?	590843 , 5463668	16.6	10.6	76.2	42.9	33.9	30.5	2.7	17	13
Harrison Lake		CX=COAXIAL CP=COPLANAR	Note: EM values shown above are local amplitudes			*Estimated depth may be unreliable because the stronger part of the conductor may be deeper or to one side of the flight line, or because of a shallow dip or magnetite/overburden effects.					

## EM Anomaly List

Label Fid	Interp	XUTM (m.) YUTM (m.)	CX 5500HZ Real (ppm)	CX 5500HZ Quad (ppm)	CP 7200HZ Real (ppm)	CP 7200HZ Quad (ppm)	CP 900HZ Real (ppm)	CP 900HZ Quad (ppm)	Cond. (siemens)	DIKE DEPTH (m)	Mag. Corr (nT)
B 4001.2	L?	590907 , 5463743	12.2	11.3	146.0	100.9	51.0	59.7	1.6	13	0
C 4029.7	D	591206 , 5464056	20.6	12.2	53.1	54.3	17.6	22.8	3.2	19	0
D 4053.8	B	591439 , 5464387	35.2	12.9	113.5	68.9	41.8	54.1	7.3	11	0
E 4075.2	B	591719 , 5464726	23.9	20.6	103.7	93.1	19.2	47.7	2.1	17	0
F 4130.0	H	592181 , 5465309	0.8	0.1	27.5	6.5	20.1	8.7	---	---	0
G 4138.4	H	592298 , 5465451	16.3	9.7	30.2	40.6	18.1	13.9	2.9	14	25
H 4148.0	B	592463 , 5465636	8.2	7.0	57.8	22.6	23.0	23.1	---	---	0
<b>LINE 10160 FLIGHT 4</b>											
A 3922.2	L?	590825 , 5463470	14.7	12.8	109.3	53.7	51.5	44.7	1.8	17	0
B 3862.7	D	591466 , 5464237	27.5	10.6	110.8	54.7	47.5	52.8	6.2	4	0
C 3857.8	B	591522 , 5464303	4.9	4.3	103.8	43.3	47.5	49.5	1.2	38	136
D 3836.6	B	591750 , 5464612	17.8	9.7	117.8	66.0	30.3	57.5	3.4	22	213
E 3781.8	D	592202 , 5465159	11.5	0.9	56.2	14.2	40.8	21.9	---	---	0
F 3779.0	B	592253 , 5465223	6.1	1.7	56.2	8.2	40.8	21.9	---	---	0
<b>LINE 10170 FLIGHT 4</b>											
A 3320.9	H	590787 , 5463268	19.9	8.4	28.4	22.2	52.8	4.3	4.9	22	0
B 3346.6	H	591073 , 5463606	12.7	8.5	25.6	28.4	1.7	9.5	2.3	20	0
C 3358.9	B	591241 , 5463836	9.0	5.5	30.8	29.0	8.0	13.8	2.3	36	0
D 3391.8	D	591469 , 5464104	9.0	5.3	31.9	17.5	17.3	15.9	2.4	33	21
E 3424.4	B	591732 , 5464426	31.9	11.3	152.9	49.4	80.3	71.5	7.4	13	0
F 3451.8	D	592024 , 5464779	6.5	9.4	5.3	18.7	2.9	2.8	0.8	18	27
G 3471.5	D	592132 , 5464899	11.1	8.3	51.4	47.0	8.6	21.3	1.9	31	0
H 3488.0	H	592249 , 5465072	0.0	3.5	31.7	37.0	37.5	15.5	---	---	0
I 3609.8	S	593808 , 5466975	2.2	7.9	4.8	36.6	7.9	4.6	---	---	0
<b>LINE 10180 FLIGHT 4</b>											
A 3229.9	II	590629 , 5462960	24.6	3.1	123.6	21.0	117.2	34.2	30.8	15	31
B 3221.4	B	590772 , 5463089	5.8	2.3	0.0	163.6	5.7	0.0	---	---	0
C 3217.7	D	590830 , 5463145	41.8	38.2	225.0	163.6	64.0	87.6	2.4	0	0
Harrison Lake		CX=COAXIAL CP=COPLANAR	Note: EM values shown above are local amplitudes			*Estimated depth may be unreliable because the stronger part of the conductor may be deeper or to one side of the flight line, or because of a shallow dip or magnetite/overburden effects.					
Page 5											

## EM Anomaly List

Label Fid	Interp	XUTM (m.) YUTM (m.)	CX 5500HZ Real (ppm)	CX 5500HZ Quad (ppm)	CP 7200HZ Real (ppm)	CP 7200HZ Quad (ppm)	CP 900HZ Real (ppm)	CP 900HZ Quad (ppm)	Cond. (siemens)	DIKE DEPTH (m)	Mag. Corr (nT)
D 3206.9	B	590926 , 5463308	8.1	5.8	9.3	11.9	15.5	1.8	1.9	21	0
E 3176.9	B	591270 , 5463702	10.0	11.5	27.1	30.1	6.8	13.4	1.1	11	0
F 3149.3	B	591595 , 5464095	38.2	15.7	138.6	62.4	59.0	61.9	6.3	9	25
G 3130.8	B	591813 , 5464385	36.9	14.5	109.1	32.5	70.2	48.2	6.6	4	63
H 3114.3	D	592044 , 5464651	8.3	9.5	11.8	41.3	6.4	2.3	1.1	26	32
I 3094.6	B	592260 , 5464904	11.7	3.3	83.4	6.9	54.8	33.3	7.3	27	0
<b>LINE 10190 FLIGHT 4</b>											
A 2604.0	H	590718 , 5462861	9.5	0.8	49.4	35.2	49.6	11.1	---	---	56
B 2620.2	E	590949 , 5463150	18.1	6.7	50.6	51.6	24.7	19.1	5.7	27	0
C 2632.6	B	591079 , 5463291	17.4	11.9	55.4	51.7	9.6	21.0	2.5	24	0
D 2671.8	B?	591540 , 5463876	6.5	11.6	40.2	49.9	8.2	17.4	0.6	17	0
E 2693.3	H	591696 , 5464056	13.7	14.4	121.4	29.6	87.7	45.7	1.4	14	0
F 2701.0	D	591755 , 5464132	23.7	31.4	107.2	84.7	42.1	53.8	1.3	7	0
G 2712.0	B	591880 , 5464281	12.9	3.1	69.0	11.1	36.6	30.1	9.6	38	0
H 2763.7	II	592340 , 5464849	0.0	2.2	17.7	6.4	13.0	5.3	---	---	0
I 2778.3	B	592523 , 5465081	8.2	10.5	29.5	28.0	10.5	11.3	0.9	27	0
<b>LINE 10200 FLIGHT 3</b>											
A 7260.3	H	590490 , 5462425	21.5	10.6	48.8	30.9	11.6	25.8	4.1	22	0
B 7282.1	H	590691 , 5462664	11.7	16.6	75.2	65.4	31.3	26.6	1.0	4	0
C 7304.5	B	590981 , 5463070	16.2	5.4	56.3	20.8	31.4	23.4	6.3	16	0
D 7349.3	H	591608 , 5463835	14.0	16.2	71.2	87.0	14.4	28.4	1.3	11	37
E 7366.4	B	591761 , 5463996	24.9	2.0	98.7	38.8	54.4	37.7	---	---	0
F 7396.6	B	592150 , 5464446	49.5	29.3	244.8	145.2	48.7	107.4	4.3	3	47
G 7399.0	B	592175 , 5464478	42.5	17.9	244.8	145.2	48.7	107.4	6.3	7	43
H 7408.3	B	592246 , 5464560	29.8	35.9	161.4	147.5	17.4	58.7	1.6	6	49
I 7434.9	H	592395 , 5464771	11.4	9.8	44.1	27.6	15.9	16.4	1.6	8	0
J 7450.3	B	592552 , 5464992	11.1	9.9	44.8	48.3	9.1	15.9	1.6	15	0
<b>LINE 10210 FLIGHT 3</b>											
A 7232.4	D	590504 , 5462278	45.3	11.6	165.4	83.0	76.3	76.3	13.1	5	0
Harrison Lake		CX=COAXIAL CP=COPLANAR	Note: EM values shown above are local amplitudes			*Estimated depth may be unreliable because the stronger part of the conductor may be deeper or to one side of the flight line, or because of a shallow dip or magnetite/overburden effects.					

### EM Anomaly List

Label Fid	Interp	XUTM (m.) YUTM (m.)	CX 5500HZ Real (ppm)	CX 5500HZ Quad (ppm)	CP 7200HZ Real (ppm)	CP 7200HZ Quad (ppm)	CP 900HZ Real (ppm)	CP 900HZ Quad (ppm)	Cond. (siemens)	DIKE DEPTH (m)	Mag. Corr (nT)
B 7216.6	II	590753 , 5462586	14.6	8.4	94.7	30.3	50.9	41.3	3.0	8	0
C 7207.1	II	590956 , 5462830	31.4	18.3	186.1	53.9	71.2	84.8	3.7	4	0
D 7191.4	II	591251 , 5463198	10.8	16.8	45.8	45.1	3.6	14.8	0.9	8	0
E 7169.3	S?	591574 , 5463570	0.9	4.1	18.5	29.6	7.8	7.0	---	---	0
F 7148.6	H	591847 , 5463936	6.5	5.5	53.1	30.8	26.1	22.4	1.4	27	0
G 7128.5	B	592191 , 5464363	12.8	6.3	111.6	62.5	50.2	49.3	3.4	26	18
H 7121.2	B	592238 , 5464499	20.0	12.9	134.4	64.2	47.9	54.7	2.8	14	0
I 7092.5	B?	592377 , 5464626	15.1	7.8	130.3	54.6	41.9	60.6	3.4	13	0
J 7077.0	H	592550 , 5464838	9.2	7.2	41.4	36.1	9.7	18.7	1.7	18	0
K 6965.9	S	594154 , 5466772	5.4	7.2	0.1	52.0	0.1	8.3	---	---	0
<b>LINE 10220 FLIGHT 3</b>											
A 6622.4	D	590541 , 5462154	38.4	21.1	107.9	41.9	10.4	42.5	4.3	8	0
B 6642.6	B	590785 , 5462473	54.3	17.0	207.9	32.4	142.7	93.4	10.4	11	0
C 6653.3	B	590941 , 5462677	18.4	15.4	128.5	60.1	37.7	58.7	2.0	8	0
D 6659.7	B	591050 , 5462809	21.4	13.0	146.1	47.2	46.9	73.8	3.1	13	0
E 6661.6	D	591082 , 5462851	32.8	13.0	146.1	47.2	46.9	73.8	6.4	10	35
F 6671.5	B	591237 , 5463049	0.4	0.2	43.0	32.5	27.3	17.9	---	---	25
G 6701.9	B	591614 , 5463498	17.2	21.2	71.6	128.3	2.6	47.7	1.3	3	0
H 6758.7	D	592251 , 5464260	39.5	26.0	122.7	54.6	48.1	54.8	3.5	5	0
I 6770.5	B	592347 , 5464391	19.6	18.4	148.8	83.9	36.7	69.2	1.8	16	0
J 6777.4	D	592401 , 5464451	15.7	18.6	167.4	39.5	102.1	85.4	1.3	2	0
K 6800.7	H	592695 , 5464823	7.6	12.1	63.3	81.0	16.8	24.1	0.7	14	0
L 6923.8	S	594232 , 5466722	0.2	9.8	5.8	59.5	2.9	10.9	---	---	0
<b>LINE 10230 FLIGHT 3</b>											
A 6566.1	B	590808 , 5462328	59.9	12.7	333.4	79.2	231.2	143.0	18.7	2	0
B 6516.6	B?	591688 , 5463402	13.7	12.7	53.6	57.4	40.5	21.9	1.6	0	0
C 6480.0	E	592207 , 5464053	18.0	26.0	113.5	134.0	0.0	34.1	1.1	10	44
D 6477.0	S?	592246 , 5464101	10.0	6.6	113.5	134.0	2.3	34.2	2.2	34	0
Harrison Lake		CX=COAXIAL CP=COPLANAR	Note: EM values shown above are local amplitudes			*Estimated depth may be unreliable because the stronger part of the conductor may be deeper or to one side of the flight line, or because of a shallow dip or magnetite/overburden effects.					

## EM Anomaly List

Label Fid	Interp	XUTM (m.) YUTM (m.)	CX 5500HZ Real (ppm)	CX 5500HZ Quad (ppm)	CP 7200HZ Real (ppm)	CP 7200HZ Quad (ppm)	CP 900HZ Real (ppm)	CP 900HZ Quad (ppm)	Cond. (siemens)	DIKE DEPTH (m)	Mag. Corr (nT)
E 6472.3	B	592309 , 5464179	16.1	21.0	131.2	127.9	36.1	64.2	1.2	2	0
F 6462.3	D	592428 , 5464328	77.1	38.1	228.3	138.7	105.3	107.9	6.3	4	0
G 6453.6	D	592575 , 5464485	19.5	39.2	106.5	127.5	0.2	31.0	0.8	2	67
H 6444.8	H	592729 , 5464674	3.0	7.0	45.0	41.6	15.9	20.2	---	---	0
<b>LINE 10240 FLIGHT 3</b>											
A 6024.0	B	590700 , 5462042	43.4	22.7	273.8	61.8	203.8	140.5	4.8	8	0
B 6033.9	B	590863 , 5462251	78.2	24.8	521.7	67.7	441.1	218.2	11.5	8	0
C 6072.8	H	591583 , 5463164	11.5	10.0	23.4	19.7	15.4	10.0	1.6	21	0
D 6089.3	B?	591740 , 5463352	5.0	7.3	46.0	66.4	43.2	17.4	0.7	35	0
E 6131.4	S?	592318 , 5464041	13.5	11.4	92.3	201.6	2.0	33.2	1.8	14	0
F 6140.3	B	592441 , 5464187	46.7	28.6	298.6	244.3	141.9	140.4	4.0	4	15
G 6157.2	D	592653 , 5464445	28.8	29.4	202.3	182.7	36.5	83.1	1.9	12	0
H 6159.4	D	592679 , 5464479	14.4	21.0	202.3	182.7	36.5	83.1	1.0	7	0
I 6165.5	B	592749 , 5464579	19.0	21.0	118.0	77.5	32.2	49.6	1.5	14	0
J 6277.1	S	594074 , 5466220	4.9	11.1	29.7	87.5	20.7	12.6	---	---	0
<b>LINE 10250 FLIGHT 3</b>											
A 5973.1	D	590521 , 5461674	63.3	27.7	216.9	112.3	104.2	106.3	6.9	0	0
B 5959.9	B	590768 , 5461962	26.2	4.8	144.7	25.2	168.0	69.5	17.6	15	0
C 5954.6	H	590889 , 5462112	36.8	14.3	258.0	55.4	172.1	107.9	6.8	8	26
D 5951.2	E	590961 , 5462210	38.7	14.3	258.0	82.7	172.1	107.9	7.3	8	0
E 5911.3	B	591727 , 5463152	6.2	6.6	46.2	24.7	26.3	21.8	1.1	14	0
F 5870.7	S?	592341 , 5463909	10.8	28.6	63.1	123.3	3.7	22.5	0.5	0	14
G 5861.7	D	592492 , 5464101	60.9	34.5	226.0	151.1	50.2	91.4	4.8	0	0
H 5841.9	B	592834 , 5464511	51.5	22.3	237.9	144.3	91.6	104.6	6.5	9	28
<b>LINE 10260 FLIGHT 3</b>											
A 5392.2	E	590573 , 5461579	70.3	34.3	377.1	180.6	184.3	173.2	6.2	9	0
B 5405.2	II	590800 , 5461859	81.9	27.1	381.7	76.9	304.8	160.3	11.0	3	0
C 5419.3	D	591022 , 5462136	27.9	11.8	222.6	97.9	86.7	104.0	5.5	13	0
Harrison Lake		CX=COAXIAL CP=COPLANAR	Note: EM values shown above are local amplitudes			*Estimated depth may be unreliable because the stronger part of the conductor may be deeper or to one side of the flight line, or because of a shallow dip or magnetite/overburden effects.					

## EM Anomaly List

Label Fid	Interp	XUTM (m.) YUTM (m.)	CX 5500HZ Real (ppm)	CX 5500HZ Quad (ppm)	CP 7200HZ Real (ppm)	CP 7200HZ Quad (ppm)	CP 900HZ Real (ppm)	CP 900HZ Quad (ppm)	Cond. (siemens)	DIKE DEPTH (m)	Mag. Corr (nT)
D 5423.5	B	591079 , 5462203	32.6	8.7	222.6	97.9	86.7	104.0	11.1	16	0
E 5442.8	H	591431 , 5462614	8.8	14.0	33.8	56.8	0.3	18.3	0.8	13	0
F 5462.9	B	591779 , 5463076	39.3	21.4	137.0	77.7	59.4	67.0	4.4	11	0
G 5505.6	E	592398 , 5463832	4.3	18.9	47.0	126.2	1.5	22.9	0.3	0	0
H 5513.7	B	592531 , 5463998	30.2	28.4	138.1	135.9	22.2	46.2	2.1	6	0
I 5526.9	D	592715 , 5464219	56.9	37.1	188.0	132.7	31.0	65.3	4.0	5	0
J 5532.9	D	592763 , 5464283	20.6	18.9	185.6	81.5	21.5	65.3	1.9	9	0
K 5540.3	B	592830 , 5464369	36.7	26.6	218.3	21.4	154.6	95.1	3.0	5	0
L 5542.9	D	592860 , 5464405	31.7	17.5	218.3	34.4	154.6	95.1	4.0	11	0
M 5552.6	B	592990 , 5464560	23.6	21.2	135.0	116.9	40.7	57.0	2.0	9	0
N 5568.7	B	593213 , 5464825	4.0	3.4	29.9	28.8	13.7	12.9	---	---	0
<b>LINE 10270 FLIGHT 3</b>											
A 5214.0	B	590704 , 5461566	38.5	15.4	220.9	79.9	142.7	84.9	6.6	11	0
B 5207.0	H	590823 , 5461719	22.9	2.1	180.2	15.1	186.3	47.0	---	---	0
C 5201.2	E	590948 , 5461861	29.2	8.3	61.6	16.6	48.4	20.6	9.7	0	0
D 5194.4	D	591072 , 5462026	43.4	18.8	221.0	90.7	96.5	103.8	6.1	0	0
E 5191.4	B	591120 , 5462094	44.6	24.8	221.0	90.7	96.5	103.8	4.5	0	0
F 5171.4	H	591497 , 5462552	6.4	14.8	64.4	79.7	7.9	26.8	---	---	117
G 5151.5	B	591853 , 5462997	64.7	42.7	245.7	115.5	93.1	114.6	4.1	7	208
H 5136.2	S	592102 , 5463314	2.6	8.3	16.9	51.9	5.4	8.3	---	---	0
I 5121.5	B?	592374 , 5463633	8.6	10.9	17.5	4.9	2.5	4.6	1.0	19	0
J 5109.3	B	592556 , 5463871	37.5	48.8	129.2	148.8	14.8	44.0	1.5	3	0
K 5095.7	D	592746 , 5464107	61.6	57.9	267.1	229.6	13.4	99.8	2.6	3	98
L 5093.4	D	592767 , 5464133	50.6	57.9	267.1	229.6	13.4	99.1	2.0	8	98
M 5082.7	D	592858 , 5464241	41.8	13.8	187.4	56.1	143.6	87.9	8.9	10	0
N 5070.9	H	593027 , 5464472	28.1	28.0	191.9	146.6	46.5	75.1	1.9	7	0
O 5052.0	B	593274 , 5464770	1.0	0.9	39.4	21.8	20.5	11.6	---	---	0
<b>LINE 10280 FLIGHT 3</b>											
A 4598.6	H	590755 , 5461486	55.5	15.9	311.6	77.6	253.2	103.1	11.9	13	0
Harrison Lake		CX=COAXIAL CP=COPLANAR	Note: EM values shown above are local amplitudes			*Estimated depth may be unreliable because the stronger part of the conductor may be deeper or to one side of the flight line, or because of a shallow dip or magnetite/overburden effects.					

### EM Anomaly List

Label Fid	Interp	XUTM (m.) YUTM (m.)	CX 5500HZ Real (ppm)	CX 5500HZ Quad (ppm)	CP 7200HZ Real (ppm)	CP 7200HZ Quad (ppm)	CP 900HZ Real (ppm)	CP 900HZ Quad (ppm)	Cond. (siemens)	DIKE DEPTH (m)	Mag. Corr (nT)
B 4606.8	II	590887 , 5461647	47.3	11.3	329.0	38.9	299.6	95.3	14.6	11	0
C 4630.3	H	591152 , 5461976	17.6	20.5	137.8	106.9	39.5	60.9	1.3	14	0
D 4649.5	D	591373 , 5462230	13.2	12.3	51.4	44.7	6.0	20.6	1.6	18	0
E 4662.3	B	591546 , 5462457	13.5	13.8	98.8	127.0	11.4	45.1	1.4	21	147
F 4681.5	B?	591875 , 5462870	10.4	13.3	75.6	78.0	0.3	30.3	1.0	23	262
G 4687.2	B	591982 , 5463002	11.1	10.7	75.6	78.0	28.8	29.2	---	---	0
H 4723.4	H	592643 , 5463805	10.3	11.2	65.5	67.8	12.6	21.4	1.2	18	0
I 4746.7	E	592867 , 5464083	12.3	25.3	156.2	89.5	39.7	67.5	0.7	9	0
J 4753.9	B	592910 , 5464147	26.5	8.8	156.2	75.7	60.2	67.5	7.6	17	0
K 4764.3	D	592992 , 5464267	30.9	30.0	120.6	116.7	27.5	48.6	2.0	7	0
L 4774.1	E	593096 , 5464399	5.7	8.2	36.9	32.3	19.6	19.8	---	---	0
<b>LINE 10290 FLIGHT 3</b>											
A 4550.4	II	590896 , 5461489	19.0	3.0	77.6	16.1	112.2	15.0	---	---	0
B 4541.9	B	591066 , 5461669	55.6	14.2	101.4	23.3	80.3	35.2	14.1	0	0
C 4531.5	B	591190 , 5461839	41.2	27.0	122.5	85.8	36.0	50.2	3.5	4	10
D 4510.3	D	591409 , 5462134	32.2	28.3	92.6	75.6	7.8	36.6	2.3	4	0
E 4500.3	B	591545 , 5462307	61.7	52.1	276.3	213.0	41.3	111.1	3.0	3	119
F 4497.7	B?	591584 , 5462358	38.6	41.1	276.3	213.0	68.0	111.1	1.9	5	111
G 4461.2	B?	592389 , 5463339	9.2	11.4	29.4	37.5	2.0	6.1	---	---	0
H 4436.5	D	592867 , 5463941	15.3	13.8	31.5	38.6	0.2	15.8	1.7	22	46
I 4424.3	H	592996 , 5464100	6.8	4.3	68.3	50.7	29.3	31.5	2.0	32	0
<b>LINE 10300 FLIGHT 3</b>											
A 3939.6	E	591197 , 5461717	38.5	25.0	160.7	102.4	13.4	82.3	3.5	3	0
B 3947.0	D	591236 , 5461768	10.8	4.8	188.5	100.9	98.5	88.2	3.8	42	0
C 3951.0	B	591253 , 5461784	40.2	24.4	188.5	100.9	98.5	88.2	3.8	18	0
D 3999.6	B	591554 , 5462138	16.7	14.7	163.1	99.5	88.2	74.5	1.8	11	0
E 4003.5	D	591604 , 5462202	1.9	7.9	74.4	29.6	80.8	28.4	---	---	52
F 4009.0	B	591670 , 5462297	7.7	2.9	74.4	27.7	80.8	28.4	---	---	43
Harrison Lake		CX=COAXIAL CP=COPLANAR	Note: EM values shown above are local amplitudes			*Estimated depth may be unreliable because the stronger part of the conductor may be deeper or to one side of the flight line, or because of a shallow dip or magnetite/overburden effects.					
<b>Page 10</b>											

## EM Anomaly List

Label Fid	Interp	XUTM (m.) YUTM (m.)	CX 5500HZ Real (ppm)	CX 5500HZ Quad (ppm)	CP 7200HZ Real (ppm)	CP 7200HZ Quad (ppm)	CP 900HZ Real (ppm)	CP 900HZ Quad (ppm)	Cond. (siemens)	DIKE DEPTH (m)	Mag. Corr (nT)
G 4049.5	D	592407 , 5463194	2.7	10.9	29.1	62.3	0.1	9.2	---	---	0
H 4070.6	B	592695 , 5463557	7.6	6.7	78.7	57.1	15.1	34.3	1.4	34	0
I 4077.5	B?	592776 , 5463654	6.7	12.4	78.7	24.0	15.1	34.3	0.6	20	27
J 4114.6	B?	592997 , 5463916	8.0	12.0	14.5	30.4	7.4	10.7	0.8	28	0
K 4236.2	S	594406 , 5465675	3.5	11.9	21.4	86.7	11.4	14.5	---	---	0
<b>LINE 10310 FLIGHT 3</b>											
A 3573.2	B	591277 , 5461638	27.4	28.6	92.0	48.7	64.0	38.8	1.8	0	0
B 3552.9	D	591478 , 5461901	15.2	7.1	68.1	14.4	6.8	27.7	3.9	30	0
C 3541.4	B	591640 , 5462107	30.8	9.5	172.9	69.9	132.9	71.0	8.8	19	0
D 3536.7	D	591725 , 5462210	15.0	8.1	189.5	76.2	156.2	80.3	3.2	22	0
E 3533.3	B	591789 , 5462283	26.6	6.9	189.5	32.2	156.2	80.3	10.8	26	0
F 3512.9	D	592213 , 5462809	8.0	15.2	26.9	46.8	7.5	9.0	0.6	13	0
G 3492.0	B	592600 , 5463293	9.4	5.1	59.7	16.5	4.0	19.0	---	---	0
H 3478.1	D	592755 , 5463515	17.9	12.1	60.7	52.9	11.7	25.2	2.6	0	0
I 3442.9	B?	593085 , 5463917	1.7	4.5	23.7	33.2	7.2	11.5	---	---	0
<b>LINE 10320 FLIGHT 3</b>											
A 2956.6	B	591371 , 5461612	34.6	26.3	146.3	97.9	43.3	67.2	2.8	0	0
B 2974.0	H	591570 , 5461860	26.1	13.0	149.3	84.9	105.9	66.9	4.3	21	0
C 2994.5	H	591892 , 5462251	25.7	3.5	196.4	5.7	209.1	45.8	27.8	24	0
D 3069.7	H	592847 , 5463445	29.6	31.3	126.9	111.2	18.9	48.2	1.8	0	0
E 3131.1	B	593305 , 5464003	1.8	1.2	21.6	11.2	15.7	8.0	---	---	0
F 3223.4	S	594525 , 5465505	2.1	8.3	34.0	82.8	22.6	14.4	---	---	0
<b>LINE 10330 FLIGHT 3</b>											
A 2896.6	B	591558 , 5461669	23.1	11.4	117.8	68.1	67.1	51.8	4.2	0	0
B 2885.7	B	591784 , 5461939	19.6	5.5	46.2	24.8	30.9	23.3	8.6	30	43
C 2872.8	B	591999 , 5462207	7.5	1.1	66.0	10.9	68.6	28.3	---	---	0
D 2844.6	D	592492 , 5462832	10.6	19.4	39.0	65.4	2.5	13.1	0.7	7	21
E 2800.0	H	592969 , 5463445	6.8	5.0	30.9	39.8	7.3	6.0	---	---	0
Harrison Lake		CX=COAXIAL CP=COPLANAR	Note: EM values shown above are local amplitudes			*Estimated depth may be unreliable because the stronger part of the conductor may be deeper or to one side of the flight line, or because of a shallow dip or magnetite/overburden effects.					



## EM Anomaly List

Label Fid	Interp	XUTM (m.) YUTM (m.)	CX 5500HZ Real (ppm)	CX 5500HZ Quad (ppm)	CP 7200HZ Real (ppm)	CP 7200HZ Quad (ppm)	CP 900HZ Real (ppm)	CP 900HZ Quad (ppm)	Cond. (siemens)	DIKE DEPTH (m)	Mag. Corr (nT)
F 2751.3	B	593336 , 5463869	12.9	6.3	87.2	35.9	50.5	34.9	3.5	3	0
<b>LINE 10340 FLIGHT 3</b>											
A 2328.2	B	591452 , 5461398	27.8	15.2	58.6	56.0	6.7	27.9	3.9	3	0
B 2335.6	D	591525 , 5461494	27.7	16.6	43.2	65.3	2.1	22.5	3.5	7	34
C 2349.1	B	591614 , 5461578	5.7	10.0	74.4	24.4	65.6	24.3	0.6	21	0
D 2376.6	B	591927 , 5461993	16.6	5.4	75.3	8.4	68.4	30.0	6.6	28	35
E 2390.7	D	592062 , 5462153	12.3	6.8	23.3	16.0	1.2	34.9	2.9	27	0
F 2398.7	B	592119 , 5462223	17.3	6.2	90.4	15.3	78.4	34.9	5.8	21	0
G 2428.7	H	592433 , 5462612	6.3	5.1	44.9	24.4	20.4	19.8	---	---	0
H 2440.5	B?	592591 , 5462798	6.9	12.5	52.3	38.7	10.3	18.1	0.6	13	0
I 2449.4	H	592699 , 5462921	7.0	6.4	62.0	34.2	16.0	24.1	1.3	32	0
J 2514.2	H	593286 , 5463666	3.9	4.4	77.2	61.7	22.7	27.1	0.9	34	0
K 2521.8	B	593345 , 5463749	11.0	9.7	63.1	36.9	40.3	24.7	1.6	7	0
L 2610.8	S	594592 , 5465282	4.8	14.2	25.1	83.9	19.4	14.7	---	---	0
<b>LINE 10350 FLIGHT 3</b>											
A 2189.7	H	591685 , 5461516	7.5	4.7	71.9	28.9	51.0	34.2	---	---	0
B 2177.5	D	591893 , 5461789	11.1	6.4	54.8	34.0	17.1	27.0	2.7	28	0
C 2156.3	B	592127 , 5462028	14.8	5.6	79.1	29.0	21.6	20.6	5.2	20	0
D 2131.3	D	592401 , 5462432	22.8	25.6	129.8	128.3	43.2	55.1	1.5	17	132
E 2121.3	B	592496 , 5462518	32.5	16.4	366.5	158.2	132.3	150.4	4.6	11	0
F 2065.9	D	593277 , 5463497	31.4	23.0	103.2	76.6	37.3	45.8	2.8	6	60
G 2053.3	B	593368 , 5463626	12.2	5.8	85.2	60.8	38.1	32.6	3.6	31	0
H 2044.0	B?	593433 , 5463718	8.7	5.4	37.1	19.2	20.5	20.6	---	---	0
I 1937.5	S	594691 , 5465242	2.2	5.2	7.9	71.1	6.8	10.8	---	---	40
<b>LINE 10360 FLIGHT 3</b>											
A 1591.0	D	592130 , 5461914	11.5	7.9	130.4	55.1	78.0	67.8	2.1	20	0
B 1597.5	D	592200 , 5461998	32.2	14.4	130.4	51.8	78.0	67.8	5.3	4	0
C 1624.9	B	592550 , 5462421	86.5	37.2	445.3	134.5	249.2	189.5	7.8	7	88
Harrison Lake		CX=COAXIAL CP=COPLANAR	Note: EM values shown above are local amplitudes			*Estimated depth may be unreliable because the stronger part of the conductor may be deeper or to one side of the flight line, or because of a shallow dip or magnetite/overburden effects.					

**EM Anomaly List**

Label Fid	Interp	XUTM (m.) YUTM (m.)	CX 5500HZ Real (ppm)	CX 5500HZ Quad (ppm)	CP 7200HZ Real (ppm)	CP 7200HZ Quad (ppm)	CP 900HZ Real (ppm)	CP 900HZ Quad (ppm)	Cond. (siemens)	DIKE DEPTH (m)	Mag. Corr (nT)
D 1638.5	D	592694 , 5462592	25.1	24.0	23.1	23.4	8.2	4.6	1.9	0	0
E 1703.9	D	593371 , 5463438	21.4	12.9	44.8	33.0	19.0	18.7	3.1	17	0
F 1721.5	B	593497 , 5463607	16.9	4.2	121.6	62.2	43.8	48.3	9.8	23	0
<b>LINE 10370 FLIGHT 3</b>											
A 1458.7	D	592214 , 5461852	14.9	8.5	128.0	57.9	36.0	60.0	3.0	26	0
B 1449.6	B	592283 , 5461935	4.3	3.7	138.9	37.4	59.5	72.7	1.2	39	0
C 1424.0	D	592594 , 5462331	26.1	17.8	227.5	109.7	119.8	94.5	2.9	13	0
D 1420.6	B	592636 , 5462373	19.7	17.8	227.5	109.7	119.8	94.5	1.9	3	0
E 1410.3	H	592752 , 5462511	6.7	5.8	98.1	36.6	54.8	46.9	1.4	28	0
F 1376.2	H	593209 , 5463141	6.3	1.9	35.2	27.5	12.3	16.5	---	---	0
G 1329.0	H	593576 , 5463569	4.9	4.0	45.8	29.4	17.1	23.3	---	---	0
H 1310.2	H	593706 , 5463672	6.1	10.2	74.7	50.4	21.8	42.5	0.7	23	0
<b>LINE 10380 FLIGHT 3</b>											
A 1026.4	II	592372 , 5461897	21.6	17.3	113.9	83.2	13.4	42.8	2.2	5	12
B 1054.9	B	592782 , 5462411	18.9	11.6	72.2	38.8	30.0	32.9	2.9	17	21
C 1066.1	B	592928 , 5462595	19.5	11.2	94.2	27.5	59.5	40.3	3.2	10	0
D 1089.7	H	593274 , 5463000	7.4	5.8	74.4	40.6	17.6	29.8	1.6	27	0
E 1112.7	D	593531 , 5463342	19.6	15.7	36.7	29.3	8.5	18.9	2.2	29	15
F 1124.4	H	593612 , 5463460	14.0	12.8	88.5	73.0	27.7	42.4	1.6	12	0
G 1135.0	B?	593729 , 5463594	17.1	14.8	89.7	44.2	39.5	35.9	1.9	12	0
<b>LINE 10390 FLIGHT 3</b>											
A 861.3	II	592775 , 5462215	8.2	9.7	91.1	61.8	13.7	36.9	1.0	23	0
B 830.1	H	593303 , 5462892	6.9	11.7	42.0	40.4	10.3	20.2	0.7	12	0
C 807.5	B?	593641 , 5463283	6.7	3.8	54.2	27.4	15.0	23.7	2.3	46	0
<b>LINE 10400 FLIGHT 4</b>											
A 566.3	II	593076 , 5462430	4.6	8.2	32.2	52.6	3.3	14.3	0.6	18	0
B 607.0	B	593586 , 5463068	14.3	12.5	45.7	48.9	4.0	17.8	1.7	18	0
C 614.4	D	593680 , 5463189	20.2	8.9	55.7	27.2	37.3	26.5	4.6	15	0
Harrison Lake		CX=COAXIAL CP=COPLANAR	Note: EM values shown above are local amplitudes			*Estimated depth may be unreliable because the stronger part of the conductor may be deeper or to one side of the flight line, or because of a shallow dip or magnetite/overburden effects.					

## EM Anomaly List

Label Fid	Interp	XUTM (m.) YUTM (m.)	CX 5500HZ Real (ppm)	CX 5500HZ Quad (ppm)	CP 7200HZ Real (ppm)	CP 7200HZ Quad (ppm)	CP 900HZ Real (ppm)	CP 900HZ Quad (ppm)	Cond. (siemens)	DIKE DEPTH (m)	Mag. Corr (nT)
<b>LINE 10410 FLIGHT 4</b>											
A 771.5	B?	593664 , 5462980	11.1	12.7	27.1	26.5	8.1	7.5	---	---	0
B 765.4	B?	593769 , 5463111	12.4	8.2	35.0	26.5	29.4	181.9	2.3	23	0
<b>LINE 10420 FLIGHT 4</b>											
A 966.5	H	593394 , 5462501	6.8	2.4	46.9	34.1	15.5	21.6	---	---	0
B 989.6	B?	593741 , 5462957	11.7	14.7	35.5	20.1	11.5	7.7	1.1	20	0
<b>LINE 10430 FLIGHT 4</b>											
A 1217.5	D	593044 , 5461879	12.5	16.5	92.3	78.4	5.0	36.8	1.1	20	0
<b>LINE 10440 FLIGHT 4</b>											
A 1300.0	B?	593064 , 5461800	6.1	8.3	39.4	43.5	7.0	20.0	---	---	0
B 1307.7	B?	593168 , 5461916	5.7	2.3	57.7	14.2	26.0	35.6	---	---	0
<b>LINE 10450 FLIGHT 4</b>											
A 1526.4	L?	594053 , 5462814	36.3	12.3	168.1	207.9	1247.8	396.0	8.1	16	0
B 1521.8	L	594137 , 5462925	9.5	14.9	154.6	162.8	200.9	306.7	0.8	8	0
<b>LINE 10460 FLIGHT 4</b>											
A 1885.6	L	593878 , 5462478	22.4	18.6	104.2	174.5	812.6	98.5	2.1	14	58
B 1895.5	L	594068 , 5462707	24.9	9.5	57.0	13.0	95.6	324.5	6.1	14	0
<b>LINE 10470 FLIGHT 4</b>											
A 2025.2	L?	593880 , 5462276	50.6	26.9	113.0	89.1	171.8	74.8	4.9	6	39
B 2017.9	L	594058 , 5462452	25.3	7.4	42.8	36.4	31.6	79.6	8.9	13	0
C 1998.1	H	594418 , 5462932	9.8	26.6	209.1	294.6	14.4	84.2	0.5	7	0
<b>LINE 10480 FLIGHT 4</b>											
A 2148.4	L	593892 , 5462181	19.8	10.5	52.4	66.2	27.2	362.1	3.6	12	11
B 2173.0	H	594408 , 5462787	6.6	10.0	78.8	118.9	26.5	46.3	0.7	22	0
C 2181.2	E	594571 , 5463005	19.5	19.3	130.1	131.8	6.3	33.2	1.7	0	0
<b>LINE 10490 FLIGHT 4</b>											
A 2284.0	L	593887 , 5462114	21.2	13.8	76.0	91.8	27.2	25.1	2.9	10	13
B 2273.3	L?	594073 , 5462374	8.9	2.5	8.3	5.0	19.1	3.3	---	---	0
Harrison Lake		CX=COAXIAL CP=COPLANAR	Note: EM values shown above are local amplitudes			*Estimated depth may be unreliable because the stronger part of the conductor may be deeper or to one side of the flight line, or because of a shallow dip or magnetite/overburden effects.					

## EM Anomaly List

Label Fid	Interp	XUTM (m.) YUTM (m.)	CX 5500HZ Real (ppm)	CX 5500HZ Quad (ppm)	CP 7200HZ Real (ppm)	CP 7200HZ Quad (ppm)	CP 900HZ Real (ppm)	CP 900HZ Quad (ppm)	Cond. (siemens)	DIKE DEPTH (m)	Mag. Corr (nT)
C 2258.9	H	594443 , 5462664	8.4	9.2	58.5	87.3	13.9	29.3	1.1	22	0
D 2249.9	H	594645 , 5462895	8.2	13.4	168.7	163.5	35.9	70.7	0.7	11	0
E 2245.2	E	594738 , 5463014	17.8	16.2	24.3	157.9	0.1	6.8	1.8	7	62
<b>LINE 19010 FLIGHT 5</b>											
A 2372.9	H	592679 , 5466574	16.1	10.0	142.9	73.8	44.8	69.4	2.7	26	0
B 2353.7	H	592316 , 5466846	21.6	10.1	99.0	58.9	24.2	41.0	4.4	20	92
<b>LINE 19020 FLIGHT 5</b>											
A 2227.2	H	590927 , 5465666	35.4	31.2	178.0	144.0	35.5	82.2	2.3	4	45
B 2208.6	L	591316 , 5465502	75.9	23.7	67.8	33.3	64.6	32.2	11.7	0	0
C 2200.5	L	591393 , 5465479	18.0	7.6	67.8	19.5	64.6	32.2	4.8	2	0
D 2186.6	L?	591524 , 5465407	19.0	2.9	89.4	23.4	60.0	36.3	---	---	0
E 2164.7	D	591777 , 5465272	41.6	32.9	82.1	46.6	5.2	33.4	2.8	0	0
F 2132.1	H	592153 , 5464922	19.6	16.6	64.6	30.8	30.2	26.3	2.0	8	0
G 2123.1	B	592332 , 5464778	24.7	27.3	81.4	63.1	23.5	30.1	1.6	0	0
H 2103.2	D	592582 , 5464561	38.1	59.9	110.6	167.5	0.7	37.6	1.3	0	53
I 2085.3	D	592822 , 5464391	79.1	31.5	321.5	116.8	159.9	144.2	8.4	1	92
J 2082.5	B	592869 , 5464357	79.1	29.7	321.5	141.1	159.9	144.2	9.1	7	92
K 2075.9	B	592979 , 5464272	37.4	21.9	116.1	84.8	33.2	45.9	3.9	4	0
L 1978.6	B	593484 , 5463792	11.7	5.2	82.8	31.3	56.3	35.8	3.9	27	0
M 1957.6	H	593599 , 5463453	11.2	18.3	89.8	60.5	22.4	39.5	0.8	20	0
<b>LINE 19030 FLIGHT 5</b>											
A 1799.8	L	593887 , 5461571	54.1	29.6	110.4	164.8	8.2	533.6	4.9	2	0
B 1770.6	L?	593290 , 5461998	25.4	21.2	81.4	66.0	16.2	47.6	2.2	0	0
C 1708.0	B	592542 , 5462562	89.5	73.3	205.8	145.5	80.6	84.0	3.5	0	44
D 1488.2	H	591142 , 5463758	13.0	9.2	44.0	50.8	3.8	13.2	2.2	28	0
E 1465.2	H	591013 , 5463916	14.3	5.5	30.9	43.0	18.1	10.7	5.0	23	0
F 1428.0	L?	590889 , 5464140	15.4	6.9	56.5	15.3	60.4	22.9	4.2	23	11
G 1420.4	L	590807 , 5464195	12.2	0.0	56.5	0.0	60.3	30.1	---	---	0
Harrison Lake		CX=COAXIAL CP=COPLANAR	Note: EM values shown above are local amplitudes			*Estimated depth may be unreliable because the stronger part of the conductor may be deeper or to one side of the flight line, or because of a shallow dip or magnetite/overburden effects.					

---

**APPENDIX E**

**STATEMENT OF QUALIFICATIONS**

---

## APPENDIX E

### STATEMENT OF QUALIFICATIONS

I, Paul A. Smith, of the City of Scarborough, Province of Ontario, do hereby certify that:

1. I am a geophysicist, residing at 65 Dogwood Crescent, Scarborough, Ontario, M1P 3N5.
2. I am a graduate of DeVry Technical Institute, Toronto (Electronics – 1962) and the Nova Scotia Land Survey Institute, (Cartography – 1966).
3. I have been actively engaged in geophysical exploration since 1962.
4. I am presently employed by Fugro Airborne Surveys Corp.
5. The statements made in this report represent my best opinion and judgment.
6. I have no direct or indirect financial interest in the property described in this report.
7. I am a member of the Society of Exploration Geophysicists (SEG), the Canadian Exploration Geophysical Society (KEGS), and the Canadian Institute of Mining, Metallurgy and Petroleum (CIM).



Paul A. Smith  
Geophysicist

---

**APPENDIX F**

**RADIOMETRIC PROCESSING  
CONTROL FILE**

---





-APPENDIX F.2-

RDN_BTC	, RADON - UR IN TC CONSTANT	=0
RDN_AK	, RADON - UR IN K COEFFICIENT	=0.0
RDN_BK	, RADON - UR IN K CONSTANT	=0
RDN_ATH	, RADON - UR IN TH COEFFICIENT	=0.0
RDN_BTH	, RADON - UR IN TH CONSTANT	=0
RDN_AUPU	, RADON - UR IN UPU COEFFICIENT	=0.0
RDN_BUPU	, RADON - UR IN UPU CONSTANT	=0
RDN_A1	, RADON - U IN UPU	=0
RDN_A2	, RADON - TH IN UPU	=0.0
ALPHA	, COMPTON TH > U	=0.2480
BETA	, COMPTON TH > K	=0.3860
GAMMA	, COMPTON U > K	=0.7820
BACKA	, GRASTY BACKSCATTER U > TH (0.05)	=0.0
BACKB	, GRASTY BACKSCATTER K > TH (0.0)	=0.0
BACKG	, GRASTY BACKSCATTER K > U (0.0)	=0.0
ATN_TC	, HEIGHT ATTENUATION OF TC	=0.001628
ATN_K	, HEIGHT ATTENUATION OF K	=0.002168
ATN_U	, HEIGHT ATTENUATION OF U	=0.00972
ATN_TH	, HEIGHT ATTENUATION OF TH	=0.001987
SENS_K	, CPS PER PERCENT POTASSIUM ON GROUND	=0.0
SENS_U	, CPS PER PPM URANIUM ON GROUND	=0.0
SENS_TH	, CPS PER PPM THORIUM ON GROUND	=0.0

-----  
GENERAL PARAMETERS:

S_FREQ	, RADIOMETRIC SAMPLES PER SECOND	=1
ALT_OFF	, HEIGHT OF SENSOR ABOVE ALTIMETER (ft)	=0
ALT_DTM	, SURVEY HEIGHT DATUM (ft)	=200
ALT_MAX	, MAXIMUM ALTITUDE (1000ft)	=500

-----  
FLIGHT RANGES TO PROCESS, FLIGHTS TO PROCESS, FLIGHTS TO SKIP:

/ flight ranges to process  
/ specific flights to process  
/ specific flights to skip

-----  
LINE RANGES TO PROCESS, LINES TO PROCESS, LINES TO SKIP:

1 999999  
/ line ranges to process  
/ specific lines to process  
/ specific lines to skip



49:21:14.80 N  
115:46:32.90 W

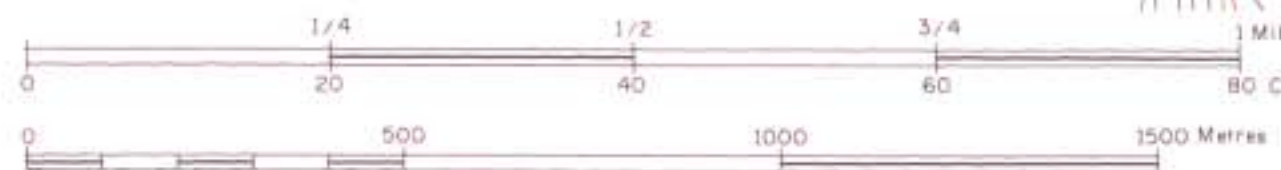
49:21:14.80 N  
115:41:13.10 W

589000 589500 590000 590500 591000 591500 592000 592500 593000 593500 594000 594500 595000

5467500 5467000 5466500 5466000 5465500 5465000 5464500 5464000 5463500 5463000 5462500 5462000

HARRISON

DIGITAL MAPPING BY  
**INTERIOR FORESTATION CO. LTD.**  
 P.O. BOX 874 CHANBROOK B.C. V1C 4J6  
 PHONE (604) 426-5300 FAX (604) 426-5311



SCALE: 1:10,000



Marguerite Island  
Camille Island

LAKE

L.S.13

L.S.12

L.S.11

L.S.10

L.S.9

L.S.8

L.S.7

L.S.6

L.S.5

L.S.4

L.S.3

L.S.2

L.S.1

L.1834

L.S.8

L.S.1

Crowhurst Bay

U.R.E.P.

U.R.E.P.

U.R.E.P.

U.R.E.P.

ENTRANCE

RESTRICTED

TRAP 28

TRAP 29

TRAP 30

TRAP 31

TRAP 32

TRAP 33

TRAP 34

TRAP 35

TRAP 36

TRAP 37

TRAP 38

TRAP 39

TRAP 40

TRAP 41

TRAP 42

TRAP 43

TRAP 44

TRAP 45

**ABO CLAIM GROUP**

**EAGLE PLAINS RESOURCES**

**BASE MAP 26717**

DATE: March 2001	DRAWN / MAPPED: TERMUENDE 2001	BCGS MAP SHEET: 092H032
SCALE: 1:10,000		FIGURE No.

49:18:0 N  
115:46:32.90 W

49:18:0 N  
115:41:13.10 W

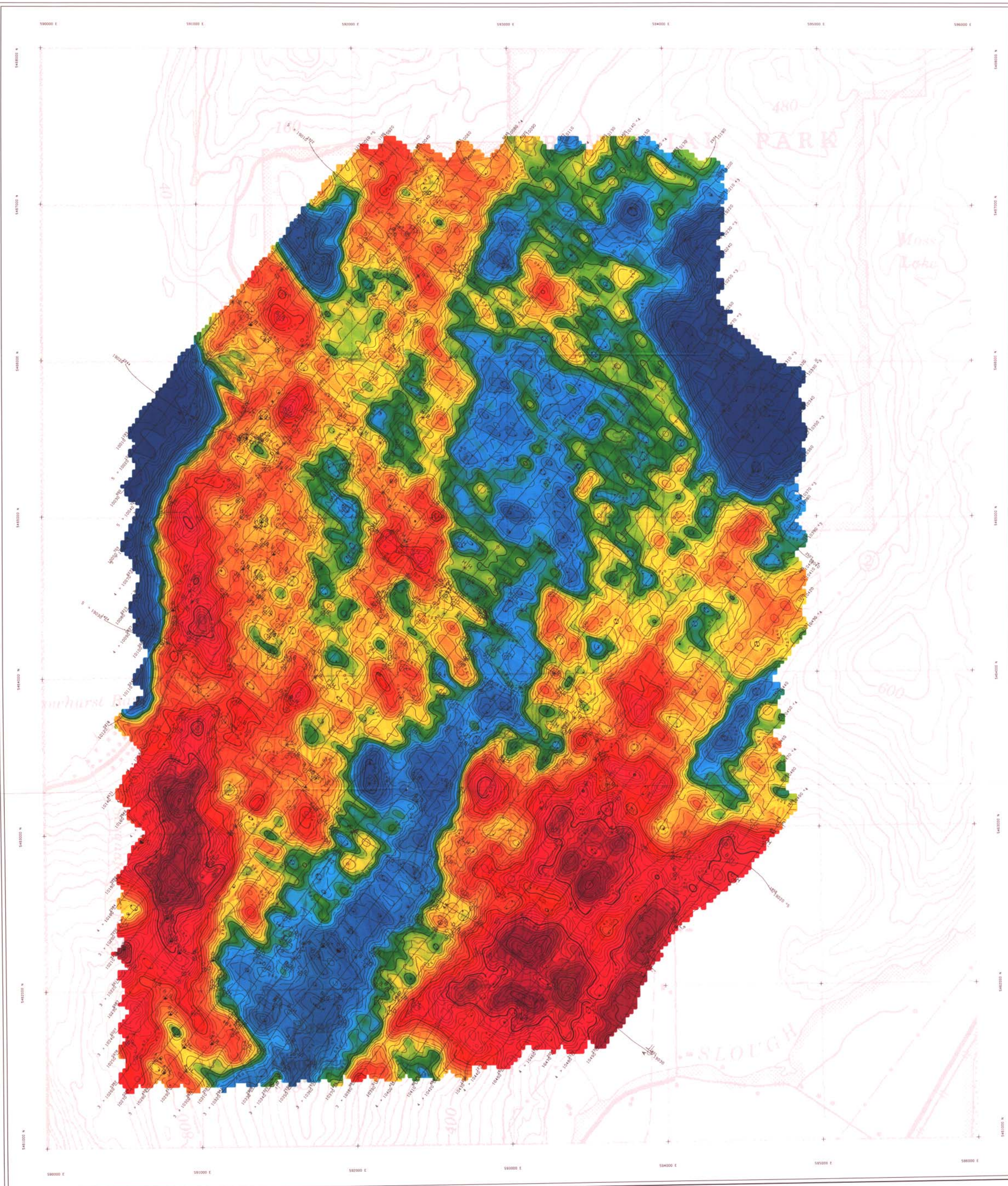
589500 590000 590500 591000 591500 592000 592500 593000 593500 594000 594500 595000

5462500 5462000 5461500 5461000 5460500 5460000 5459500 5459000 5458500 5458000 5457500 5457000

Harrison  
top SANDS

I.R.  
A BIRD





**TECHNICAL SUMMARY**

Navigation: Differentially-corrected GPS  
 Data reduction grid interval: 25 metres  
 Terrain clearance: Helicopter, Spectrometer 57 m  
 Electromagnetic sensor 30 m  
 Magnetometer sensor 30 m  
 Data sampling interval: 0.1 second  
 Magnetometer / sensitivity: Cesium / 0.01 nT  
 Electromagnetic system: DIGEM  
 Spectrometer: CR820

Frequency	Sensitivity	Coil Orientation
1000 Hz	06 ppm	Vertical coplanar
5500 Hz	12 ppm	Vertical coplanar
900 Hz	12 ppm	Horizontal coplanar
7200 Hz	24 ppm	Horizontal coplanar
56000 Hz	60 ppm	Horizontal coplanar

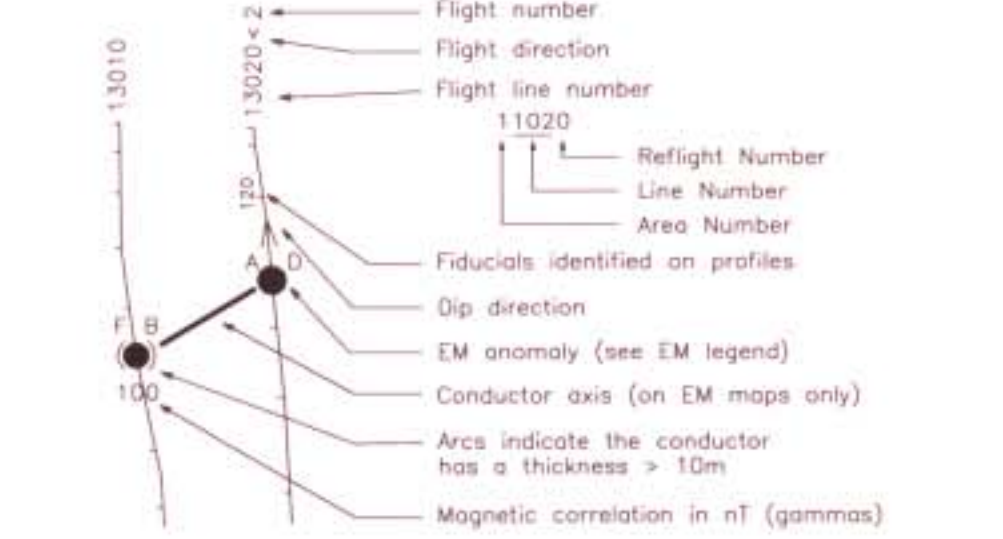


**ELECTROMAGNETIC ANOMALIES**

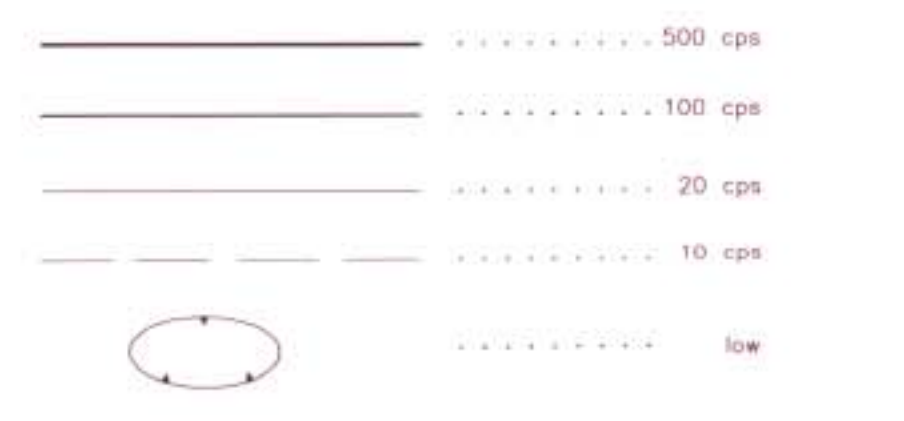
Grade	Anomaly	Conductance
7	●	>100 siemens
6	●	50-100 siemens
5	●	20-50 siemens
4	●	10-20 siemens
3	●	5-10 siemens
2	●	1-5 siemens
1	●	< 1 siemens
	*	Questionable anomaly

Anomaly identifier	Interpretive symbol	Conductor ("mode")
Depth is greater than 15 m	○	B Bedrock conductor ("thin die")
30 m	○	D Narrow bedrock conductor ("thin die")
45 m	○	S Conductive cover ("horizontal thin sheet")
60 m	○	H Broad conductive rock unit, deep conductive weathering, thick conductive cover ("half space")
	○	E Edge of broad conductor ("edge of half space")
	○	L Culture, e.g. power line, metal building or fence

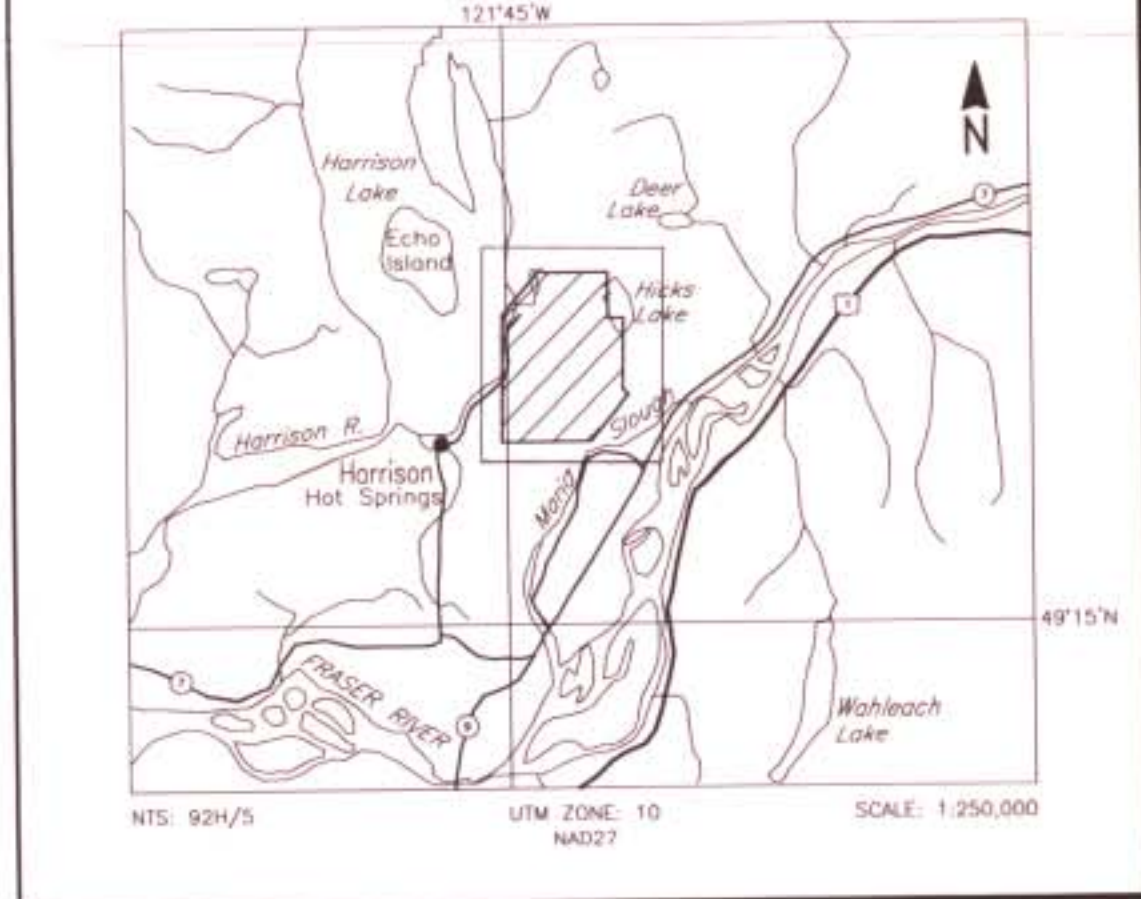
**FLIGHT LINES WITH EM ANOMALIES**



**CONTOUR INTERVALS**



**LOCATION MAP**

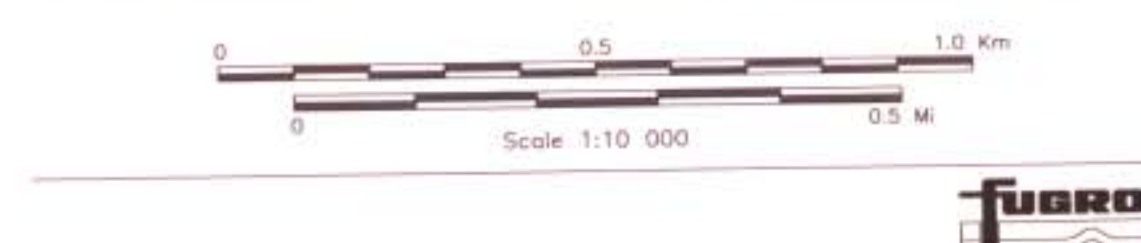


**TOKLAT RESOURCES INC.**  
 HARRISON LAKE AREA, B.C.

**RADIOMETRIC TOTAL COUNT**

DIGEM SURVEY: NTS: 92H/5 GEPHYSICIST: [Signature]  
 DATE: OCTOBER, 2001 JOB: 2066 SHEET: 1

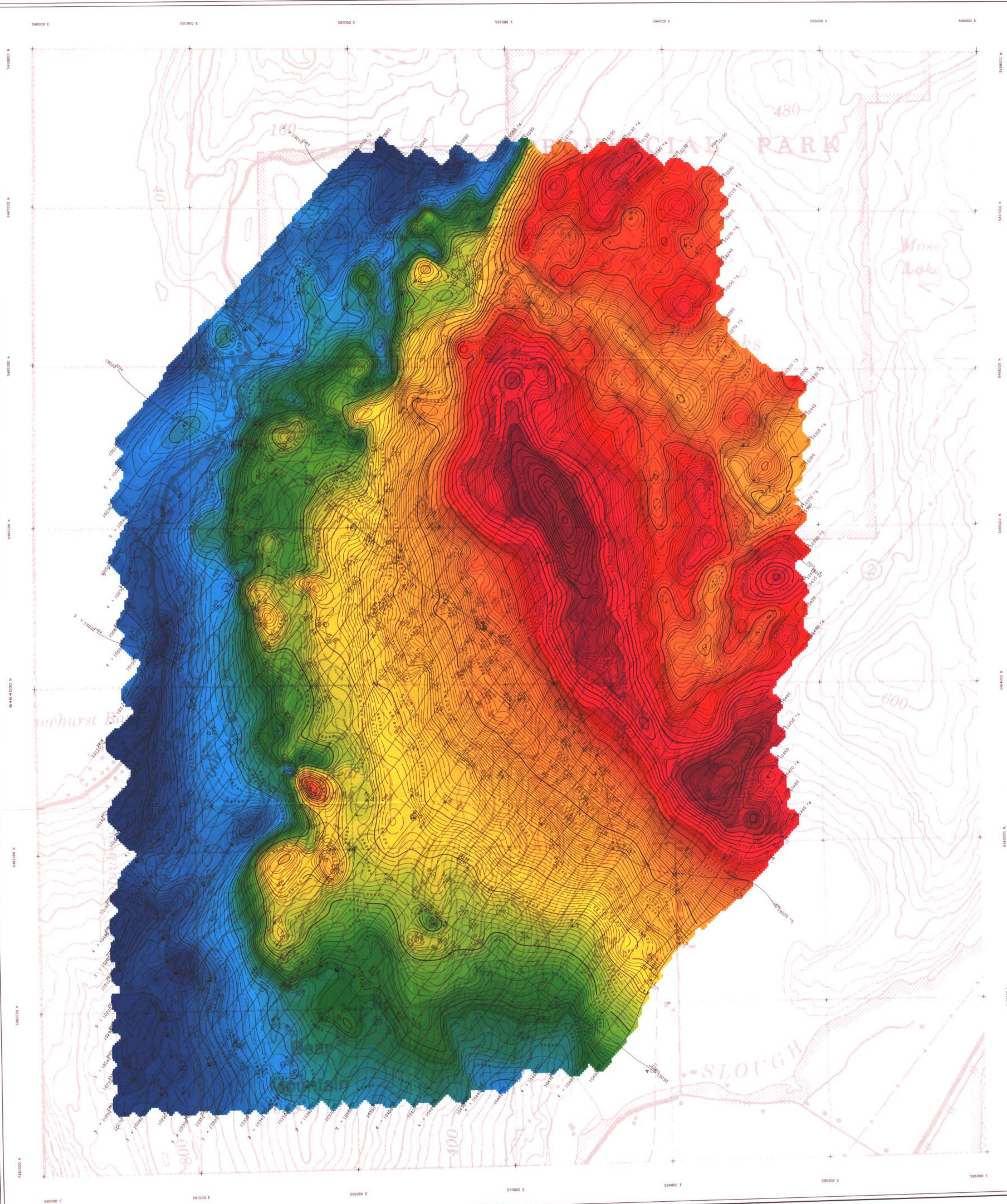
Fugro Airborne Surveys



GEOLOGICAL SURVEY BRANCH

26,717





**TECHNICAL SUMMARY**

Navigation: Differentially-corrected GPS  
 Data reduction grid interval: 25 metres  
 Terrain clearance: Helicopter, Spectrometer 57 m  
 Electromagnetic sensor 30 m  
 Magnetometer 30 m  
 Data sampling interval: 0.1 second  
 Magnetometer / sensitivity: Cesium / 0.01 nT  
 Electromagnetic system: DIGHEM  
 Spectrometer: GR820

Frequency	Sensitivity	Coil Orientation
1000 Hz	06 ppm	Vertical coplanar
5500 Hz	12 ppm	Vertical coplanar
900 Hz	12 ppm	Horizontal coplanar
7200 Hz	24 ppm	Horizontal coplanar
56000 Hz	60 ppm	Horizontal coplanar

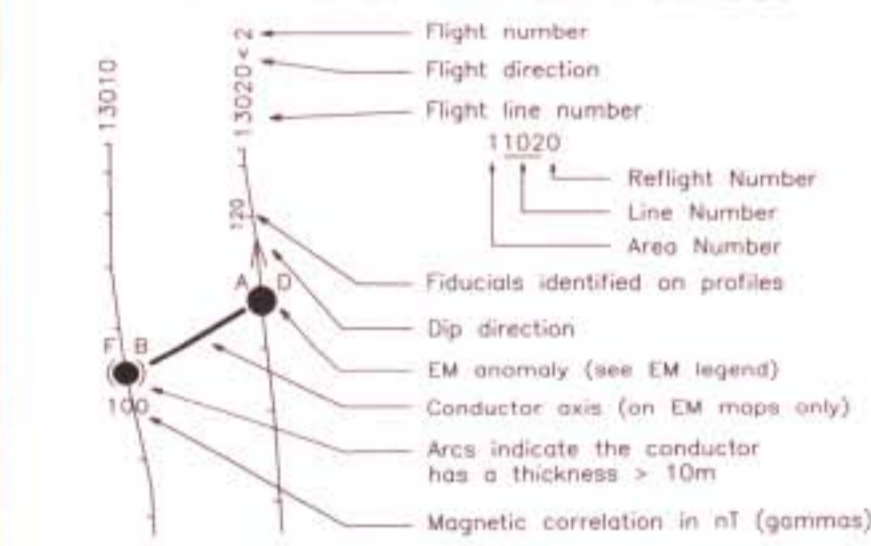


**ELECTROMAGNETIC ANOMALIES**

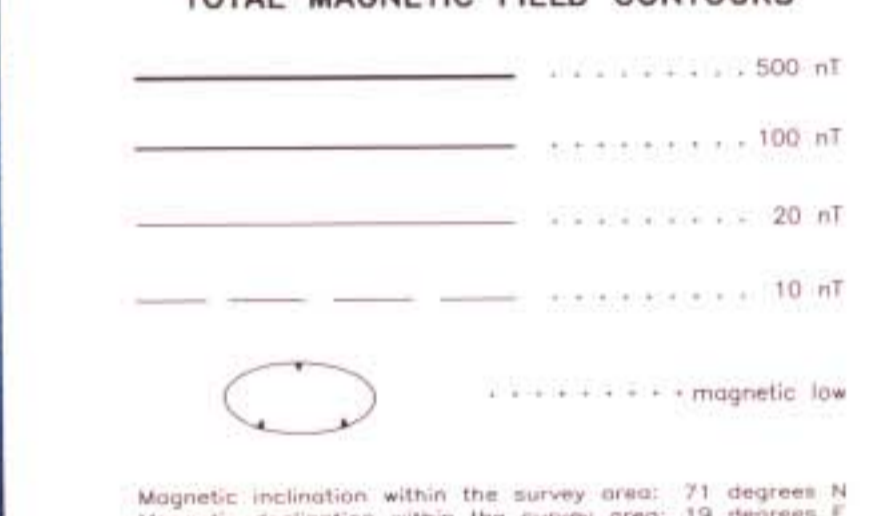
Grade	Anomaly	Conductance
7	●	>100 siemens
6	●	50-100 siemens
5	●	20-50 siemens
4	●	10-20 siemens
3	●	5-10 siemens
2	●	1-5 siemens
1	●	< 1 siemens
-	*	Questionable anomaly

Interpretive symbol	Interpretive symbol	Interpretive symbol
B	B	B
B	B	B
S	S	S
H	H	H
E	E	E
L	L	L

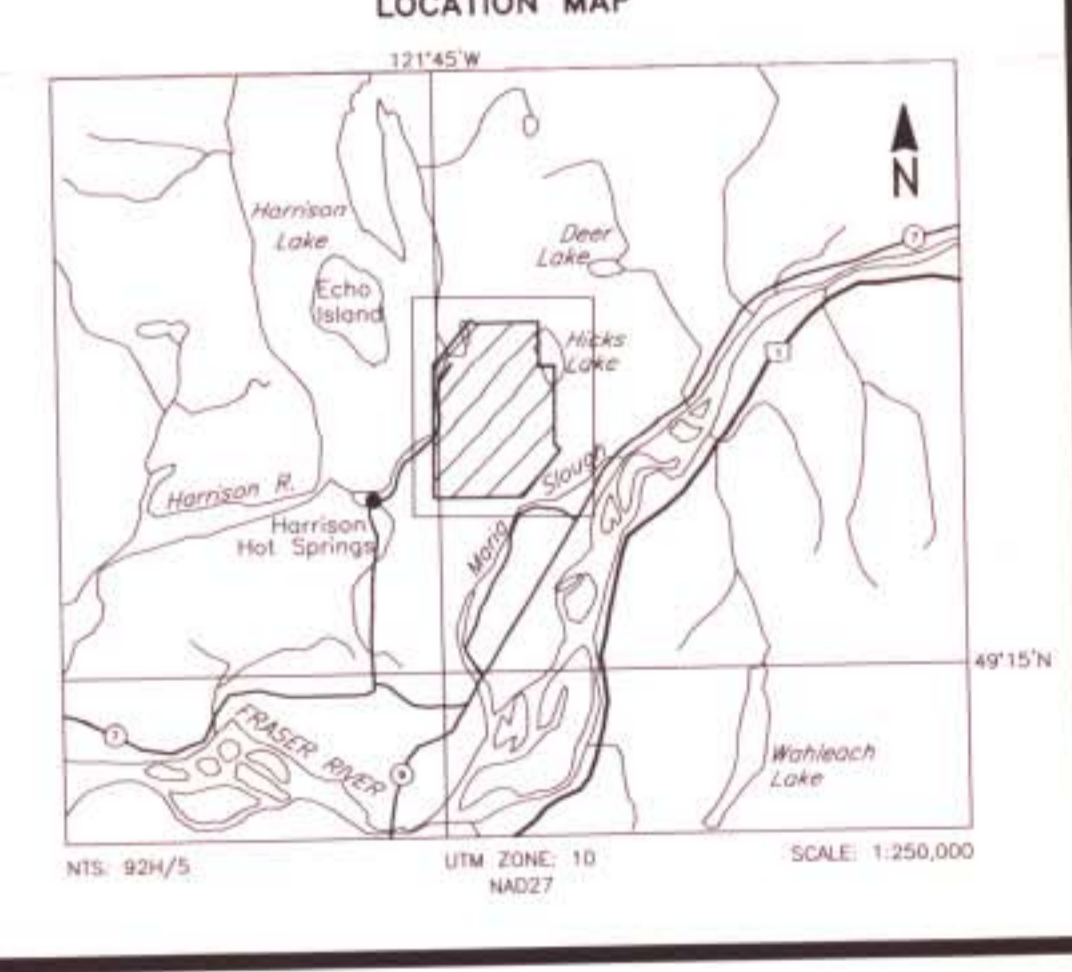
**FLIGHT LINES WITH EM ANOMALIES**



**TOTAL MAGNETIC FIELD CONTOURS**



**LOCATION MAP**

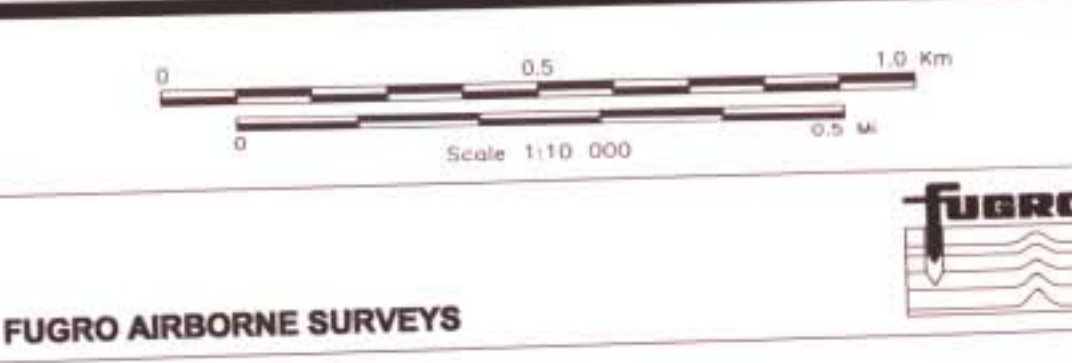


**TOKLAT RESOURCES INC.**  
**HARRISON LAKE AREA, B.C.**

**TOTAL MAGNETIC FIELD** ③

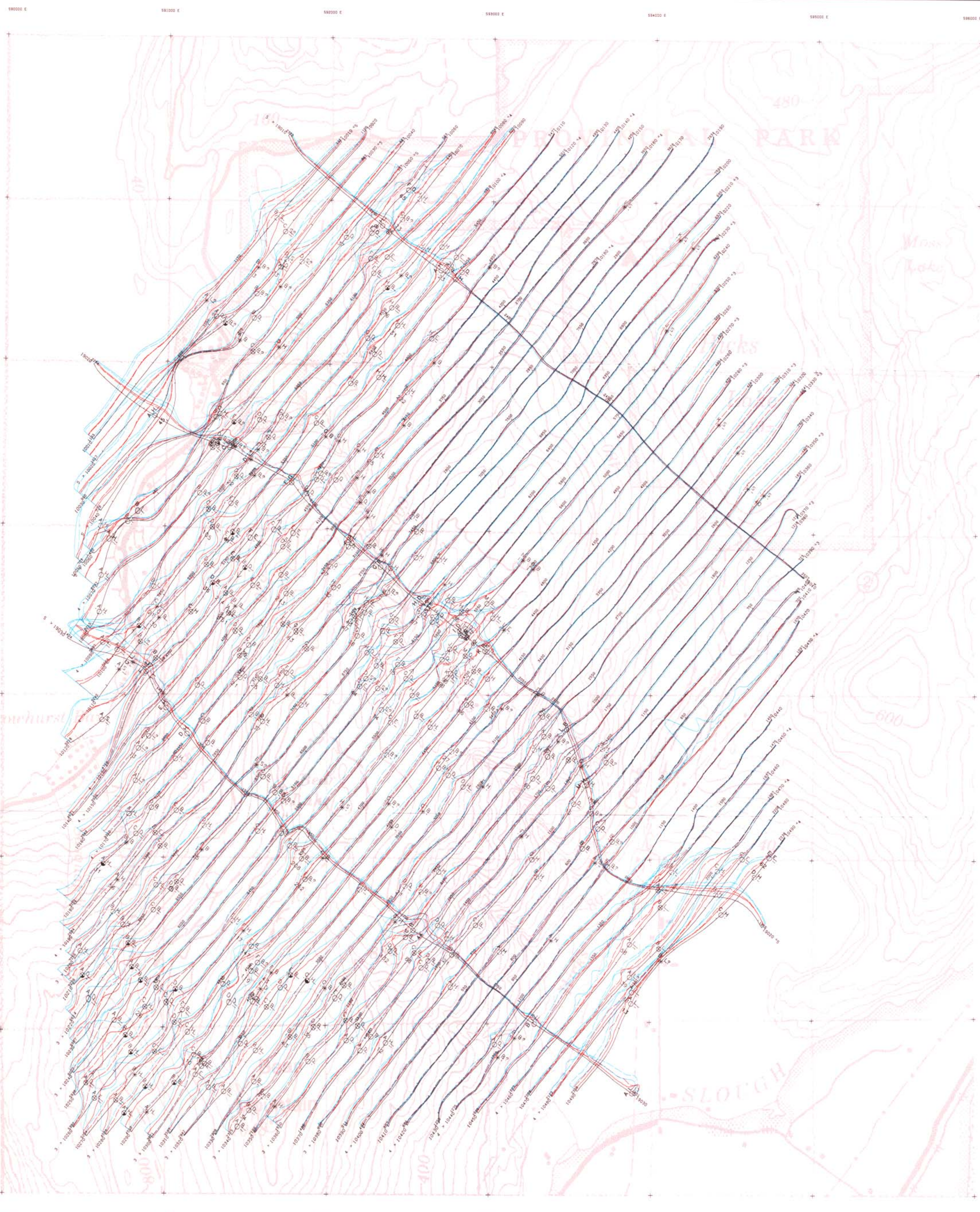
DICHEM SURVEY	NTS: 92H/5	GEOPHYSICIST: [Signature]
DATE: OCTOBER, 2001	JOB: 2066	SHEET: 1

Fugro Airborne Surveys



GEOLOGICAL SURVEY BRANCH  
 26.717





**TECHNICAL SUMMARY**

Navigation: Differentially-corrected GPS  
 Data reduction grid interval: 25 metres  
 Terrain clearance: Helicopter, Spectrometer 57 m  
 Electromagnetic sensor 30 m  
 Magnetometer 30 m  
 Data sampling interval: 0.1 second  
 Magnetometer / sensitivity: Cesium / 0.01 nT  
 Electromagnetic system: DiGEM  
 Spectrometer: GR20

Frequency	Sensitivity	Coil Orientation
1000 Hz	06 ppm	Vertical coaxial
5500 Hz	12 ppm	Vertical coaxial
900 Hz	12 ppm	Horizontal coplanar
7200 Hz	24 ppm	Horizontal coplanar
56000 Hz	60 ppm	Horizontal coplanar

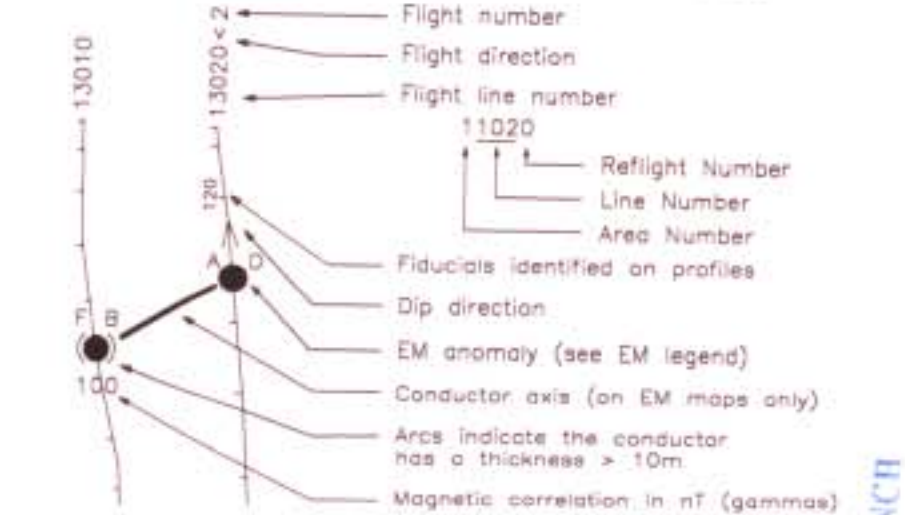


**ELECTROMAGNETIC ANOMALIES**

Grade	Anomaly	Conductance
7	●	>100 siemens
6	●	50-100 siemens
5	●	20-50 siemens
4	●	10-20 siemens
3	○	5-10 siemens
2	○	1-5 siemens
1	○	<1 siemens
-	*	Questionable anomaly

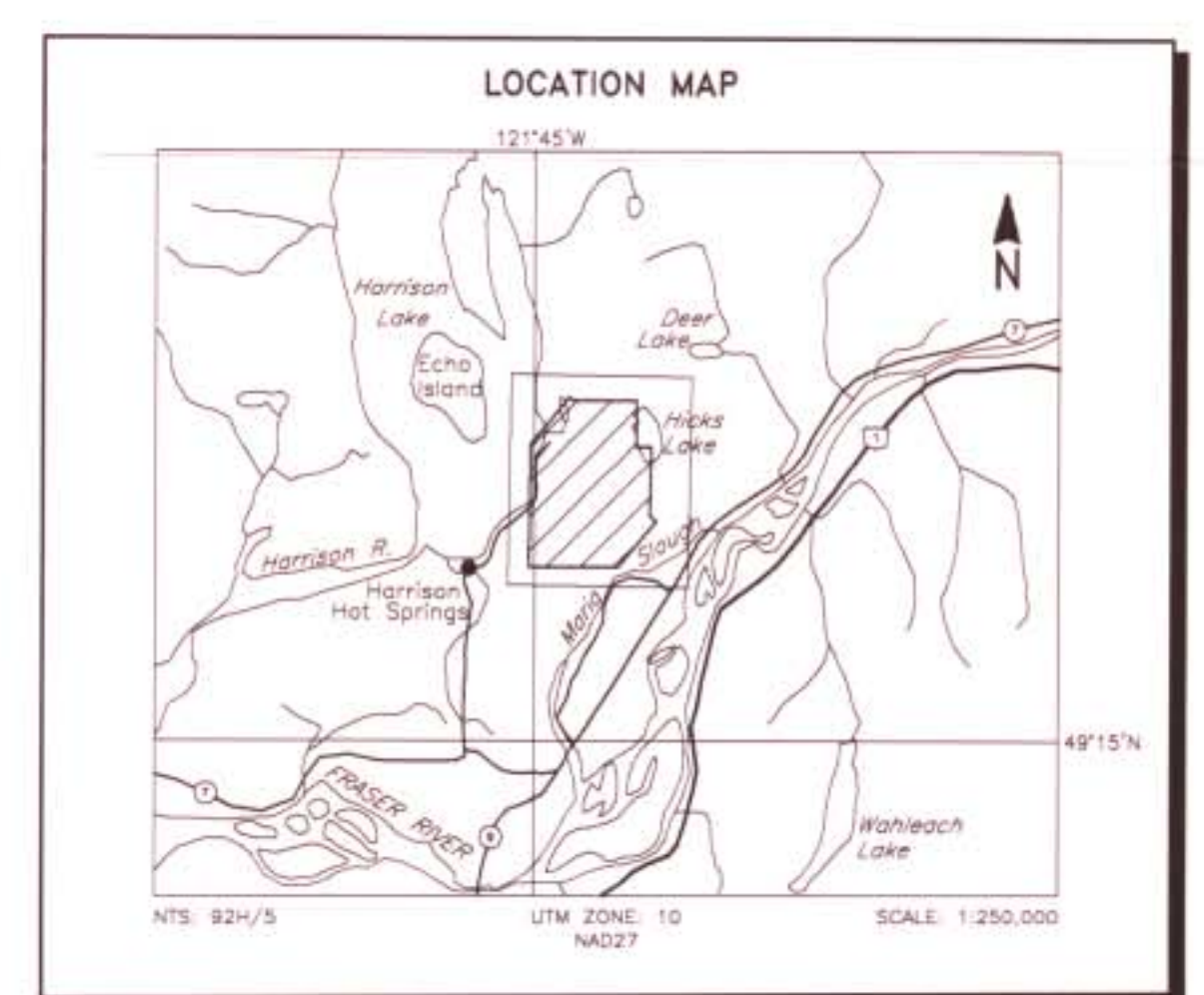
Anomaly Identifier	Interpretive symbol	Interpretive symbol
Depth is greater than: 15 m 30 m 40 m 60 m	○ ○ ○ ○	Inphase and Quadrature of coaxial coil is greater than: 5 ppm 10 ppm 15 ppm 20 ppm
Conductor ("mode")	B	Bedrock conductor
Narrow bedrock conductor ("thin die")	D	Narrow bedrock conductor ("thin die")
Conductive cover ("horizontal thin sheet")	S	Conductive cover ("horizontal thin sheet")
Broad conductive rock unit, deep conductive weathering, thick conductive cover ("half space")	H	Broad conductive rock unit, deep conductive weathering, thick conductive cover ("half space")
Edge of broad conductor ("edge of half space")	E	Edge of broad conductor ("edge of half space")
Culture, e.g. power line, metal building or fence	L	Culture, e.g. power line, metal building or fence

**FLIGHT LINES WITH EM ANOMALIES**



**EM INPHASE & QUADRATURE PROFILES**

Coaxial inphase 10 ppm/mm	—
Coaxial quadrature 10 ppm/mm	- - -
Coplanar inphase 20 ppm/mm	—
Coplanar quadrature 20 ppm/mm	- - -

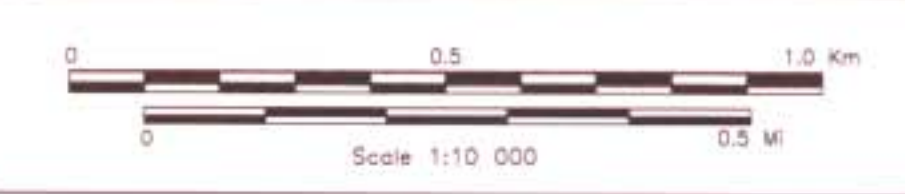


**TOKLAT RESOURCES INC.**  
 HARRISON LAKE AREA, B.C.

**EM COLOUR PROFILES**  
 (5500 Hz Cx, 7200 Hz Cp)

DiGEM SURVEY: NTS: 92H/5      GEOPHYSICIST: [Signature]  
 DATE: OCTOBER, 2001      JOB: 2066      SHEET: 1

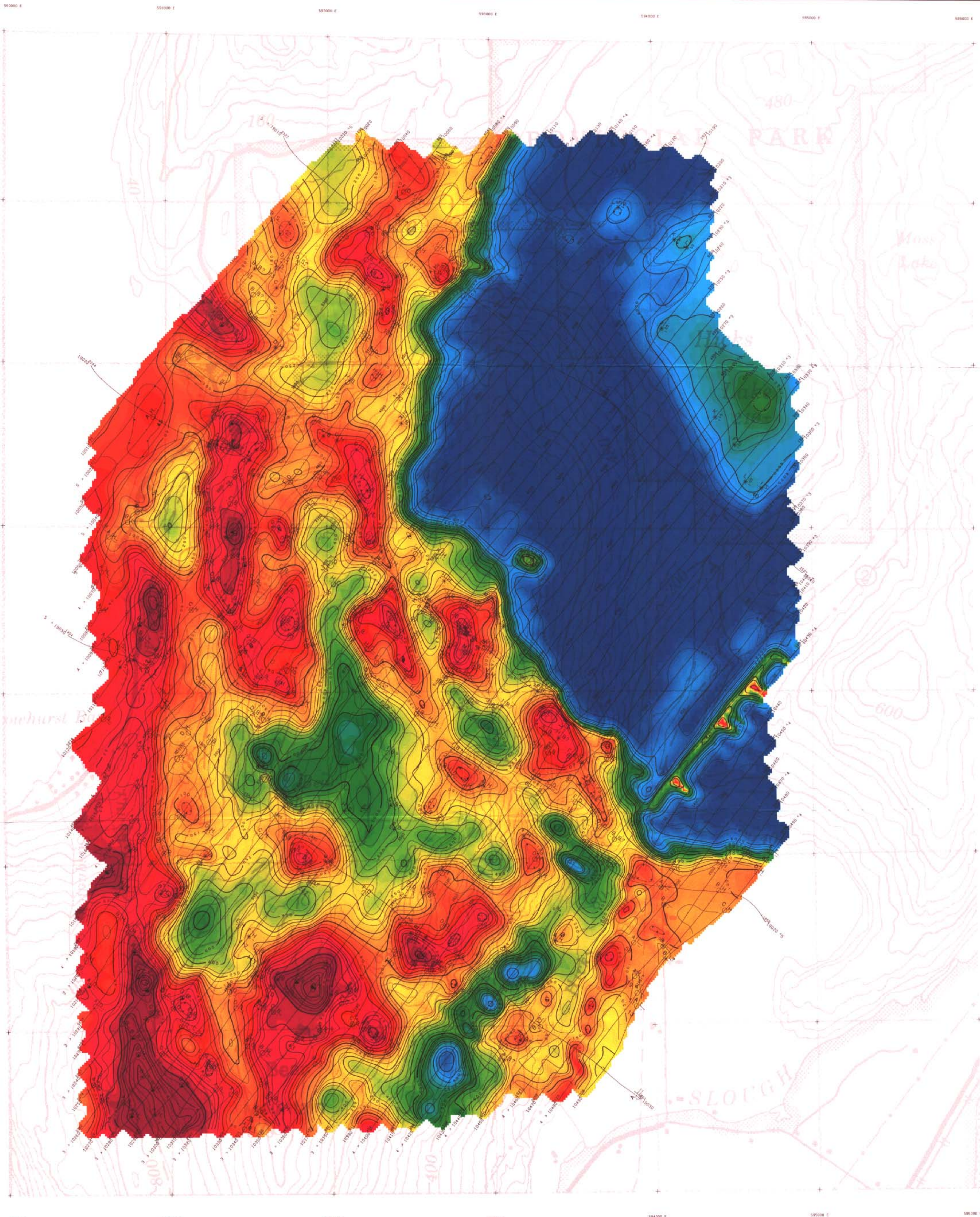
Fugro Airborne Surveys



GEOLOGICAL SURVEY BRANCH

26,717





**TECHNICAL SUMMARY**

Navigation	Differentially-corrected GPS
Data reduction grid interval	25 metres
Terrestrial clearance	helicopter, Spectrometer 5.7 m
	Electromagnetic sensor 30 m
	Magnetometer 30 m
Data sampling interval	0.1 second
Magnetometer / sensitivity	Cesium / 0.01 nT
Electromagnetic system	DIGEM
Spectrometer	GR820

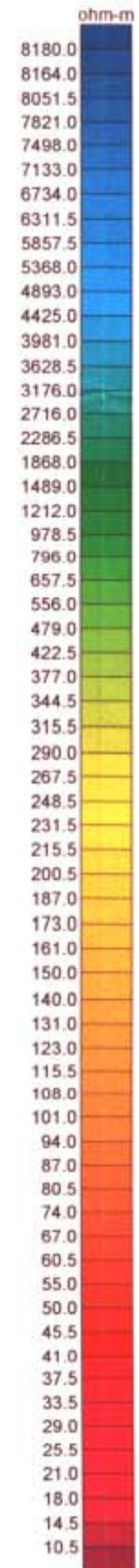
  

Frequency	Sensitivity	Coil Orientation
1000 Hz	06 ppm	Vertical coaxial
5500 Hz	12 ppm	Vertical coaxial
900 Hz	12 ppm	Horizontal coplanar
7200 Hz	24 ppm	Horizontal coplanar
56000 Hz	60 ppm	Horizontal coplanar



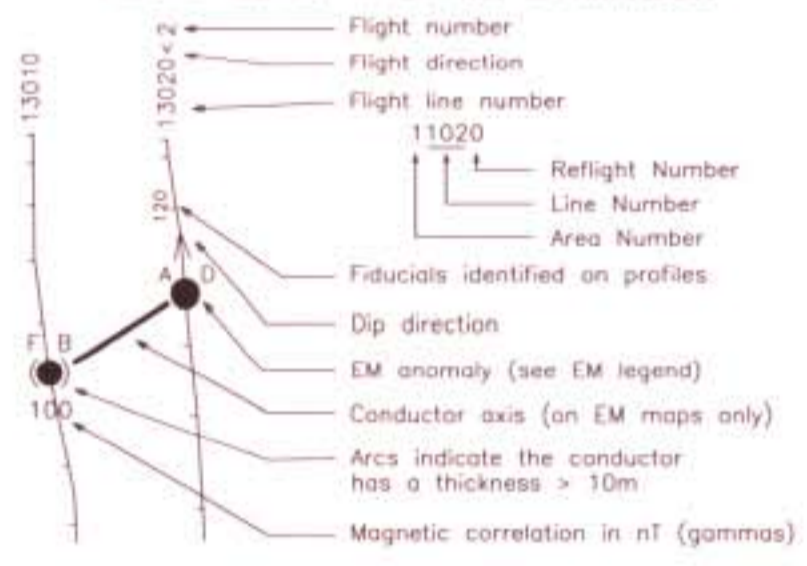
**ELECTROMAGNETIC ANOMALIES**

Grade	Anomaly	Conductance
7	●	>100 siemens
6	●	50-100 siemens
5	●	20-50 siemens
4	●	10-20 siemens
3	●	5-10 siemens
2	●	1-5 siemens
1	●	< 1 siemens
-	●	Questionable anomaly

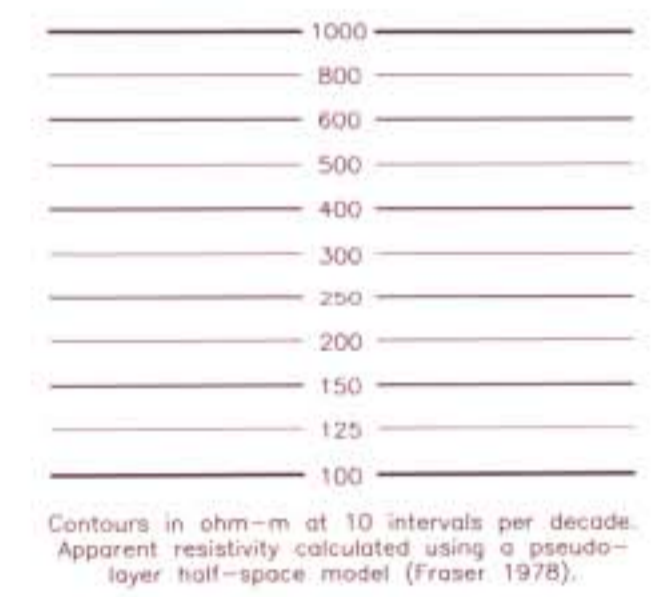


Interpretive symbol	Conductor ("model")
B	Bedrock conductor
D	Narrow bedrock conductor ("thin dike")
S	Conductive cover ("horizontal thin sheet")
H	Broad conductive rock unit, deep conductive weathering, thick conductive cover ("half space")
E	Edge of broad conductor ("edge of half space")
L	Culture, e.g. power line, metal building or fence

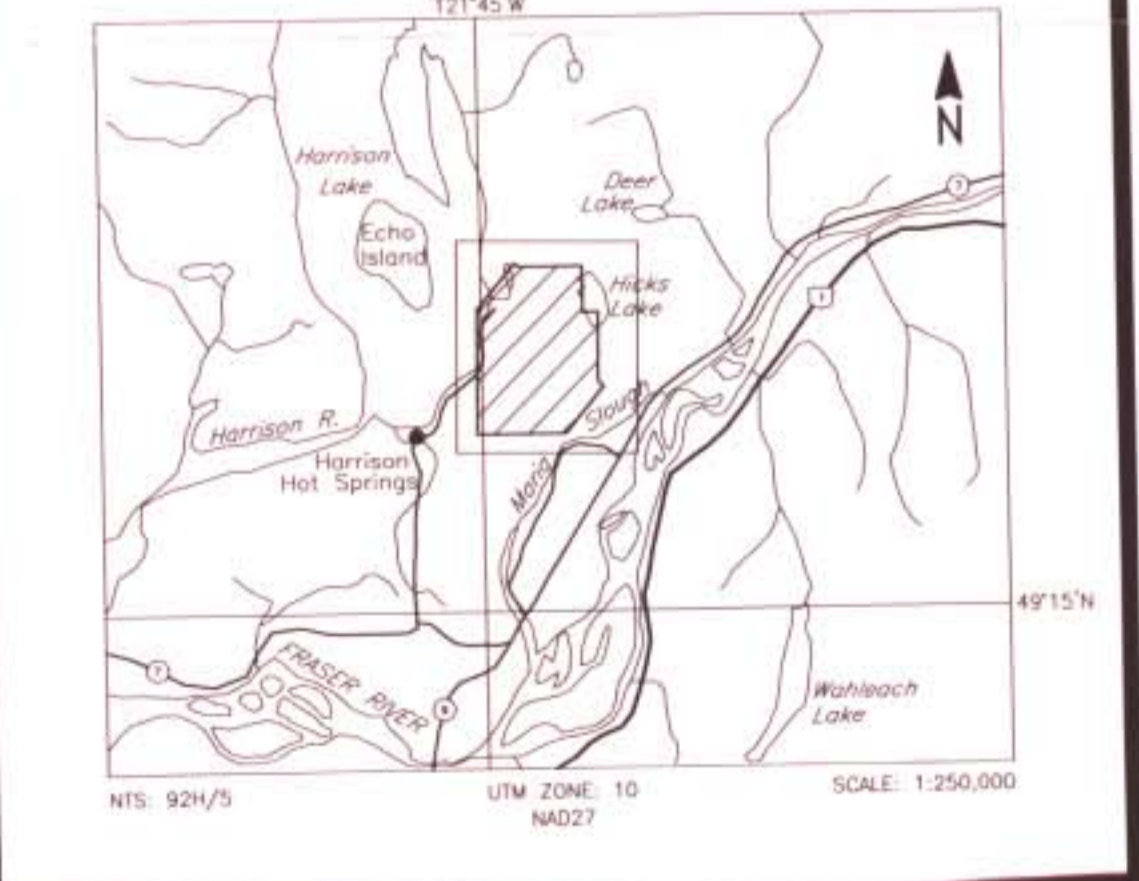
**FLIGHT LINES WITH EM ANOMALIES**



**RESISTIVITY CONTOURS**



**LOCATION MAP**

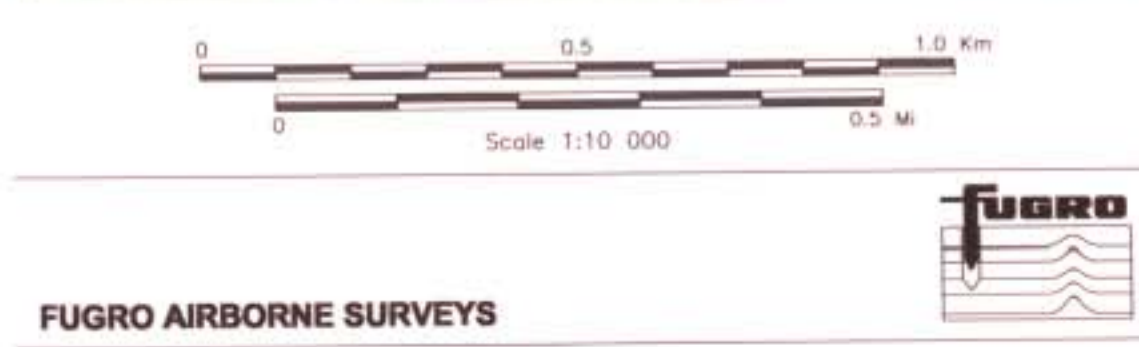


**TOKLAT RESOURCES INC.**  
**HARRISON LAKE AREA, B.C.**

**APPARENT RESISTIVITY** 5  
**7200 Hz COPLANAR**

DIGEM SURVEY	NTS: 92H/5	GEOPHYSICIST: [Signature]
DATE: OCTOBER, 2001	JOB: 2066	SHEET: 1

Fugro Airborne Surveys



GEOLOGICAL SURVEY BRANCH

26,717